Study of vegetation – atmosphere interactions over vineyards: CO_2 fluxes and turbulent transport mechanics

Nadia Vendrame

University of Padova
2016

University of Padova

Department of Agronomy, Food, Natural resources, Animals and Environment

---

DOCTORAL COURSE IN CROP SCIENCE

CYCLE: XXIX

STUDY OF VEGETATION–ATMOSPHERE INTERACTIONS OVER VINEYARDS: CO_2 FLUXES AND TURBULENT TRANSPORT MECHANICS

Head of the course: Prof. Antonio Berti

Supervisor: Prof. Andrea Pitacco

Ph.D student: Nadia Vendrame

Declaration

I hereby declare that this submission is my own work and that, to the best of my knowledge and belief, it contains no material previously published or written by another person nor material which to a substantial extent has been accepted for the award of any other degree or diploma of the university or other institute of higher learning, except where due acknowledgment has been made in the text.

January 31st, 2017 Nadia Vendrame

A copy of the thesis will be available at *http://paduaresearch.cab.unipd.it/*

Dichiarazione

Con la presente affermo che questa tesi è frutto del mio lavoro e che, per quanto io ne sia a conoscenza, non contiene materiale precedentemente pubblicato o scritto da un'altra persona né materiale che è stato utilizzato per l'ottenimento di qualunque altro titolo o diploma dell'università o altro istituto di apprendimento, a eccezione del caso in cui ciò venga riconosciuto nel testo.

31 gennaio, 2017 Nadia Vendrame

Una copia della tesi sarà disponibile presso *http://paduaresearch.cab.unipd.it/*

Index

Abstract iii

Riassunto v

Chapter I: General introduction 1

References 5

Chapter II: Study of the annual carbon budget of a temperate–climate vineyard 7

1 Introduction 8
2 Methods 11
2.1 *Site description* 11
2.2 *Instrumentation* 12
2.3 *Data processing* 13
3 Results and discussion 14
3.1 *Annual carbon budget of the vineyard: ecosystem and soil fluxes* 14
3.2 *Comparison of eddy covariance and soil chamber CO_2 fluxes* 17
3.3 *Interannual variability of ecosystem carbon fluxes* 20
4 Conclusions 24
5 References 25

Chapter III: Effect of evolving canopy structure on turbulence statistics in a hedgerow vineyard 27

1 Introduction 28
2 Methods 32
2.1 *Site description and experimental setup* 32
2.2 *Turbulence measurements* 33
2.3 *Characterization of canopy structure* 33
2.4 *Data processing and period selection* 34
3 Results 36
4 Discussion 45
5 Conclusions 49
6 References 50

Chapter IV: Organized turbulent motions in a hedgerow vineyard: effect of evolving canopy structure 53

1 Introduction 54
2 Methods 59
2.1 *Site description and experimental setup* 59
2.2 *Turbulence measurements* 60
2.3 *Characterization of canopy structure* 60
2.4 *Data analysis* 62
2.4.1 Data processing and period selection 62
2.4.2 Quadrant analysis 62
2.4.3 Quadrant event duration analysis 63
3 Results 66
3.1 *Quadrant analysis* 66
3.2 *Quadrant event duration analysis* 77
4 Discussion 85
5 Conclusions 90

6 References ***91***
Summary and conclusions ***95***
Ringraziamenti ***99***
Acknowledgements ***100***

Abstract

The study of vegetation–atmosphere exchanges is today of great interest in order to understand and model plant responses to environmental conditions and their potential influence on global climate change. A special attention is usually given to carbon dioxide (CO_2) fluxes and, in general, natural ecosystems such as forests received more attention. In the present work we investigated vegetation–atmosphere interactions over vineyards, focusing on the annual carbon budget and turbulent transport processes driving exchanges of mass and energy.

Vineyard is a complex ecosystem with distributed sources/sinks of scalars (water vapour, carbon dioxide, heat), where vines and soil surface combine to give the overall flux of the canopy. In Northern Italy vineyard inter-row is often grassed, playing then an important role in the whole carbon budget. In this context, the partitioning of net ecosystem CO_2 exchange (NEE) into soil and vine components deserves a special attention. We monitored vineyard NEE applying the eddy covariance (EC) method for three years, while soil CO_2 flux measurements have been carried on using soil chambers (transparent and dark). In 2015, the annual carbon budget of the vineyard was about -80 g C m^{-2} y^{-1}, however the largest part of carbon assimilation was due to grassed soil compartment (-60 g C m^{-2} y^{-1}). The interannual variability of seasonal carbon budget showed to be high and significantly affected by heat waves and drought spells in summer. During the growing season of 2014, characterized by plenty of rainfall, NEE reached its maximum value of about -250 g C m^{-2}.

The organization in rows of the vineyard determines a peculiar turbulent transport dynamics within the canopy. However, the morphological structure of the vineyard is greatly variable over the year, shifting from an empty canopy during vine dormancy to dense foliage in summer. We investigated the influence of foliage development on turbulence statistics deploying a vertical array of sonic anemometers. Turbulent flow showed to be greatly influenced by canopy structure. Without leaves, turbulent regime is typical of a rough–wall boundary layer flow, whereas at full foliage development it assumes the features of a mixing–layer flow, even if the inflection point at canopy top is weak, due to sparseness of the vineyard. Coherent structures involved in momentum transport and their temporal scales have been also investigated, showing the increasing

importance of sweeps throughout the growing season. The average duration of dominating coherent structures was in the order of 6 – 10 s and no clear influence by canopy structure evolution was detected.

The research demonstrated the importance of long–term monitoring of vegetation–atmosphere exchanges, and also the complexity of turbulent transport dynamics in the canopy space. However, only a thorough comprehension of this mechanics could lead to a solid interpretation of the role of vegetation in fundamental biogeochemical cycles.

Riassunto

Lo studio delle interazioni tra vegetazione e atmosfera è oggi un tema di grande interesse nell'ottica di migliorare la comprensione della risposta delle piante alle variabili ambientali e la modellizzazione del loro ruolo nel cambiamento climatico globale. Particolare attenzione è di solito rivolta ai flussi di anidride carbonica (CO_2) e, in genere, gli ecosistemi naturali come le foreste hanno ricevuto una maggiore attenzione. In questa ricerca sono state studiate le interazioni vegetatione-atmosfera su una coltura agraria importante per il bacino mediterraneo, quale il vigneto, focalizzandosi sul monitoraggio del bilancio annuale di carbonio e approfondendo lo studio della meccanica del trasporto turbulento che è alla base degli scambi di energia e materia.

Il vigneto è un sistema complesso con diverse sorgenti e *sink* di scalari (vapore d'acqua, anidride carbonica, calore), in cui le due principali componenti, vite e suolo, compongono il flusso totale della *canopy* in un rapporto che varia nel corso dell'anno. Nei vigneti del Nord Italia, l'interfila è solitamente non lavorata e inerbita, giocando un ruolo importante nel bilancio del carbonio del sistema. In questo contesto, risulta cruciale la ripartizione dello scambio netto di CO_2 dell'ecosistema (Net Ecosystem Exchange, NEE) nelle componenti suolo e vite. Nel corso di questa indagine, la NEE di un vigneto è stata monitorata per tre anni utilizzando la tecnica micrometeorologica dell' *eddy covariance* (EC), mentre la misura dei flussi di CO_2 al suolo è stata effettuata con camere (a cupola trasparente e oscura). Nel 2015, il bilancio annuale di carbonio del vigneto è stato di circa – 80 g C m^{-2} a^{-1}, dimostrando quindi la capacità di agire da *sink*, ma la maggior parte dell'assimilazione è risultata legata al suolo inerbito (– 60 g C m^{-2} a^{-1}). In ogni caso, il sistema ha dimostrato un'elevata variabilità interannuale del bilancio del carbonio stagionale, in cui ondate di calore e periodi di siccità estivi hanno giocato un ruolo primario. Nella stagione 2014, caratterizzata da un regime di precipitazione abbondante, la NEE ha raggiunto il valore massimo di circa – 250 g C m^{-2}.

L'organizzazione del vigneto in filari determina una particolare dinamica del trasporto turbolento dentro *canopy*. Inoltre, la struttura morfologica del vigneto è altamente variabile durante il corso dell'anno, passando da una *canopy* praticamente vuota nel periodo di dormienza della vite a una situazione dove il fogliame è denso e concentrato nelle file al culmine della stagione vegetativa. L'influenza dello sviluppo della densità fogliare sulle

statistiche della turbolenza è stato studiato installando un profilo verticale di anemometri ad ultrasuoni. Il flusso turbolento è risultato fortemente influenzato dalla struttura della *canopy*. Senza foglie, il regime turbolento è caratteristico di un flusso di parete, mentre con lo sviluppo completo del fogliame assume le proprietà tipiche di un flusso con *mixing–layer*, sebbene il flesso al limite superiore della *canopy* sia poco accentuato, a causa della bassa densità fogliare del vigneto. Infine, è stata condotta un'analisi specifica delle strutture coerenti coinvolte nel trasporto di quantità di moto e sulle loro scale temporali. L'importanza di eventi discendenti che trasportano aria più veloce del flusso medio (*sweeps*) è aumentata nel corso della stagione. La durata media delle strutture coerenti dominanti è stato nell'ordine di 6 – 10 s e, in questo caso, non è stata riscontrata nessuna chiara correlazione con lo sviluppo della struttura della *canopy*.

Lo studio ha messo in evidenza l'importanza del monitoraggio a lungo termine degli scambi tra vegetazione e atmosfera, ma anche la complessità dei fenomeni di trasporto turbolento che li caratterizzano. Tuttavia, solo la piena comprensione della meccanica di questi processi può portare alla corretta interpretazione del ruolo della vegetazione nei cicli biogeochimici più fondamentali.

Chapter I:

General introduction

Exposed to large and periodical variation of microclimate, influencing themselves many of its features, terrestrial plants are rarely in equilibrium with the surrounding environment, rather exchanging substantial amounts of energy and mass. The study of the interactions between vegetation and the atmosphere has a long history. Yet, it is still a very active field of study, both for the very practical implications directly related to agricultural and forest productivity and for the more actual concerns related to climate change.

The understanding of the structural and functional properties of plant canopies has been crucial to the development of basic and applied micrometeorology, gradually stimulating the increasing awareness of the key role of surface properties on energy partitioning and the regulation of fundamental mass exchanges between Biosphere, Geosphere and Atmosphere. The flux of water vapor – the evapotranspiration – has always received deep attention, due to the many and crucial implication on the hydrological balance of the land, on the agricultural productivity and on the efficient management of irrigation. More recently, fluxes of carbon dioxide (CO_2) and other greenhouse–gases drew the attention of scientist working on natural and managed vegetation, leading to a better knowledge of crucial environmental dynamics and fundamental biogeochemical cycles.

To a keen observer, the study of vegetation–atmosphere interactions is a clear paradigm of a steady, progressive and fascinating advancement of scientific knowledge, that nicely combines several fields and competences – fundamental and environmental physics, plant physiology and morphology, fluid mechanics and thermodynamics –, requiring a wide range of technical skills to disentangle a complex picture of interactions. This word is really crucial, as it epitomizes the very fundamental feature of vegetation canopies: the intricacy of feedbacks between structure and function, between physics and physiology, between geosphere and biosphere, all these playing a winning role in sustaining life and mitigating the asperities of the bare physical environment.

Being at the floor of the atmospheric boundary layer, the study of vegetation canopies has been a mainstay of experimental research in micrometeorology for many years. The word *canopy* has itself a long history: the English language loaned it from the Old French word *conope* (*canapé*, in Modern French), meaning "bed–curtain". The French words derived from Medieval Latin *canopeum*, dissimilated from Latin *conopeum*. Romans introduced the word from the Greek κωνωπείον, that stands for the "Egyptian couch with mosquito curtains” from κώνωψ (mosquito, gnat) which is of unknown origin. The same word (*canapé*) in French, Italian, Spanish and Portuguese now means “sofa, couch”. However, the very first attempts to study and understand its role in energy partitioning and governing water vapor release into the atmosphere has been initially quite primitive, considering the most common canopy used in these research – the natural grass – as a green, wet, and rough carpet, with a limited depth. Nonetheless, the measurements taken close to this intriguing boundary of the lower atmosphere sparked out the very first understanding of the drag experienced by wind in the boundary layer (Taylor, 1918) and of thermodynamics of evaporation (Bowen, 1926). At that time, the view of turbulent transport was understandably simplified, proposing an analogy with molecular diffusion that had its pivotal concept in the *Austausch coeffizient* proposed by Schmidt (1925), that has been practically used until the 80’s. In this long span of time, a steady advancement of practical and theoretical knowledge about canopy properties and processes took place anyway, peaking with the contribution of Penman (1948) and his scholar Monteith (1963, 1965), which were able to merge aerodynamic and thermodynamic determinants of evaporation in a unique model, and apply it satisfactorily to natural surfaces and plant canopies.

Even at that time, the awareness of a more complex and realistic picture of vegetation, which can be rarely simplified to a plain surface, was not completely uncommon. Several Authors were actively seeking a thorough knowledge of the internal canopy microclimate, which should consider the complex radiative regime and wind flow as influenced by the foliage. These Authors were rejecting the reduction of the complexity of the canopy to a simple homogeneous layer where sources and sinks of every property coincide. Already in 1963, just after John Monteith had presented his model to the Symposium on “Environmental Control of Plant Growth” held in Canberra, several researchers (Philip, Swinbank, Businger, Inoue) questioned his simplified approach. Actually, among the same proceedings, Eichi Inoue was attacking the complexity of canopy microenvironment with a very detailed study of internal profiles of momentum and scalar quantities. Indeed, the Japanese school of Agricultural Meteorology was carrying out throughout all the 60’s a very thorough work on canopy micrometeorology, with a long series of contributions (especially by Inoue and Uchijima), which culminated with Uchijima and Wright (1964).

However, these very nice contributions from Japan became gradually less known, and finally faded away.

Main focus of all these studies was on water consumption of crop canopies, and the improvement of crop productivity. Fluxes of carbon dioxide were rarely measured, because of technical obstacles. Gradually, however, the need to understand plant growth increased, together with a raised attention to forest ecosystems. Field measurements, based on the classical flux–gradient approach that was holding since decades, when performed above these tall canopies, were often questionable. The faith in the flux–gradient approach had in the paper by Thom (1975) the final celebration, but soon after several researchers – most of them from Australia – raised a motivated criticism to this approach (Raupach, 1979; Denmead, 1985).

The concern about the fundamental mechanics of transport, however, did not hurt much the research community, as the study of vegetation–atmosphere interactions did benefit from a fundamental technological help, i.e. the availability of instruments to practice the eddy covariance technique. The focus shifted from the wish to understand fundamental properties of plant canopies to the practical commitment of measuring fluxes, and that was easily accomplished deploying one set of instruments above the canopy, and let it run.

Internal canopy space then gradually received a faded attention for years, with most researchers working just on “fluxes” and only few still engaged in understanding its intricacies (Raupach and Thom, 1981; Shaw et al., 1983; Baldocchi and Hutchinson, 1987, 1988; Leclerc et al., 1990; Finnigan, 2000). In this work, we took the commitment to study the carbon fluxes of a vineyard, but also tried to describe and understand the complex relationship between canopy structure and its microclimate. We focused especially on the momentum fluxes and turbulent regime, trying to relate turbulent statistics to the evolution of canopy density and morphology. Although seemingly abstract and theoretical, we believe that these studies have profound implications also in the practical management of crops, improving their general sustainability and maximizing the efficiency of resource use.

References

Baldocchi, D., Hutchison, B., 1988. Turbulence in an almond orchard: Spatial variations in spectra and coherence. Boundary-Layer Meteorology 42, 293-311.

Baldocchi, D., Hutchison, B., 1987. Turbulence in an almond orchard: Vertical variations in turbulent statistics. Boundary-Layer Meteorology 40, 127-146.

Bowen, I.S., 1926. The ratio of heat losses by conduction and by evaporation from any water surface. Physical Review 27, 779-787.

Denmead, O.T., Bradley, E.F., 1985. Flux-gradient relationships in a forest canopy. In: Hutchinson, B.A., Hicks, B.B. (Eds.), The Forest-Atmosphere Interaction. D. Reidel Publishing Company, Dordrecht, pp. 421-442.

Finnigan, J., 2000. Turbulence in plant canopies. Annual Review of Fluid Mechanics 32, 519-571.

Inoue, E., 1963. The Environment of Plant Surfaces. In: Evans, L.T. (Ed.), Environmental Control of Plant Growth. Academic Press, pp. 23-32.

Leclerc, M.Y., Beissner, K.C., Shaw, R.H., den Hartog, G., Neumann, H.H., 1990. The influence of buoyancy on velocity skewness within a deciduous forest. Boundary-Layer Meteorology.

Monteith, J.L., 1963. Gas Exchange in Plant Communities. In: Evans, L.T. (Ed.), Environmental Control of Plant Growth. Academic Press, pp. 95-112.

Monteith, J.L., 1965. Evaporation and environment. In: Fogg, G. (Ed.), The State and Movement of Water in Living Organisms. Cambridge University Press, Cambridge, pp. 205-234.

Penman, H.L., 1948. Natural Evaporation from Open Water, Bare Soil and Grass. Proceedings of the Royal Society of London A: Mathematical, Physical and Engineering Sciences 193, 120-145.

Raupach, M., 1979. Anomalies in flux-gradient relationships over forest. Boundary-Layer Meteorology 16, 467-486.

Raupach, M.R., Thom, A.S., 1981. Turbulence in and above plant canopies. Annual Review of Fluid Mechanics 13, 97-129.

Schmidt, W., 1925. Der Massenaustausch in freier Luft und verwandte Erscheinungen. Henri Grand Verlag, Hamburg.

Shaw, R.H., Tavangar, J., Ward, D.P., 1983. Structure of the Reynolds Stress in a Canopy Layer. Journal of Climate and Applied Meteorology 22, 1922-1931.

Thom, A.A.S., 1975. Momentum, mass and heat exchange of plant communities. In: Monteith, J.L. (Ed.), Vegetation and the Atmosphere. Academic Press, London, pp. 57-109.

Uchijima, Z., Wright, J.L., 1964. An experimental study of air flow in a corn plant-air layer. The Bulletin of the National Institute of Agricultural Sciences (Japan) Series A 11, 19-65.

Chapter II:
Study of the annual carbon budget of a temperate–climate vineyard

1 Introduction

The monitoring of vegetation–atmosphere exchanges has gained great importance in the last decades. In the second half of the past century the research focus was mainly on improving agricultural productivity. Therefore, a lot of effort has been done studying the response of agricultural crops to environmental forcing, with a special attention on evapotranspiration flux in order to correctly manage irrigation requirements. However, in the early 1990s the attention shifted to the study of natural ecosystem responses to climate. This change was driven by the increasing awareness of global warming effects due to greenhouse gas emissions. Since vegetation plays an active role in the global atmospheric CO_2 budget through uptake by photosynthesis and release by respiration, it was mandatory to clarify the magnitude of these fluxes for major vegetation types. Thanks to these research effort, it has been confirmed that vegetation is a sink of CO_2, that today is estimated to be around 30% of total emissions (Le Quéré et al., 2015). In addition, studies on the performance of ecosystems under different and extreme environmental conditions are fundamental to improve the ability to model and predict vegetation role under future climate scenarios. In this context, the monitoring of vegetation–atmosphere exchanges in natural ecosystems, especially forests, received increasing attention leading to the establishment of regional networks of flux measurements in North America (Running et al., 1999) and Europe (Aubinet et al., 2000) in the late 1990s. Later, a coordinated effort was established to monitor fluxes at the global scale with the FLUXNET network (Baldocchi et al., 2001), which greatly helped on the harmonization of methodologies and data availability.

Although conceived already in the fifties (Swinbank, 1951), only recently scientific and technological developments allowed for the establishment of the eddy covariance (EC) method as the more reliable and robust technique to measure long–term ecosystem fluxes (Baldocchi, 2003). This method gives a direct measure of scalar fluxes (water vapor, carbon dioxide, heat, etc.) above the surface, without the use of any empirical equations. Like every micrometeorological measurements, instruments are placed in free atmosphere without altering the environmental conditions of the underlying vegetation. Traces gases as CO_2 are transported by turbulent – upward and downward – motions of air, which are sampled to determine the net flux of mass moving across the canopy–atmosphere interface.

The theoretical framework of the EC technique is the conservation equations describing the time rate of change of scalar concentration at a fixed point in space. Under ideal conditions the conservation equation can be simplified such that the vertical turbulent flux measured at a certain height is equal to the molecular flux at the surface (Baldocchi et al., 1988). The average flux is computed from the covariance between the fluctuations of vertical wind component (w') and scalar concentration (c'), $F = \rho\,\overline{w'c'}$, where ρ is air density. In order to correctly sample turbulent transport, fast (≥ 10 Hz) and synchronous sampling of w and c is required. The applicability of the method requires steady–state conditions, horizontal homogeneity and extensive flat surface, in order to make horizontal transport negligible over a reference time interval.

Despite site requirements, EC is nowadays the most used technique worldwide to measure vegetation–atmosphere fluxes offering several advantages. The spatial resolution of the method is suitable to sample whole ecosystem flux as it provides, with measurements at one point, an area–integrated average of the exchange between vegetation and the atmosphere (Baldocchi et al., 1988). Additionally, the temporal scale ranges from hours to years, allowing continuous and long–term monitoring of ecosystem fluxes (Baldocchi, 2003).

The ecosystem CO_2 flux measured by the EC method is often called net ecosystem exchange (NEE) being the sum of two large opposite fluxes: ecosystem respiration (R_{ECO}) and gross primary productivity (GPP). In order to achieve a better understanding of the relative importance of processes governing ecosystem functioning, the partitioning of NEE into GPP and R_{ECO} is desirable. Furthermore, eddy covariance fluxes are today widely used for calibration and validation of ecosystem models. In this context, the partitioning of NEE into its components is often achieved using flux–partitioning algorithms (Reichstein et al., 2005). However, plant canopies are usually complex systems, where multiple sources and sinks are distributed across a layer, not easily represented as a simple surface. Focusing on soil compartment, direct measurements of underlying fluxes can be achieved using chambers. Dark chambers have been used to measure soil respiration (R_{SOIL}), while transparent chambers can measure the NEE of grassed soil (Riederer et al., 2014). Several authors used both soil chambers and eddy covariance to cross–validate the two techniques under different conditions (Goulden et al., 1996; Van Gorsel et al., 2007).

The major part of long–term ecosystem flux measurements have been carried out in forest sites, due to the primary role played by these biomes as sink of CO_2 globally. However, other types of natural and managed ecosystems have been monitored, reaching a general overview of NEE seasonal patterns for different plant functional types (Table 1 in Baldocchi, 2008). Among them, agricultural crops are shown to achieve the highest short–term rates of carbon uptake, but their annual budget is usually positive or close to neutral due to long periods when the land is bare, therefore losing carbon. However, perennial crops (e.g. vineyards, orchards, olive trees) can behave differently: they grow a permanent woody structure, stand undisturbed in the same field for decades, originate woody pruning debris, and are often grass–covered. Only few long–term studies have been performed over this kind of crops (Pitacco and Meggio, 2015). These canopies are characterized by high structural variability and, often, the floor of vineyard inter–rows is grassed, leading to the coexistence of two vegetation components with different annual cycles. The grass cover is active during the mayor part of the year, while the annual cycle of grapevine begins in spring with bud break and terminates in autumn with leaf fall, followed then by winter dormancy. Therefore, vineyard NEE is determined by the combination of grass and vine performances along the year.

In order to study vineyard–atmosphere exchanges, an eddy covariance station has been set up in a flat extensive vineyard in Northern–East Italy. The flux measurements started in May 2014 and are still ongoing as part of a long–term monitoring program. In the following discussion we will analyze interannual variability of CO_2 fluxes for the growing seasons of 2014, 2015 and 2016. Additionally, a detailed comparison of NEE with soil CO_2 flux measured by chambers will be discussed focusing on year 2015. General considerations on the annual carbon budget of vineyard and NEE partitioning into grapevine and soil components will be given.

2 *Methods*

2.1 *Site description*

Eddy covariance measurements have been carried out in an extensive flat vineyard (*Vitis Vinifera*), cv *Sauvignon Blanc* grafted on 3309C, located in North–Eastern Italy (45°44'25.80"N 12°45'1.40"E). The vineyard, established in 2001, is about 33 ha with vine rows oriented to 35 – 125 °N. Rows are spaced 2.2 m apart and are approximately 0.5 m wide, while the canopy height at full development is 2 m. The vineyard inter–rows are covered by permanent grass, regularly mowed during the season and the soil below plants is chemically weeded for a strip of about 0.7 m.

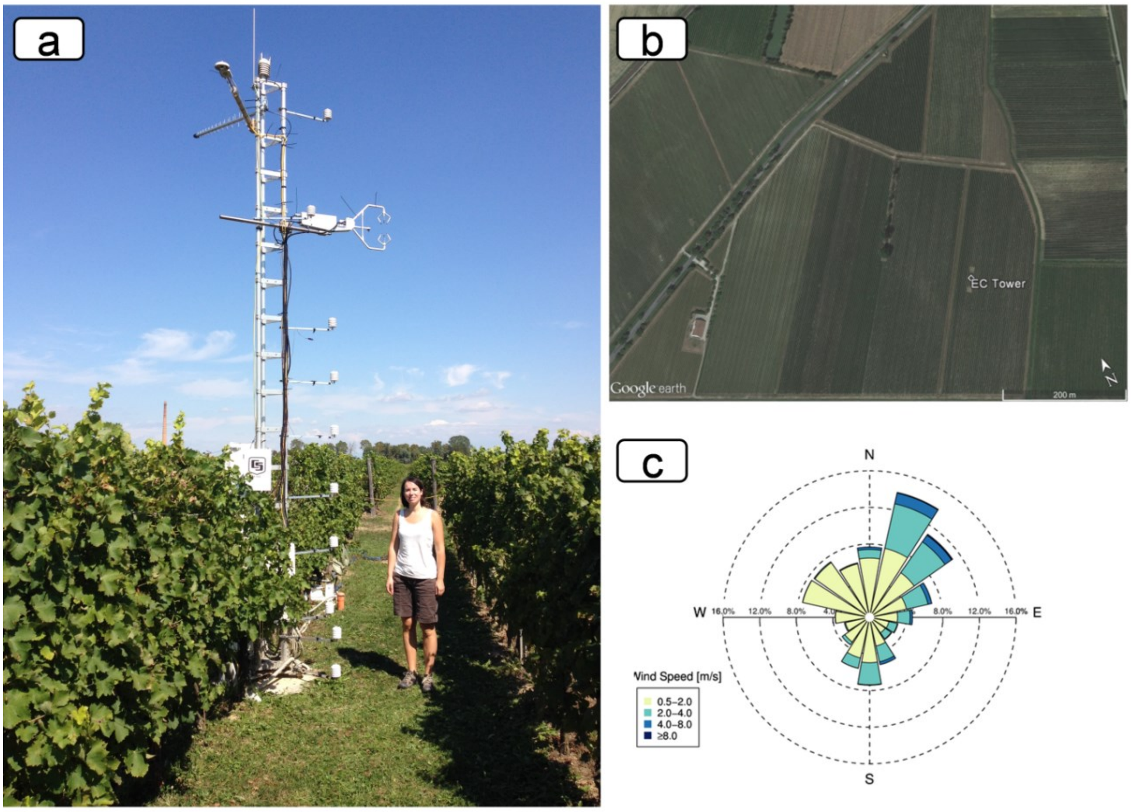

Fig. 1 Eddy covariance tower at Lison di Pramaggiore, NE Italy (a), satellite image of the vineyard (b) and wind rose plot for 2015 (c).

The 5 m high, self–supporting lattice tower is located in the southern part of the field, in order to have the most homogenous fetch. The area is characterized by a regular sea breeze regime, with average morning wind direction from N –NE and turning in the afternoon to S – SW.

The area is part of the so–called lower plain Venice region. The soil consists mainly of fine sediments and silty matrix, deposited by pristine rivers, as well as by more recent fluvial deposits, usually giving the coarser fraction. To these have been added lagoon sediments and marsh, which are dominated by clay fraction.

Yearly average temperature is between 12.5 and 13.5 °C, while yearly average rainfall is in the range of 800–1100 mm. These climatic features made viticulture a successful and widespread crop, so far not requiring irrigation input. However, in the recent years farmers started to provide additional water supply to maintain high quality production even during the recurring summer heat waves and drought spells.

2.2 *Instrumentation*

Flux measurements have been conducted using a CPEC200 closed–path system (Campbell Scientific, Inc., Logan, UT, USA), that is composed of a CSAT3A sonic anemometer and EC155 closed–path IRGA. Sonic and IRGA measurements have been synchronously polled and collected by a CR3000 datalogger (Campbell Scientific, Inc., Logan, UT, USA) with a sampling frequency of 20 Hz. The instruments have been deployed at 4 m height, that is two times the vegetation height at full development. The sonic anemometer has been mounted pointing towards East, in order to have the maximum number of periods with good data according to local wind regime. Fetch was adequate for the prevailing wind directions.

In addition, several ancillary meteorological variables have been monitored. Short–wave and long–wave radiation have been measured using a CNR4 net radiometer (Kipp & Zonen) placed at 4.5 m on the top of a row, in order to have the best representative footprint of the canopy. At the top of the tower, standard meteorological variables (air temperature, humidity and pressure, wind speed and direction, rainfall) have been collected using Vaisala WXT520 integrated meteorological sensor. Soil temperature has been monitored at several depths (0.02, 0.05, 0.10, 0.20, 0.50 m) and water content has been measured at 0.04, 0.10 and 0.20 m using Decagon 5TM and CSI CS616 probes, respectively. Soil heat flux has been measured at four locations along a diagonal transect between two rows at 0.08 m depth using Hukseflux HFP01 plates. All meteorological variables have been collected every 1 s and soil variables every 15 s, whereas statistics have been saved every 30 minutes.

Soil CO_2 flux measurements have been carried out using an automatic dynamic chamber system Li-8100 (LI-COR Biosciences, Lincoln, NE, USA). The system was composed by six soil chambers connected to an infrared gas analyzer (LI-8100) by a dedicated multiplexer (LI-8150). In addition, soil temperature and soil water content probes have been measured close to each chamber. Every 30 minutes, fluxes were estimated from the rate of CO_2 concentration change inside the chamber during a close time of 2 min 35 s. After each chamber measurement a dead–band of 45 s was included. Five dark chambers, measuring soil respiration, have been deployed over different soil conditions: chemically weeded row; grassed inter–row; manually weeded inter–row and "trenched" plot, an area where root growth was avoided by a fine–mesh fabric in order to measure heterotrophic respiration. One transparent chamber has been placed on the grassed inter–row, measuring grass Net Primary Productivity (NPP).

2.3 *Data processing*

Eddy covariance raw data have been saved in daily files, separated later into 30–min chunk files. The raw data processing has been performed using Li-Cor EddyPro® open source software. Standard processing and corrections (despiking, double axis rotation and spectral corrections) for EC measurements have been applied. Statistics, quality parameters and fluxes have been calculated over 30–min time intervals. Periods with rain, wind blowing from behind the sonic anemometer (225–315°N) and unrealistic values (e.g. negative fluxes during nighttime) were excluded. The gap–filling method by Desai et al. (2005) has been applied to replace missing data due to filtering, sensor malfunctioning or calibration.

For the comparison between ecosystem and soil fluxes, two soil chamber measurements have been used: grassed inter–row NPP and bare soil row respiration flux (R_{SOIL}), measured by transparent and dark chamber respectively. Data filtering has been performed applying a despiking algorithm and gaps where filled using linear interpolation. We calculated the overall soil CO_2 flux (Fc_{SC}) as the area–weighted sum of the two fluxes $Fc_{SC} = NPP\ A_{InterRow} + R_{SOIL}\ A_{Row}$, where $A_{InterRow} = 0.66$ and $A_{Row} = 0.34$ are the fractional area occupied by grassed inter–row and bare row soil respectively.

3 Results and discussion

3.1 *Annual carbon budget of the vineyard: ecosystem and soil fluxes*

The annual time course of daily carbon fluxes and main meteorological variables is presented in Fig. 2. The net vineyard carbon flux measured with eddy covariance (Fc_{EC}) and the overall soil carbon flux (Fc_{SC}) showed different patterns through the year.

During winter time, until end of February, both fluxes were small and positive showing similar patterns, meaning that the vineyard was overall a net source of CO_2. However, the magnitude of Fc_{EC} was slightly larger compared to Fc_{SC}, probably due to above ground vine respiration (not measured by soil chambers) and differences in footprint between the two methods. In March net daily fluxes started to be negative and showed good agreement between ecosystem and soil scale. During this period CO_2 assimilation was only due to grass photosynthesis, since vines were still dormant.

Vine bud break occurred at the end of April, but the fluxes remained of the same magnitude until end of May. At this point of the season, vine foliage became significant, reaching full growth in early July. Indeed, from June Fc_{EC} started to be greater in magnitude compared to Fc_{SC} due to active photosynthesis of the vine and the recurring of several heat waves, which caused the reduction in volumetric soil water content down to 20% of available water. The grass cover dried up first and, after few days, vines also reduced dramatically the photosynthesis, with the system sometimes becoming a net source of CO_2. Few rain events in August restored the soil water content and, consequently, Fc_{EC} became negative again. However, soil carbon flux remained positive, indicating that grass did not recover promptly from water stress.

In September the magnitude of both fluxes decreased; vine leaves were still present but the photosynthesis was low and soil flux remained positive. In late October, after several rain events, grass recovered and started to assimilate again until the end of November. However, this pattern was not registered by eddy covariance. The difference between the two methods could be explained by CO_2 release due to decomposition of fallen leaves, which is not accounted in chamber measurements. In addition, the difference in footprint may play a central role. In the EC footprint, there were several temporary patches of bare soil because of previous perturbation by heavy tractors transit. Moreover, in winter some areas were often flooded for several days after rain due to low soil permeability. The combination of these factors, could lead to an overestimation of grass photosynthesis measured at one point by the transparent chamber compared to the average grassed floor of the vineyard. The inter–row, where soil chamber measurements have been taken, were not subjected to heavy tractor transit and therefore the grass and soil conditions were undisturbed compared to other areas in the EC footprint.

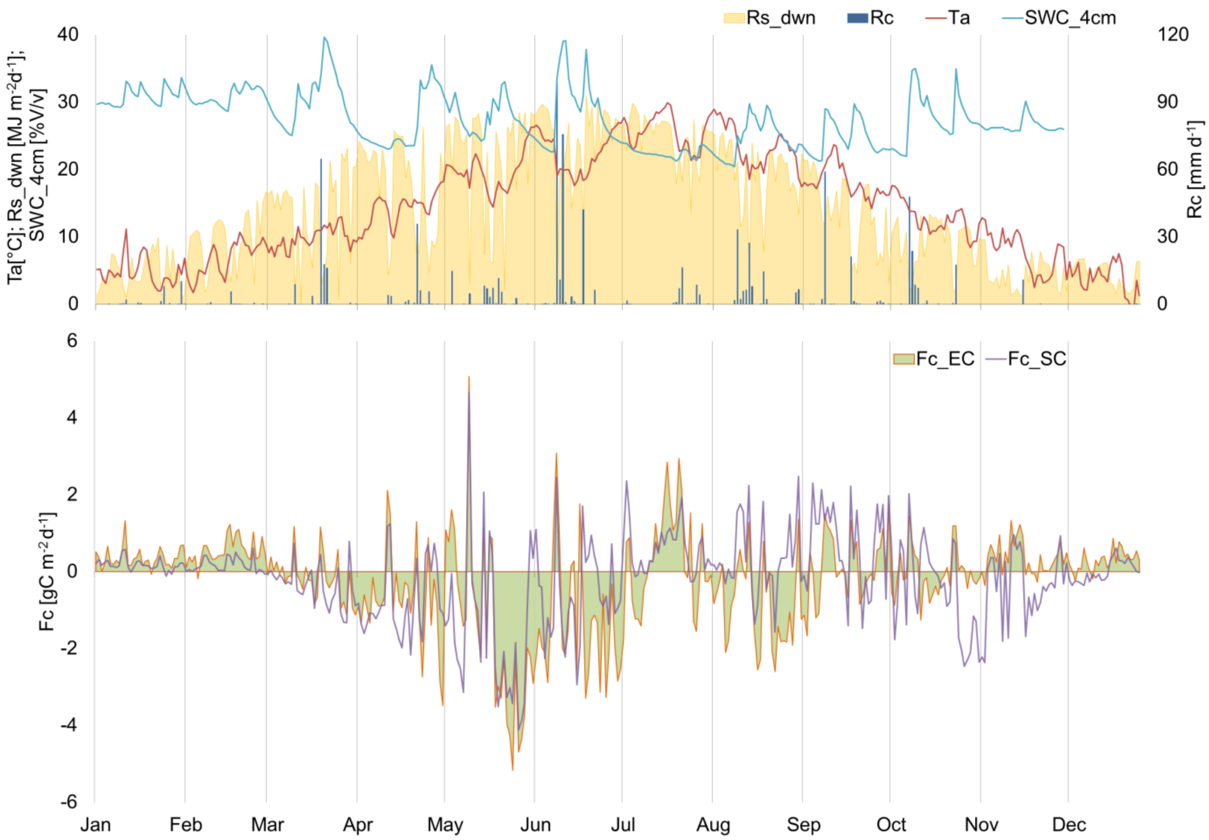

Fig. 2 Upper: Time series of meteorological variables: global radiation (yellow); daily precipitation (blue); air temperature (red); soil water content at 4 cm (purple). Bottom: Annual time course of daily integral carbon fluxes: whole vineyard flux by eddy covariance (green); soil surface flux by chambers (purple).

A more readable pattern on the capacity of the vineyard to act as carbon sink can be obtained looking at cumulated carbon fluxes (Fig. 3). The cumulated soil flux crossed the zero line, becoming a net sink of carbon, at the beginning of April, almost one and a half month before the ecosystem flux. During winter time we would expect the two fluxes to be similar because of grapevine dormancy. However, from January to March, eddy covariance measured higher respiration from the vineyard compared to soil chamber flux. This difference may be explained by vine respiration and decomposition of pruning debris promoted by an increase of temperature. Furthermore, it could be related to low air mixing close to soil surface in stable conditions. Riederer et al. (2014) reported larger EC fluxes during nighttime stable conditions compared to soil chambers, explained by lower coupling of chambers to the surrounding atmosphere than EC. At our site we found the same behavior, with greater variability of nighttime Fc_{EC} compared to quite uniform and lower Fc_{SC}. For deeper analysis refer to Section 3.2.

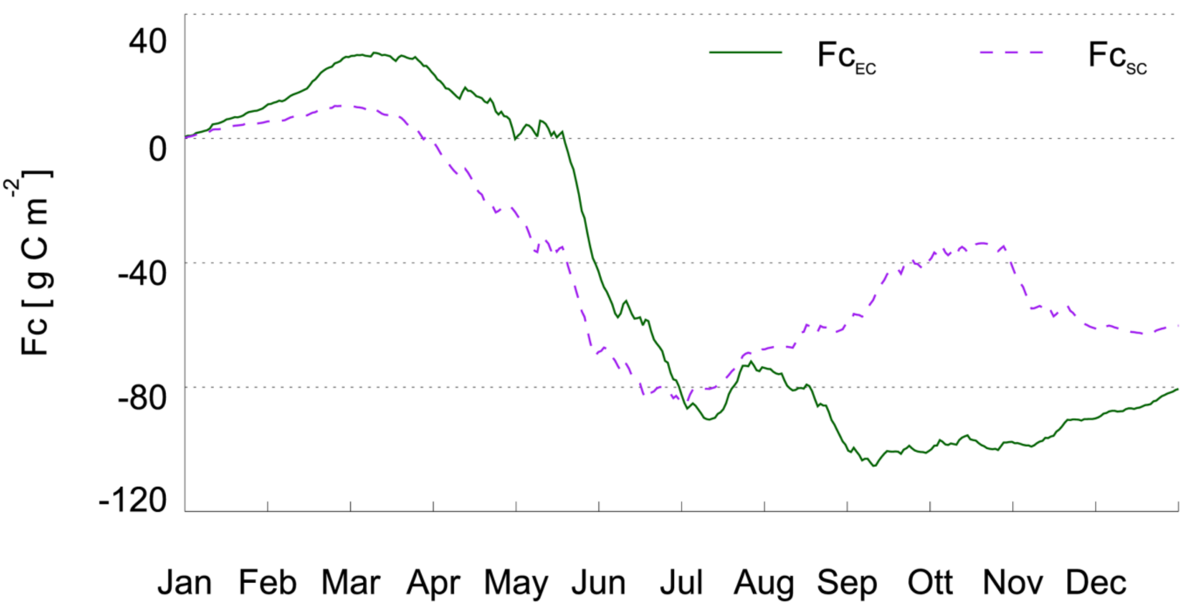

Fig. 3 Annual pattern of cumulated carbon fluxes: vineyard NEE by eddy covariance (solid line); overall soil flux by chambers (dashed line).

In April, grass photosynthesis became very active and it was able to turn down the vineyard net carbon flux to values close to zero within few weeks, becoming then negative in mid–May. Since then, both fluxes showed a steep increase in carbon assimilation and the vineyard reached the strongest sink strength in early July. The grassed soil cover was strongly affected by water stress in July, stopping the photosynthesis and releasing some of the carbon previously absorbed. Vines showed a similar response to water stress but delayed in time and less marked. In August, after few rain events, the vine was able to recover from the stress and started to assimilate again until mid–September, when grapevine reduced the metabolism before leaf fall. On the contrary, cumulated soil flux continued to decrease in magnitude until mid–September likely because grass was previously strongly affected by water stress and it did not recover until late October, when it showed an increase of CO_2 assimilation. This pattern was not registered by eddy covariance, probably due to altered grass conditions in the EC footprint as explained before. In November and December, Fc_{SC} remained stable and Fc_{EC} decreased in magnitude, meaning that eddy covariance was measuring a net release of CO_2 from the vineyard while soil chambers measured a net flux close to zero. In this period we would have again expected similar values from the two methods due to vine dormancy period, as in the first months of the year. In this case, the dissimilarity was primarily caused by the fact that soil chambers measured net daily CO_2 assimilation fluxes until mid–December and, on the contrary, EC was recording positive daily fluxes. Therefore, in this case the discrepancy was primarily referable to overestimation of grassed inter–row assimilation by the clear chamber compared to inter–rows in the EC footprint.

At the end of the year the ecosystem and soil carbon budget were about –80 g C m^{-2} y^{-1} and –60 g C m^{-2} y^{-1} respectively. The difference between the two cumulated fluxes might represent the contribution by vine assimilation. However, due to dissimilarity in footprint of the two methods, the CO_2 uptake by grassed inter–row may have been overestimated.

3.2 *Comparison of eddy covariance and soil chamber CO_2 fluxes*

As underlined in the previous section, we found unexpected discrepancy between soil and ecosystem fluxes during the vine dormancy period. We argued that for the period January–March higher respiration fluxes detected by EC can be partially explained by peculiar turbulence characteristics, especially during nighttime stable periods.

Stable stratification causes a decoupling between the lowest air layer close to ground and the upper layer, where EC instruments are placed. Often, these conditions are associated with low wind speed and dampened vertical mixing. In this context, processes like storage and lateral advection can become important, especially in tall canopies, causing a systematic underestimation of ecosystem fluxes, if measured by eddy covariance. For this reason, a friction velocity (u_*) – threshold filter is usually applied to 30–min fluxes (Aubinet et al., 2012; Goulden et al., 1996). Thus, in these conditions we expect EC fluxes to be in general lower than soil chamber fluxes.

Previous studies reported much regular chamber fluxes compared to eddy covariance during nighttime, with smooth dynamic and low variability (Janssens et al., 2000; Riederer et al., 2014). They explained this features with the weaker coupling of soil chambers to the surrounding atmosphere than EC. At our site, we found the same pattern with relatively regular soil respiration fluxes compared to EC at night (Fig. 4a), while daytime fluxes showed similar variability. Stable conditions are characterized by intermittent turbulence, often associated to large scale coherent structures. In these conditions, the flux at EC measurement height is highly intermittent, discontinuously transporting the CO_2 accumulated in the lower canopy and causing high variability in the data. On the contrary, soil chamber measurements are only slightly affected by turbulence intermittency due to the nature of the measurement itself (the flux is derived from the increase of CO_2 concentration by diffusion when the chamber is closed) and decoupling between air flow above canopy and at soil surface. In addition, it should be underlined that the build–up of CO_2 concentration in the air layer in contact with soil can reduce diffusive surface fluxes measured by the chambers.

Nighttime EC fluxes were not only more variable than chamber fluxes, but also higher on average. Prior studies related this phenomenon to periods with high wind velocity (Denmead and Reicosky, 2003; Riederer et al., 2014). We selected periods of stable nighttime conditions with $u_* > 0.1$ m s^{-1}, which has been found to be the threshold below which EC fluxes were generally smaller than soil fluxes at our site, in order to compare EC and soil chamber fluxes.

The plot in Fig. 4b confirms the findings of previous studies, with larger EC fluxes in case of high wind velocities. This could again be related to atmospheric decoupling between lower within–canopy and above–canopy layers. Under these conditions the air above canopy is well–mixed when friction velocity is sufficiently high, but vertical mixing is still dampened by stable stratification and the within–canopy airspace can remain stably stratified even as u_* above the canopy increases (Van Gorsel et al., 2011).

We tested this hypothesis analyzing turbulence data from the sonic profile experiment presented in the following chapters. Data of April, when the vines were still without leaves, have been used. Stable nighttime 30–min periods with $u_* > 0.1$ m s^{-1} have been selected and turbulence statistics at 4 and 0.5 m have been compared (Table 1).

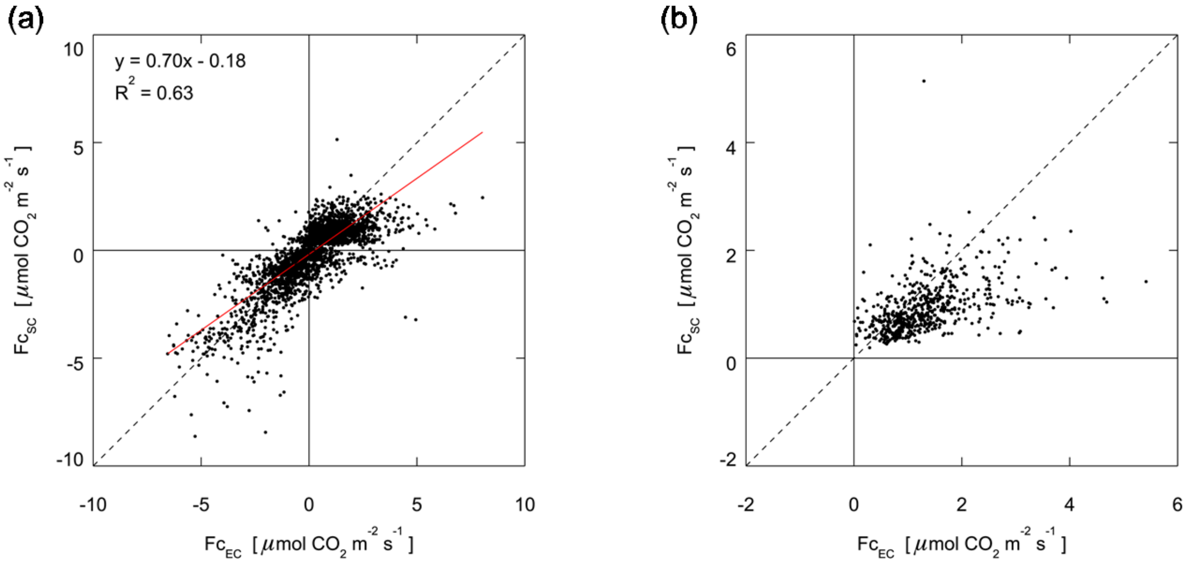

Fig. 4 Scatterplot of Fc_{EC} and Fc_{SC} for the whole period January – March 2015. **(b)** Scatterplot of Fc_{EC} and Fc_{SC} for nighttime stable conditions with $u_* > 0.1$ m s^{-1}.

As expected, average u_* and vertical velocity standard deviation (σ_w) were smaller at 0.5 m, indicating that turbulence was dampened probably due to both stable conditions and proximity to soil surface. A clear sign of the intermittent nature of the airflow in stable stratification is given by the kurtosis (*Kt*). At 0.5 m the kurtosis of horizontal (*u*) and vertical (*w*) wind velocities were much larger than at 4 m, meaning that turbulent transport was more intermittent and thus characterized by stronger stable stratification. In these conditions, the air flow at EC instrumentation height is well–mixed, allowing a correct application of the method, but the measurement of diffusive soil flux by chambers is still reduced by CO_2 build–up in the lowest air layer.

Table 1 Average friction velocity (u_*), standard deviation of *w* (σ_w), kurtosis of *u* (Kt_u) and *w* (Kt_w) at 0.5 and 4 m of stable ($z/L > 0.02$) periods with $u_* > 0.1$ m s^{-1}. In parenthesis standard deviations are reported.

Measurement height [m]	u_* [m s^{-1}]	σ_w [m s^{-1}]	Kt_u	Kt_w
0.5	0.14 (± 0.05)	0.17 (± 0.05)	0.90 (± 1.03)	2.33 (± 1.68)
4.0	0.19 (± 0.07)	0.24 (± 0.08)	0.17 (± 0.85)	1.48 (± 1.72)

3.3 *Interannual variability of ecosystem carbon fluxes*

In order to study the interannual variability of ecosystem carbon fluxes, in this section we will analyze and compare results for the growing seasons (May–September) of 2014, 2015 and 2016. We decided to focus on this period because it is fundamental for the annual carbon budget and we had available data without long gaps for all three years, except for May 2016 when we had sonic malfunctioning for few weeks and we were forced to calculate CO_2 fluxes using the gap–filling method.

Monthly mean daily patterns of 30–min CO_2 fluxes for the three growing seasons are shown in Fig. 5, while Table 2 summarizes monthly statistics of main environmental drivers and monthly carbon and water fluxes. In May average daily fluxes were similar for all years, whereas in June and July 2014 daytime Fc was much larger in absolute value compared to 2015 and 2016. In August 2015 the photosynthesis flux was still reduced, while in 2016 Fc increased in magnitude compared to the previous month, with values similar to 2014. From these patterns it is evident that in 2015 and 2016 the vineyard suffered some stress, on the contrary in 2014 it was more productive. In particular, during July 2015 and 2016 daily CO_2 fluxes deviated from the typical bell–shape curve, with the vineyard reaching the maximum assimilation in early morning and then decreasing linearly until mid–afternoon. This pattern is typical of water stress condition or elevated atmospheric vapour demand: when the photosynthesis is depleted, in response to the increase of substomal CO_2 concentration, the stomata close up in order to maintain safe leaf water potential. In general, grapevine is considered a water stress avoiding species, with a tight stomatal control (Hugalde and Vila, 2014).

The seasonal trends of cumulative carbon fluxes (Fig. 6) clearly underline differences among the three years. The fluxes showed similar patterns until mid of June, when they started to diverge. In 2014 the cumulative carbon flux steadily continued to increase during the growing season until September, reaching a final value of about –250 g C m^{-2}. In 2015 the cumulative flux started to increase in magnitude only towards the end of May and it remained always lower than the previous year. At mid–July the vineyard reached its maximum carbon assimilation, afterwards it slightly decreased and then increased again in late August, as already explained in Section 3.1, leading to a cumulative carbon flux of roughly –100 g C m^{-2}. During 2016, the ecosystem reduced its activity at mid–June and remained stable until begin of August, when it started again to be a net sink of carbon. At the end of September the cumulative carbon flux was about –150 g C m^{-2} in 2016.

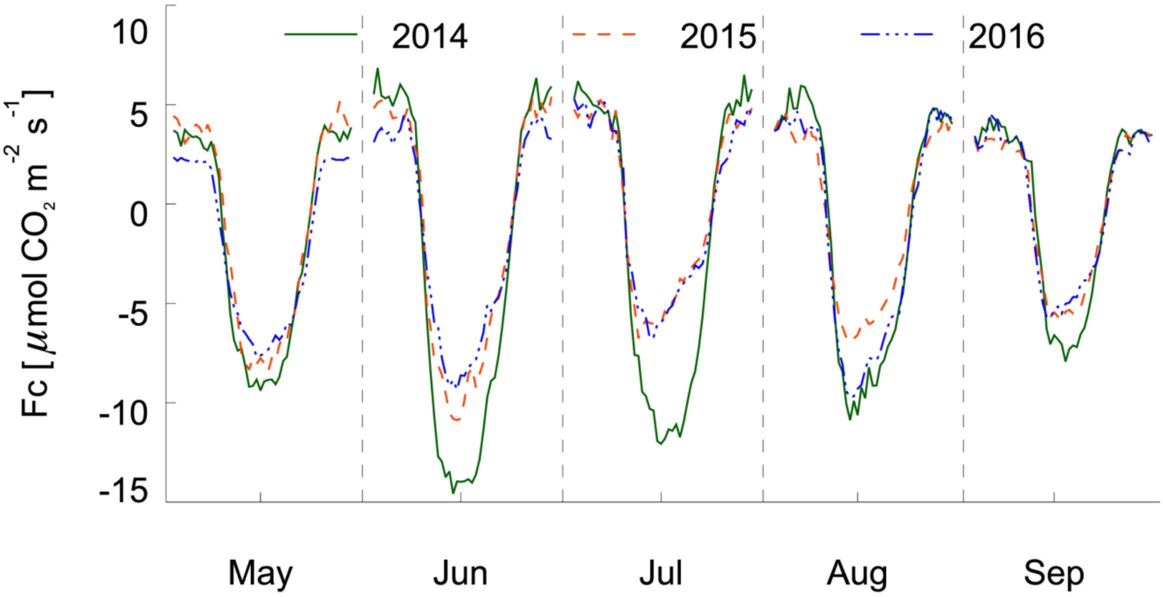

Fig. 5 Monthly mean daily pattern of ecosystem CO_2 flux by eddy covariance in 2014 (solid line), 2015 (dashed line) and 2016 (dash–dotted line).

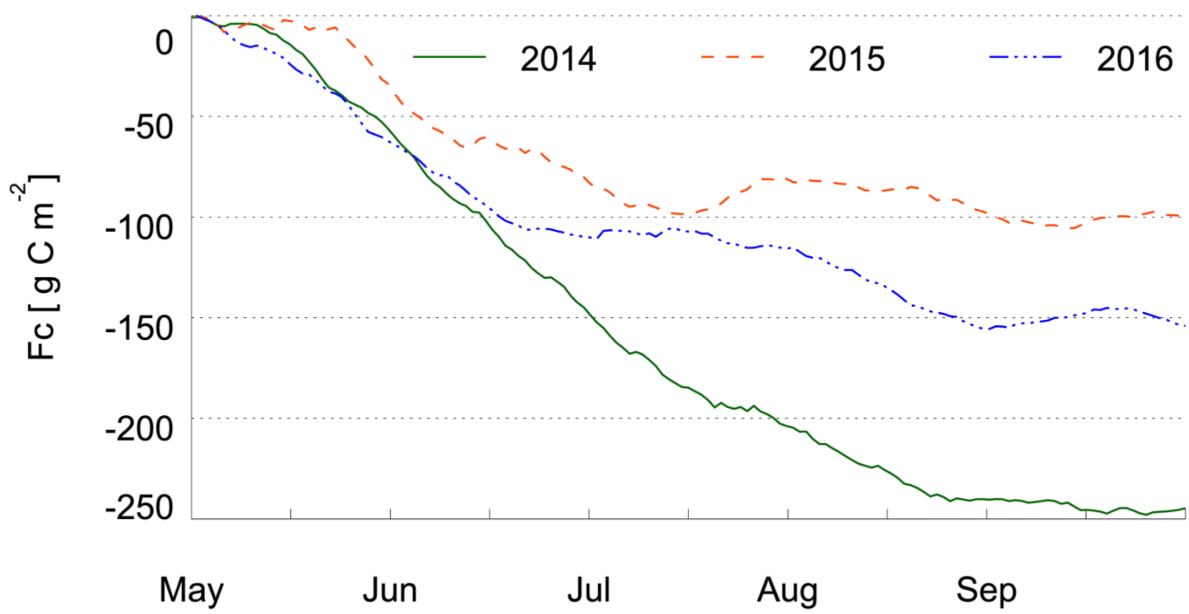

Fig. 6 Seasonal pattern of cumulated ecosystem carbon fluxes in 2014 (solid line), 2015 (dashed line) and 2016 (dash–dotted line).

From both daily pattern and cumulative flux, it is evident that the vineyard activity in June and, even more, in July was crucial for the seasonal and annual carbon budget. The 2015 growing season was characterized by unusual recurring heat waves during the period June–August, associated with very low precipitation in July, leading to water and heat stress conditions. During 2016 air temperature (*Ta*) was slightly lower and soil water content (*SWC*) higher than 2015, however monthly NEE was still consistently lower in June and July compared to 2014. The latter was characterized by lower average *Ta* and higher precipitation during the whole season, with consequent quite elevated *SWC*.

The total rainfall during the growing seasons was 600, 551 and 478 mm for 2014, 2015 and 2016 respectively. However, even if the overall precipitation was similar, the distribution among months was very different (Table 2). In 2014 the rainfall was evenly distributed over the whole growing season, with a peak in July, causing a relatively wet season. On the contrary, 2015 was characterized by few extreme events: most of the rain came in June, but just with two consecutive strong events of about 100 and 80 mm respectively. However, most of the rainfall during these events was probably lost by surface runoff due to high precipitation intensity and low soil permeability. Afterwards, July was characterized by very low rainfall (28 mm) and high air temperature. In 2016, the monthly precipitation decreased constantly from May to September, being always lower than 2014 except in May.

Rainfall is the main water supply at our study site, but during dry spells farmers try to supply water by increasing the water table height using the drainage pipe system. However, in our case it was insufficient to maintain adequate soil moisture in July 2015 and 2016. Even if *SWC* in 2016 was slightly larger than 2015, the photosynthetic response of the system was the same, probably because the evaporative demand (expressed as daytime vapour pressure deficit (*VPD*)) was considerably high in both seasons. Nevertheless, the vineyard recover in August 2016 might indicate that the stress suffered in July was lower compared to the same period of 2015.

Generally, the interannual variability of net ecosystem carbon exchange was considerably high, with 2015 being less than half compared to 2014 and 2016 being intermediate.

Table 2 Monthly mean air temperature (T air), daytime vapour pressure deficit (VPD) and soil water content (SWC) at 0.1 m depth; monthly total rainfall, net ecosystem exchange (NEE) and evapotranspiration (ET).

Year	Month	T air [°C]	Daytime VPD [kPa]	SWC 0.1 m % Vol/vol	Rain [mm]	NEE [g C m^{-2}]	ET [mm]
2014	May	17.3	1.06	–	88.4	–55.9	68.4
	Jun	21.8	1.46	–	125.1	–89.0	122.0
	Jul	21.9	1.10	52.0	192.8	–58.9	106.3
	Aug	21.2	1.02	54.0	123.0	–36.6	91.8
	Sep	18.5	0.85	54.0	71.1	–4.2	51.1
2015	May	18.3	1.01	52.1	73.5	–33.7	48.8
	Jun	22.0	1.39	49.8	239.6	–46.5	88.5
	Jul	25.9	1.79	33.3	27.6	–0.9	109.9
	Aug	24.1	1.67	38.7	114.4	–17.5	88.3
	Sep	19.1	1.09	39.1	96.1	–0.9	54.2
2016	May	16.7	0.98	43.1	138.3	–	–
	Jun	21.3	1.25	53.6	111.3	–47.9	61.9
	Jul	24.4	1.63	38.3	91.1	–5.8	109.3
	Aug	22.7	1.50	39.9	78.2	–39.8	110.7
	Sep	20.9	1.45	34.6	59.6	1.5	56.3

The vineyard carbon sink capacity showed to be very sensitive to environmental conditions in the central months of the growing season, when foliage reached the maximum development. July showed to be very critical because it was commonly the hottest month with low rainfall, leading to plant stress due to both high temperatures and soil water deficit. Under these conditions, both grapevine and grass CO_2 uptake capacity were reduced but the latter seemed to be the most strongly affected, as showed in Section 3.1. Under non–limiting water availability conditions, like in 2014, the vineyard showed to have the strongest carbon sink capacity. Nevertheless, we should consider that a wet environment is favorable for the spreading of fungal infection on grapevine leaves, eventually leading to leaf area reduction in spite of massive use of pesticides.

The occurrence of extreme climatic events, like intense but irregular precipitation and heat waves, is predicted to increase in the next years due to climate change. From our results it is evident that vineyard carbon sink capacity will be strongly affected and variable.

4 Conclusions

In our conditions, the vineyard showed to be a moderate net sink of CO_2 on annual basis. The carbon sequestration capacity was considerably lower compared to a previous long–term study in a vineyard of a nearby area (Pitacco and Meggio, 2015). The difference could be related to several factors, among them soil type, training system, vigour of the plants, climate and management of the vineyard. At our site, the soil is composed by a predominant clay fraction, this characteristic together with intensive heavy tractor transit on the inter–rows leaded to high compactness of the soil, with recurrent flooding and hypoxia episodes impacting on root system and the overall vigour of the vineyard was weakened.

Additionally, the 2015 growing season registered the lowest carbon sink capacity of the ecosystem in the period 2014–2016 due to recurring summer heat waves and drought spells, which caused a reduction in photosynthesis of both grapevine and inter–row grass. The latter was the most affected by water stress on the long–term, showing a longer period before recovering. Our results indicated that the grass component was crucial to define the vineyard as carbon sink. Thus, a less conservative soil management with inter–row ploughing, as it is common in many vineyards of other regions, could reverse the carbon budget of the system.

The potential carbon sequestration of agricultural ecosystems can be then subjected to site specific management practices, which are usually consistently higher than in natural ecosystems. Additionally, we showed that climate variability and increased frequency of extreme events can heavily impact also on NEE of agricultural crops. Thus, long–term studies of CO_2 exchanges at different sites are fundamental to assess the role of viticulture, or more in general agriculture, in the global CO_2 budget.

5 References

Aubinet, M., Feigenwinter, C., Heinesch, B., Laffineu, Q., Papale, D., Reichstein, M., Rinne, J., Van Gorsel, E., 2012. Eddy Covariance Chapter 5 Nighttime Flux Correction, in: Aubinet, M., Vesala, T., Papale, D. (Eds.), Eddy Covariance - A Practical Guide to Measurement and Data Analysis. Springer Netherlands, Dordrecht, pp. 133–157.

Aubinet, M., Grelle, A., Ibrom, A., Rannik, U., Moncrieff, J., Foken, T., Kowalski, A.S., Martin, P.H., Berbigier, P., Bernhofer, C., Clement, R., Elbers, J., Granier, A., Grünwarld, T., Morgenstern, K., Pilegaard, K., Rebmann, C., Snijders, W., Valentini, R., Vesala, T., 2000. Estimates of the annual net carbon and water exchange of forests: the EUROFLUX methodology. Adv. Ecol. Res. 30, 113–117.

Baldocchi, D., 2008. “Breathing” of the terrestrial biosphere: lessons learned from a global network of carbon dioxide flux measurement systems. Aust. J. Bot. 56, 1–26.

Baldocchi, D., 2003. Assessing the eddy covariance technique for evaluating carbon dioxide exchange rates of ecosystems: past, present and future. Glob. Chang. Biol. 9, 479–492.

Baldocchi, D., Falge, E., Gu, L.H., Olson, R., Hollinger, D., Running, S., Anthoni, P., Bernhofer, C., Davis, K., Evans, R., Fuentes, J., Goldstein, A., Katul, G., Law, B., Lee, X.H., Malhi, Y., Meyers, T., Munger, W., Oechel, W., Paw U, K.T., Pilegaard, K., Schmid, H.P., Valentini, R., Verma, S., Vesala, T., Wilson, K., Wofsy, S., 2001. FLUXNET: A New Tool to Study the Temporal and Spatial Variability of Ecosystem-Scale Carbon Dioxide, Water Vapor, and Energy Flux Densities. Bull. Am. Meteorol. Soc. 82, 2415–2434.

Baldocchi, D., Hincks, B.B., Meyers, T.P., 1988. Measuring biosphere-atmosphere exchanges of biologically related gases with micrometeorological methods. Ecology 69, 1331–1340.

Denmead, O., Reicosky, D.C., 2003. Tillage Induced Gas Fluxes: Comparison of Meteorological and Large Chamber Techniques, in: International Soil Tillage Research Organisation Conference.

Desai, A.R., Bolstad, P. V., Cook, B.D., Davis, K.J., Carey, E. V., 2005. Comparing net ecosystem exchange of carbon dioxide between an old-growth and mature forest in the upper Midwest, USA. Agric. For. Meteorol. 128, 33–55.

Goulden, M., Munger, J., Fan, S.-M., Daube, B.C., Wofsy, S.C., 1996. Measurements of carbon sequestration by long-term eddy covariance: Methods and a critical evaluation of accuracy. Glob. Chang. Biol. 2, 169–182.

Hugalde, I.P., Vila, H., 2014. Isohydric or Anisohydric Behaviour in Grapevine…a Never-Ending Controversy? Rev. Investig. Agropecu. 39, 4–10.

Janssens, I. a, Kowalski, a S., Ceulemans, R., 2000. Forest floor CO_2 fluxes estimated by eddy covariance and chamber – based model. Agric. For. Meteorol. 106, 61–69.

Le Quéré, C., Moriarty, R., Andrew, R.M., Canadell, J.G., Sitch, S., Korsbakken, J.I., Friedlingstein, P., Peters, G.P., Andres, R.J., Boden, T.A., Houghton, R.A., House, J.I., Keeling, R.F., Tans, P., Arneth, A., Bakker, D.C.E., Barbero, L., Bopp, L., Chang, J., Chevallier, F., Chini, L.P., Ciais, P., Fader, M., Feely, R.A., Gkritzalis, T., Harris, I., Hauck, J., Ilyina, T., Jain, A.K., Kato, E., Kitidis, V., Klein Goldewijk, K., Koven, C., Landschützer, P., Lauvset, S.K., Lefèvre, N., Lenton, A., Lima, I.D., Metzl, N., Millero, F., Munro, D.R., Murata, A., S. Nabel, J.E.M., Nakaoka, S., Nojiri, Y., O'Brien, K., Olsen, A., Ono, T., Pérez, F.F., Pfeil, B., Pierrot, D., Poulter, B., Rehder, G., Rödenbeck, C., Saito, S., Schuster, U., Schwinger, J., Séférian, R., Steinhoff, T., Stocker, B.D., Sutton, A.J., Takahashi, T., Tilbrook, B., Van Der Laan-Luijkx, I.T., Van Der Werf, G.R., Van Heuven, S., Vandemark, D., Viovy, N., Wiltshire, A., Zaehle, S., Zeng, N., 2015. Global Carbon Budget 2015. Earth Syst. Sci. Data 7, 349–396.

Pitacco, A., Meggio, F., 2015. Carbon budget of the vineyard – A new feature of sustainability. 38th World Congr. Vine Wine (Part 1) 5.

Reichstein, M., Falge, E., Baldocchi, D., Papale, D., Aubinet, M., Berbigier, P., Bernhofer, C., Buchmann, N., Gilmanov, T., Granier, A., Grunwald, T., Havrankova, K., Ilvesniemi, H., Janous, D., Knohl, A., Laurila, T., Lohila, A., Loustau, D., Matteucci, G., Meyers, T., Miglietta, F., Ourcival, J.-M., Pumpanen, J., Rambal, S., Rotenberg, E., Sanz, M., Tenhunen, J., Seufert, G., Vaccari, F., Vesala, T., Yakir, D., Valentini, R., 2005. On the separation of net ecosystem exchange into assimilation and ecosystem respiration: review and improved algorithm. Glob. Chang. Biol. 11, 1424–1439.

Riederer, M., Serafimovich, A., Foken, T., 2014. Net ecosystem CO_2 exchange measurements by the closed chamber method and the eddy covariance technique and their dependence on atmospheric conditions. Atmos. Meas. Tech. 7, 1057–1064.

Running, S.W., Baldocchi, D.D., Cohen, W.B., Gower, S.T., Turner, D.P., Bakwin, P.S., Hibbard, K.A., 1999. A Global Terrestrial Monitoring Network intergrating Tower Fluxes with ecosystem modeling and EOS satellite data. Remote Sens. Environ. 70, 108–127.

Swinbank, W.C., 1951. the Measurement of Vertical Transfer of Heat and Water Vapor By Eddies in the Lower Atmosphere. J. Meteorol. 8, 135–145.

Van Gorsel, E., Harman, I.N., Finnigan, J.J., Leuning, R., 2011. Decoupling of air flow above and in plant canopies and gravity waves affect micrometeorological estimates of net scalar exchange. Agric. For. Meteorol. 151, 927–933.

Van Gorsel, E., Leuning, R., Cleugh, H. a., Keith, H., Suni, T., 2007. Nocturnal carbon efflux: reconciliation of eddy covariance and chamber measurements using an alternative to the u * – threshold filtering technique. Tellus B 59, 397–403.

Chapter III:
Effect of evolving canopy structure on turbulence statistics in a hedgerow vineyard

1 Introduction

Turbulent fluxes of mass and energy between vegetation and the atmosphere are today measured around the world over different ecosystem types using the eddy covariance (EC) method (Baldocchi, 2014). The increasing number of sites where fluxes are measured concurred on improving knowledge about plant responses to environmental conditions and the role of different ecosystems in the global atmospheric CO_2 budget. EC is a micrometeorological technique that it is able to measure fluxes in free atmosphere above canopy, without altering surrounding environmental conditions. However, the applicability of the method requires well–developed atmospheric turbulence in order to perform correct measurements. Usually, data are discarded when friction velocity is below a minimum threshold, as it is common during nighttime (Aubinet et al., 2012).

Vegetation–atmosphere exchanges are determined both by physical and physiological characteristics of plants, but also by the properties of turbulent air flow within and above the canopy. Turbulence is a common condition of the lower atmosphere and it is very efficient in transporting mass and energy from the surface into the overlying atmospheric boundary layer. Even if turbulence is a chaotic motion, it is far from being purely random. Three dimensional coherent structures, called eddies, are responsible for most of the vertical transport (Finnigan, 2000; Raupach et al., 1996). The region of the atmospheric boundary layer where fluxes are measured is the surface layer (SL). Here the air flow is in equilibrium with the surface and it is characterized by small changes of vertical fluxes with height, for that reason it is often called the constant flux layer. The portion in direct contact with the vegetation and strongly influenced by roughness elements is the roughness sublayer (RSL), while the region actually occupied by plants is called canopy sublayer (CSL).

SL turbulent motion is comparable with the turbulent flow above a rough wall, where the shape of horizontal mean wind profile is approximately logarithmic. Differently, in the RSL the profile deviates from the logarithmic shape decaying exponentially. The merging of the two regimes is characterized by an inflection point around canopy height, which is distinctive of a plane mixing layer flow, due to intense drag exerted by rough elements at canopy top. At this height, large intermittent eddies are generated by hydrodynamic instability associated with the inflection point (Raupach et al., 1996). The coherent structures are of approximately canopy size and responsible for most of the transport in the CSL, leading to possible counter–gradient fluxes within this region (Denmead and Bradley, 1987).

The main difference between canopy and rough–wall flows is that vegetation absorbs momentum throughout the entire canopy depth as drag on plant elements, rather than just as friction on the ground as for a plane rough surface (Finnigan, 2000). Canopy drag varies with height depending both on vertical foliage distribution and the local velocity field itself. Thus, within–canopy distribution of scalars is determined by sources/sinks distribution together with turbulent transport within the canopy (Finnigan and Raupach, 1987; Patton and Finnigan, 2013). It is then crucial to study turbulence characteristics both above and within canopy, in order to improve the ability of understand and predict overall vegetation–atmosphere exchanges.

Raupach et al. (1996) compared results of horizontal mean velocity and turbulence statistics profiles of twelve different canopies in near–neutral atmospheric stability. They found common features in all canopy types after appropriate scaling, the so–called "family portraits". From this starting point, they developed the analogy between RSL and plane mixing layer turbulent flows, leading to a comprehensive description of turbulence characteristics in plant canopies (Finnigan, 2000). However, some differences between canopy types were attributed to vertical distribution of leaf area. Additionally, most of these studies neglected diabatic effects, which are known to be significant within the canopy (Leclerc et al., 1991, 1990).

Research on canopy turbulence requires synchronous and fast measurements of three dimensional wind velocities at several levels above and within the canopy. The implementation of such experiments is therefore very demanding in natural canopies. For this reason, studies regarding the effect of canopy density or vertical foliage distribution on turbulent flow have been mostly conducted in artificial canopies (Pietri et al., 2009; Poggi et al., 2004) or using modelling approach (Bailey and Stoll, 2013; Dupont and Brunet, 2008). These authors compared several canopy structures with varying plant density and/or vertical foliage distribution, both influencing the overall canopy roughness. They observed a shift from standard boundary–layer flow to canopy flow with increasing canopy density, with development of a stronger inflection point at canopy top due to shear increase.

Moreover, they reported that the greatest influence on canopy flow was caused by density of the upper canopy layer (Dupont and Brunet, 2008).

Even if canopy turbulence is clearly affected by canopy shape and vertical distribution of foliage density, only few studies investigated the effect of seasonal foliage changes on turbulence characteristics in natural canopies (Dupont and Patton, 2012; Leclerc et al., 1991; Shaw et al., 1988; Su et al., 2008). These experiments studied the variation of turbulent motion above and within the canopy between foliated and defoliated phase of deciduous plants (forests and orchards). They reported a decrease of momentum penetration within the canopy in the foliated period and changes in the magnitude of turbulence statistics due to presence of leaves. Furthermore, a modification of the height where mixing–layer coherent structures develop has been observed by Dupont and Patton (2012) in an almond orchard, with higher height in the foliated period. This result, combined with turbulence statistics profiles, indicates that the flow within the canopy without leaves is likely the superposition of a wall boundary–layer flow with a plane mixing–layer flow. On the other hand, typical features of canopy flow become prevalent as canopy density increases (Su et al., 2008).

Together with canopy morphology effects, the departure of atmospheric stability from near–neutral conditions has been investigated. Diabatic effects have shown to have a large impact on within–canopy turbulence and, in some cases, even greater than changes due to leaf density (Leclerc et al., 1991; Shaw et al., 1988). Therefore, both canopy structure and atmospheric stability play a central role modifying turbulence characteristics within and just above the canopy. Their combined effect should be taken into account to understand the nature of fluxes and included in turbulence closure models.

In this context, a detailed study on canopy turbulence following the continuous evolution of vegetation structure during the growing season is missing, to our knowledge. Thus, we carried out a field experiment measuring turbulence statistics in a hedgerow vineyard along with vertical development of foliage. Vineyards are characterized by large changes in leaf area density (LAD) and canopy height within few months, making it a perfect subject of study for our research.

Most studies on canopy turbulence have been conducted in tall canopies, such as forests (Amiro, 1990; Baldocchi and Meyers, 1988; Launiainen et al., 2007) due to large impact of these natural ecosystems in biogeochemical cycles, but a characterization of turbulence in shorter canopies also deserves attention. Among short canopies, vineyards represent a special case being typically organized in well–defined rows. The distance between rows is normally on the order of canopy height, making it a relatively sparse canopy, but, at the same time, foliage in the rows is very dense exerting a considerable drag on the mean flow. In the past, wind flow characteristics over vineyards have been investigated (Hicks, 1973; Weiss and Allen, 1976b), reporting influence by wind direction on canopy–atmosphere exchanges. Recent studies showed that turbulence characteristics in vineyards are similar to homogenous canopies (Francone et al., 2012; Miller et al., 2015). Nevertheless, wind direction affects the degree of penetration of boundary layer eddies into the CSL (Chahine et al., 2014) and canopy architecture causes wind challenging between the rows (Miller et al., 2015). The particular structure of vineyards recently motivated the study of the impact of row orientation on microclimatic conditions and physiological status of grapevine (Hunter et al., 2016). Vineyards have distinct sources/sinks of scalars, having a large fraction of surface occupied by inter–rows, which can be bare or grassed soil. In this context, canopy architecture can play a central role modifying the transport of mass from soil through the canopy and towards the atmosphere.

Our study aims to follow the continuous evolution of turbulence characteristics and canopy structure during the growing season of a hedgerow vineyard, from bud break to fully developed canopy. The field experiment was conducted in a flat extensive vineyard in the North–East of Italy, using a vertical array of five synchronous sonic anemometers within and above canopy.

2 Methods

2.1 Site description and experimental setup

The experiment was conducted from April to July 2015 in a flat hedgerow–trained vineyard (*Vitis Vinifera*) cv *Sauvignon Blanc* located in the North East of Italy (45°44'25.80"N 12°45'1.40"E). The vineyard is planted in rows oriented 35–125 °N, spaced 2.2 m apart and 0.5 m width; the canopy trunk space is 0.7 m and the maximum trellis height is 2 m. We decided to take the trellis height as the nominal canopy height (h) and we monitored the development of the canopy through the season. Once the vines reached 2 m, the plants were mechanically pruned to maintain this maximum height.

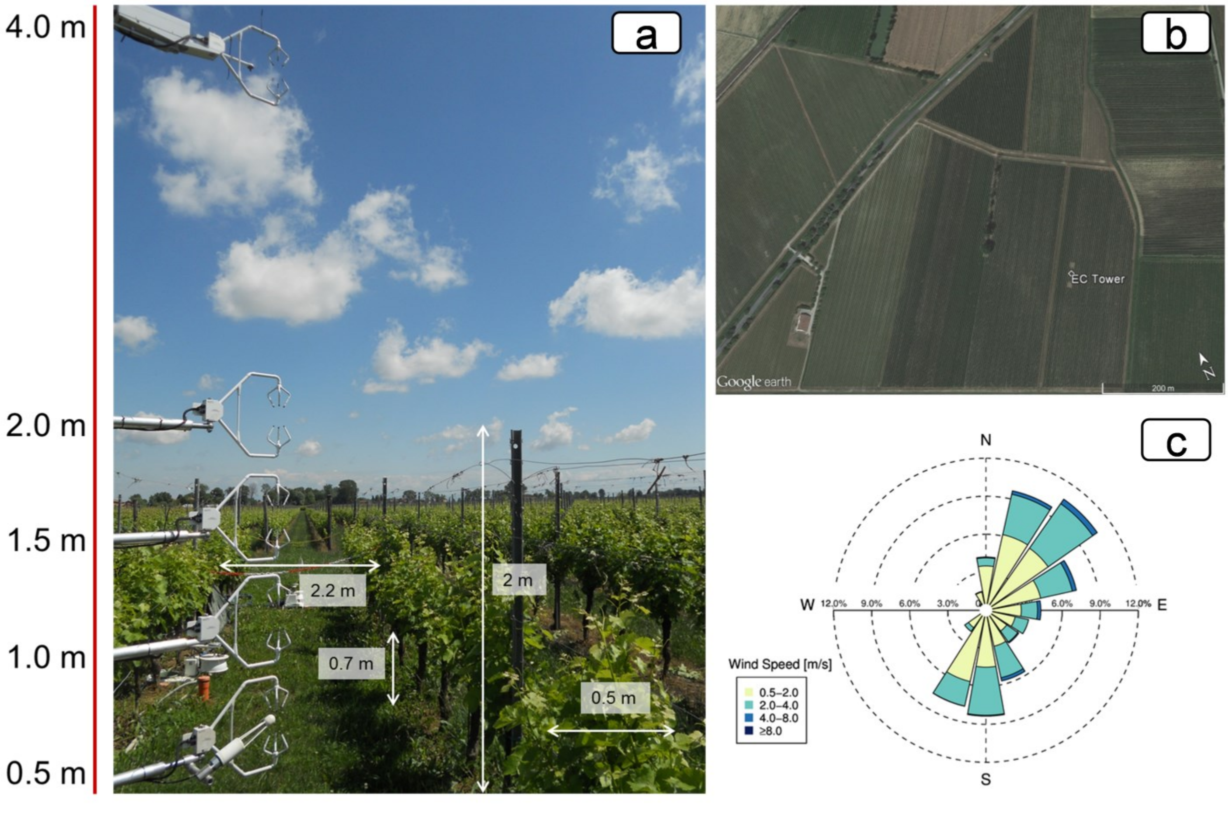

Fig. 1 Array of sonic anemometers on the 5 m tower and canopy characteristics (a), satellite image of the vineyard (b) and wind rose plot at 4 m during the measurement period (c).

2.2 *Turbulence measurements*

A vertical profile of five Campbell Scientific sonic anemometers CSAT3 has been installed on a 5 m tower. The instrument heights were selected in order to detect the changes in turbulent flow characteristics due to vegetation growth. Four sonic anemometers have been deployed in the middle of inter–row within the canopy at 0.5 m (in the trunk space), 1 m, 1.5 m and 2 m; and one at 4 m ($2h$) as surface layer reference. The anemometers have been aligned on the vertical axis and pointed towards East.

High frequency observations of wind vector components and sonic temperature were synchronously digitally sampled at 20 Hz using a CR3000 Campbell Scientific datalogger for the four sonics in the canopy. The highest sonic was collected on a separate CR3000 datalogger as part of an eddy covariance system. The clocks of the dataloggers were synchronized using a server connection once a day at midnight. The raw data were stored in binary daily files and subdivided later in 30 minutes block files. Data processing was performed on this time interval.

2.3 *Characterization of canopy structure*

Canopy foliage and shape had been regularly monitored, ca. every 14 days, from bud break (30/04) to maximum foliage development (16/07) by optical and direct methods (Fig. 2). We assessed leaf area index (LAI) using Li-Cor LAI-2000 plant canopy analyzer. Measurements have been performed on diagonal transect in the inter–row, to better characterize the row structure of the canopy, and at several locations in the footprint area.

At the same time, direct measurements of LAI have been carried on five plants in the footprint area. The number of shoots per vine was counted and randomly selected shoots have been collected from left, center and right of the vine. During the experiment we used two different direct methods to obtain LAI. During the first month, we measured the width and length of each leaf with a ruler on selected shoots. Then, we calculated the leaf area from an empirical relation calibrated on the same vineyard. Once the canopy was more developed and the number of leaves became too large, we used a destructive sampling method, measuring leaf area directly. To better correlate canopy structure with turbulence data, the canopy crown has been subdivided into three layers (0.7–1.2 m, 1.2–1.7 m, 1.7–2 m) and LAI have been measured using direct methods for each layer.

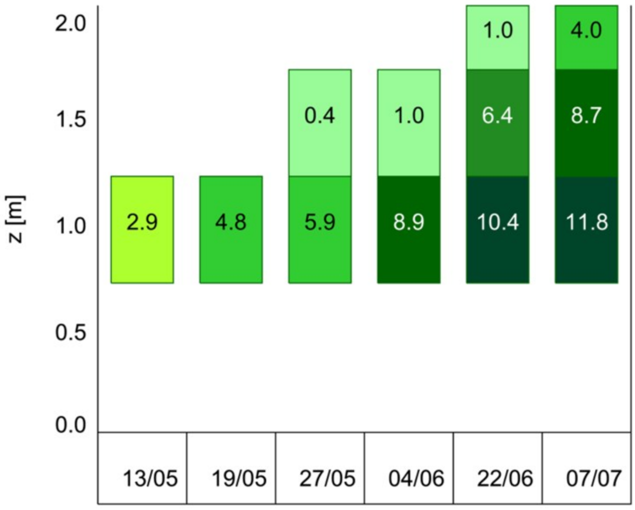

Fig. 2 Development of canopy foliage (left) and time course of Leaf Area Density [m^2 m^{-3}] for each canopy layer during the growing season (right).

In the context of turbulence characteristics analysis, a more appropriate parameter to characterize canopy structure is the leaf area density (LAD), the total leaf area in a reference volume [m^2 m^{-3}]. We calculated canopy average leaf area density as *LAD = LAI (row width) (canopy height)*, assuming a width of 0.5 m and height of 2 m (Table 3). LAD of each layer has been calculated using the height of the layer instead of canopy height (Fig. 2).

Optical and direct methods gave comparable results; thus we were confident using LAD measured with direct methods in the present work.

Table 3 Average leaf area density and canopy height during the growing season.

Sampling date	13/05	19/05	27/05	04/06	22/06	07/07
LAD [m^2 m^{-3}]	1.1	1.9	2.3	3.8	6.8	8.8
Canopy height [m]	1.0	1.2	1.3	1.5	1.9	2.0

2.4 *Data processing and period selection*

The 20 Hz data of velocity components at each height were horizontally rotated to align mean horizontal wind to the streamlines, obtaining *u* horizontal, *v* longitudinal and *w* vertical wind velocities; for each sonic the local angle of rotation has been used. To skip disturbed flow conditions, periods with average wind direction coming from the tower (225 – 315 °N) have been discarded. Periods with rain or total number of sonic diagnostic flag greater than 1800 (90 sec) were not used for the analysis. Additionally, to ensure that the flow was in turbulent motion, 30–min periods with u or w standard deviations lower than 0.1 m s^{-1} were discarded. All the calculations have been performed using IDL scripts developed for the purpose.

We subdivided the dataset in seven periods of increasing LAD, starting from an "empty" canopy (LAD assumed zero) to a final LAD of 8.8 m^2 m^{-3}. Each period, of about 14 days, was associated with a value of LAD measured in the middle of the period.

3 Results

In this section results of turbulence statistics within and above canopy are presented. The dataset was subdivided into six periods of LAD and 3 stability classes (unstable, near–neutral and stable) based on the stability parameter *z/L*, where *z* is the reference measurement height (4 m) and *L* is the Monin–Obukhov length calculated at the same height. No distinction has been made based on wind direction at this stage of the analysis. Unfortunately one sonic anemometer (at 1.5 m) suffered of some malfunctioning after the second LAD period and data from this level are missing until the last period, when the bottom sonic was moved at this height. When normalization has been applied, the friction velocity (u_*) at 4 m has been used. We decided to not use u_* at canopy height (2 m), as common use in analysis of canopy turbulence statistics, because the canopy height is not well–defined in vineyards during the growing season due to vertical development of shoot lengths. Nevertheless, we will refer to 2 m as the canopy height because it is the maximum height for the fully developed canopy and, even in periods without leaves, this space is occupied by trellis.

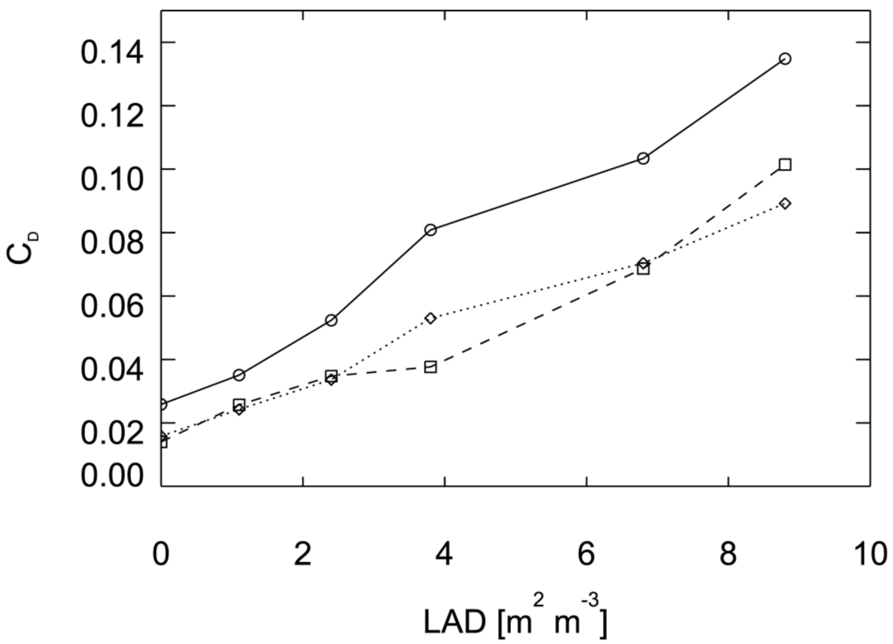

Fig. 3 Evolution of canopy drag coefficient (C_D) as a function of leaf area density (LAD), for unstable $z/L < -0.02$ (solid line), near-neutral $-0.02 \leq z/L \leq 0.02$ (dotted line) and stable $z/L > 0.02$ (dashed line) conditions.

The bulk drag coefficient (C_D) at 2 m, the nominal canopy height, may be used as reference value in models to estimate the overall drag exerted by the vineyard. The drag coefficient was calculated as the ratio between momentum flux and squared mean wind velocity ($C_D = \overline{u'w'}/U^2$). Fig. 3 shows that C_D increased almost linearly with LAD, meaning that the overall efficiency of the canopy in absorbing momentum was directly related to leaf density and vertical development of foliage, as it could be expected. However, the drag exerted by the canopy was generally higher in unstable conditions compared to near–neutral and stable stratification, which instead were showing comparable values. C_D increased from about 0.02 for the empty canopy to 0.10 for fully developed canopy in neutral and stable conditions, while in the unstable case it almost reached 0.14.

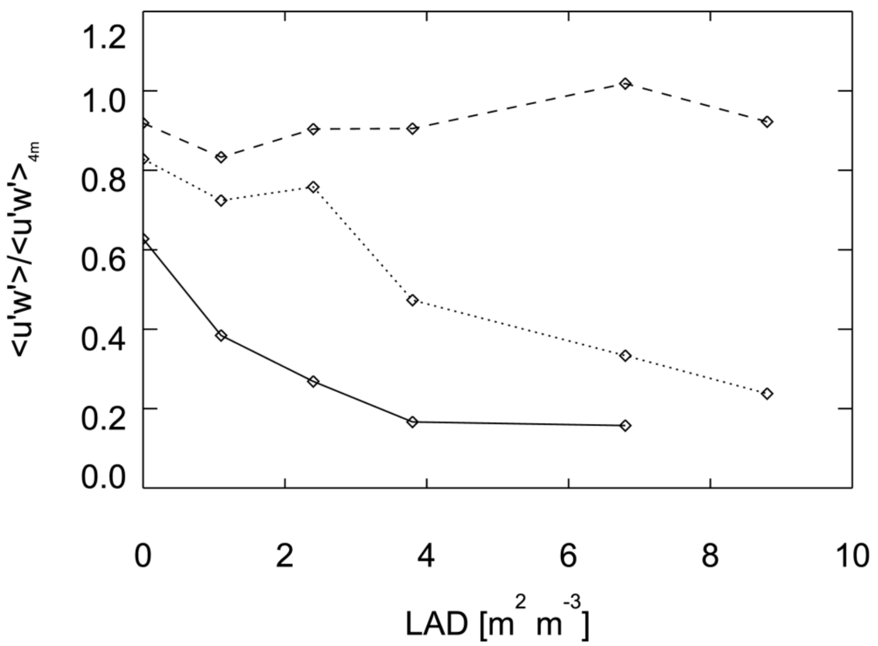

Fig. 4 Evolution of normalized momentum flux ($\overline{u'w'}/\overline{u'w'}_{4\,m}$) at 0.5 m (solid line), 1 m (dotted line) and 2 m (dashed line) as a function of leaf area density (LAD) in near-neutral conditions.

The penetration of momentum, represented as $\overline{u'w'}$ normalized by $\overline{u'w'}$ at 4 m, decreased with height within the canopy and as foliage developed (Fig. 4). For clarity only results for near–neutral conditions are shown since only slight effect by stability was found. Within the canopy the pattern was very different at 0.5 m, in the empty trunk space, and at

1 m, the first foliage layer. In the trunk space the normalized momentum flux rapidly decreased with first foliage appearance and it continued to reduce until the bottom layer of foliage was very dense. Later in the season, the amount of momentum penetrating into the trunk space was stable around 15% of above canopy flux. On the contrary, at the level just above it (1 m), stress fraction was stable around 80% at the beginning, dropping only when foliage in this layer became very dense and it progressively decreased with upper layers development, reaching about 20%. On the contrary, the normalized momentum flux at canopy top was stable around 90% during the whole experiment, indicating that momentum was almost conserved between 4 and 2 m.

Fig. 5 Vertical profiles of normalized mean horizontal velocity U/u_* for unstable ($z/L < -0.02$), near-neutral ($-0.02 \leq z/L \leq 0.02$) and stable ($z/L > 0.02$) conditions and different leaf area density (LAD) periods.

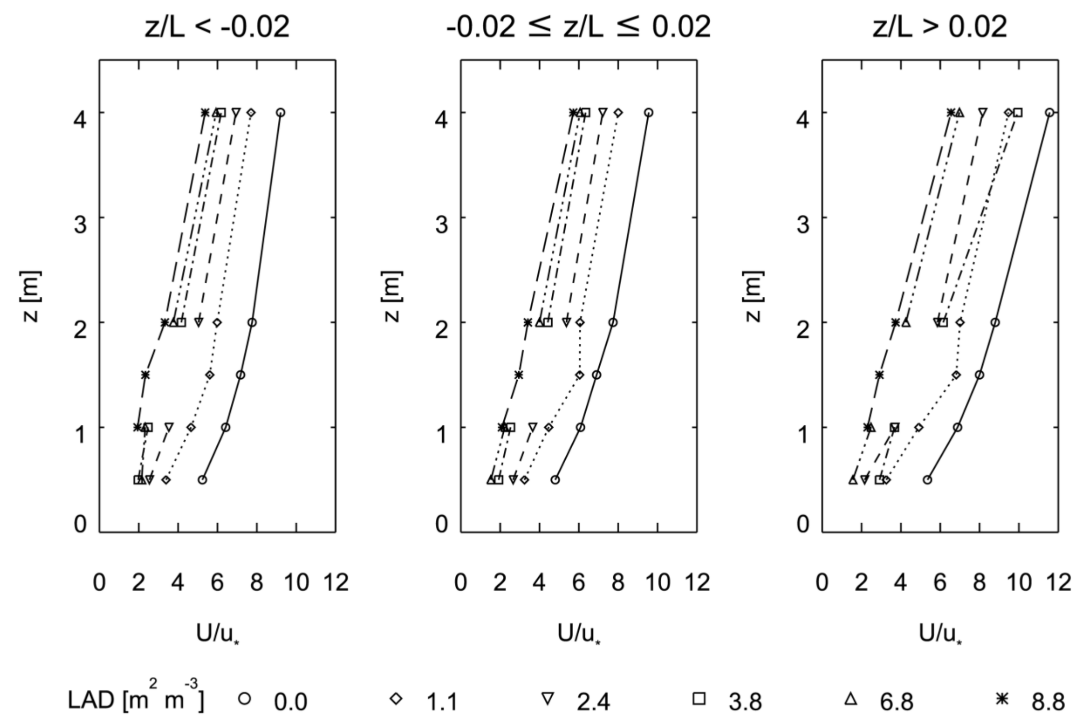

The characteristic inflection point at canopy top in the mean horizontal velocity profile was not clearly detectable in our results (Fig. 5), except for the last period in unstable conditions. Probably, this was partially due to lack of a measurement level just above the canopy, which would have allowed a more clear shape of the curve, and to sparseness of the vineyard itself. What we would have expected is an inflection point shifting up during the growing season. Nevertheless, normalized mean wind velocity decreased at all heights during the growing season.

Normalized momentum flux profiles $\overline{u'w'}/u_*$ (Fig. 6a) showed the same patterns reported before, with decrease of momentum penetration within the canopy as foliage developed. However, in unstable and stable conditions an unexpected intensification within the canopy was present for the no–leaves period.

The correlation coefficient between horizontal and vertical velocity (r_{uw}) can be interpreted as the efficiency of momentum transport (Fig. 6b). In the empty canopy r_{uw} increased getting closer to the ground. However, when the first layer of foliage developed, the peak of transport efficiency shifted to this height (1 m) and it was greatly reduced in the trunk space. With further increase of LAD in the bottom layer and with development of upper canopy, the momentum transport efficiency decreased at 1 m and the peak moved to 2 m (neutral) or 1.5 m (unstable and stable). The magnitude of r_{uw} was greater in near–neutral conditions, being around 0.3 above canopy and 0.4 as maximum value within the canopy in the upper layer of denser foliage. In unstable and stable conditions momentum transport efficiency was lower, with values around 0.25 above canopy and maximum of 0.35 within the canopy.

The normalized standard deviations of vertical (σ_w/u_*) and horizontal (σ_u/u_*) wind velocity were both attenuated by foliage development (Fig. 7). However, the effect of LAD was more pronounced on σ_u, with σ_u/u_* around 2.5 above canopy and 1.8 in the trunk space without leaves, decreasing to 1.2 at fully developed canopy. On the contrary, σ_w slightly decreased in unstable and stable conditions but it did not change much under neutral stability: it was about 1.2 above canopy and 0.7 in the trunk space for all periods. Nevertheless, the diabatic effect was similar on both standard deviations, with smaller and higher values in near–neutral and unstable conditions respectively. Results for stable stratification were placed in between, but considerably higher standard deviations were observed for the canopy without leaves in stable conditions.

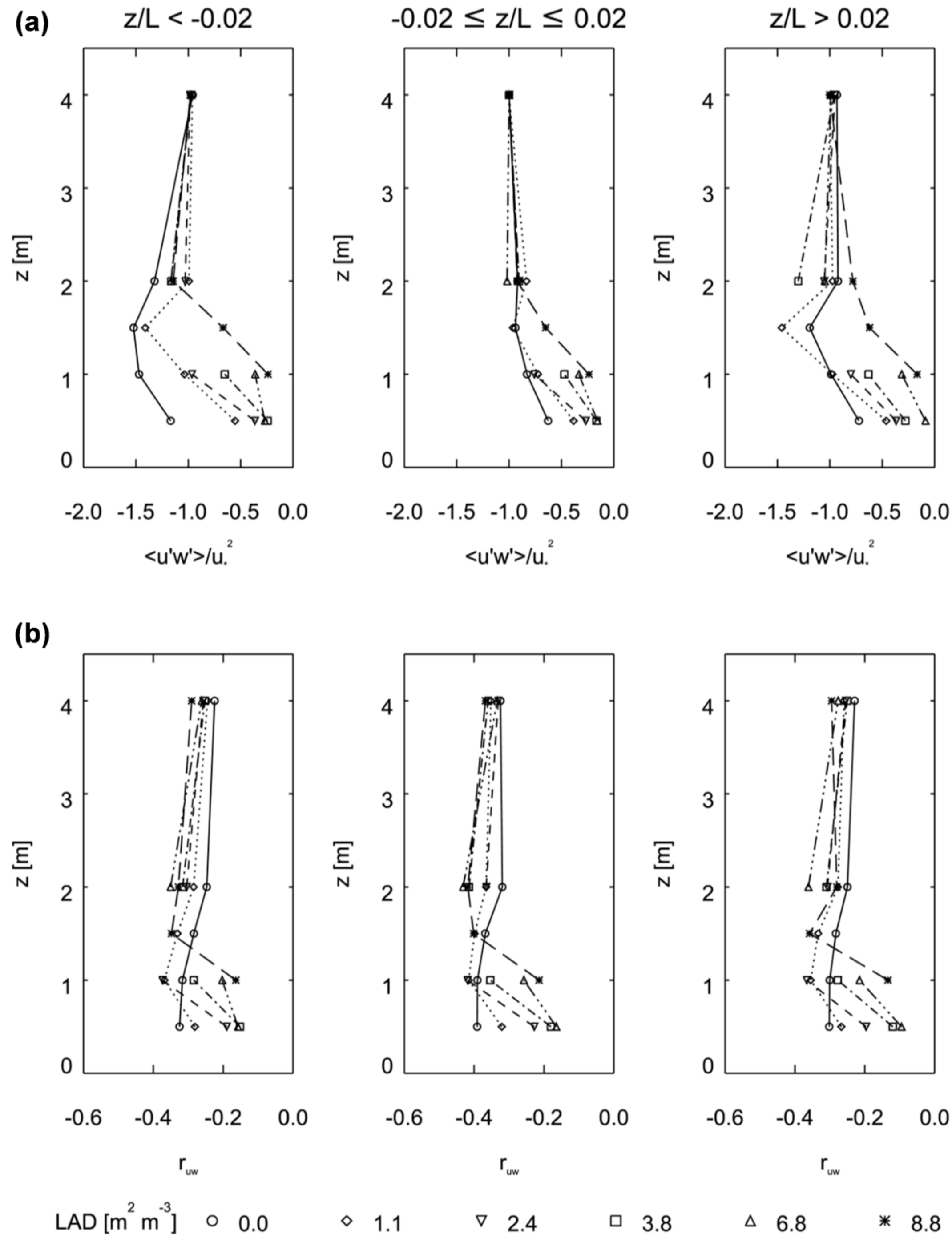

Fig. 6 Vertical profiles of normalized momentum flux (a) and correlation coefficient of horizontal and vertical velocity (b) for different stability conditions and LAD periods.

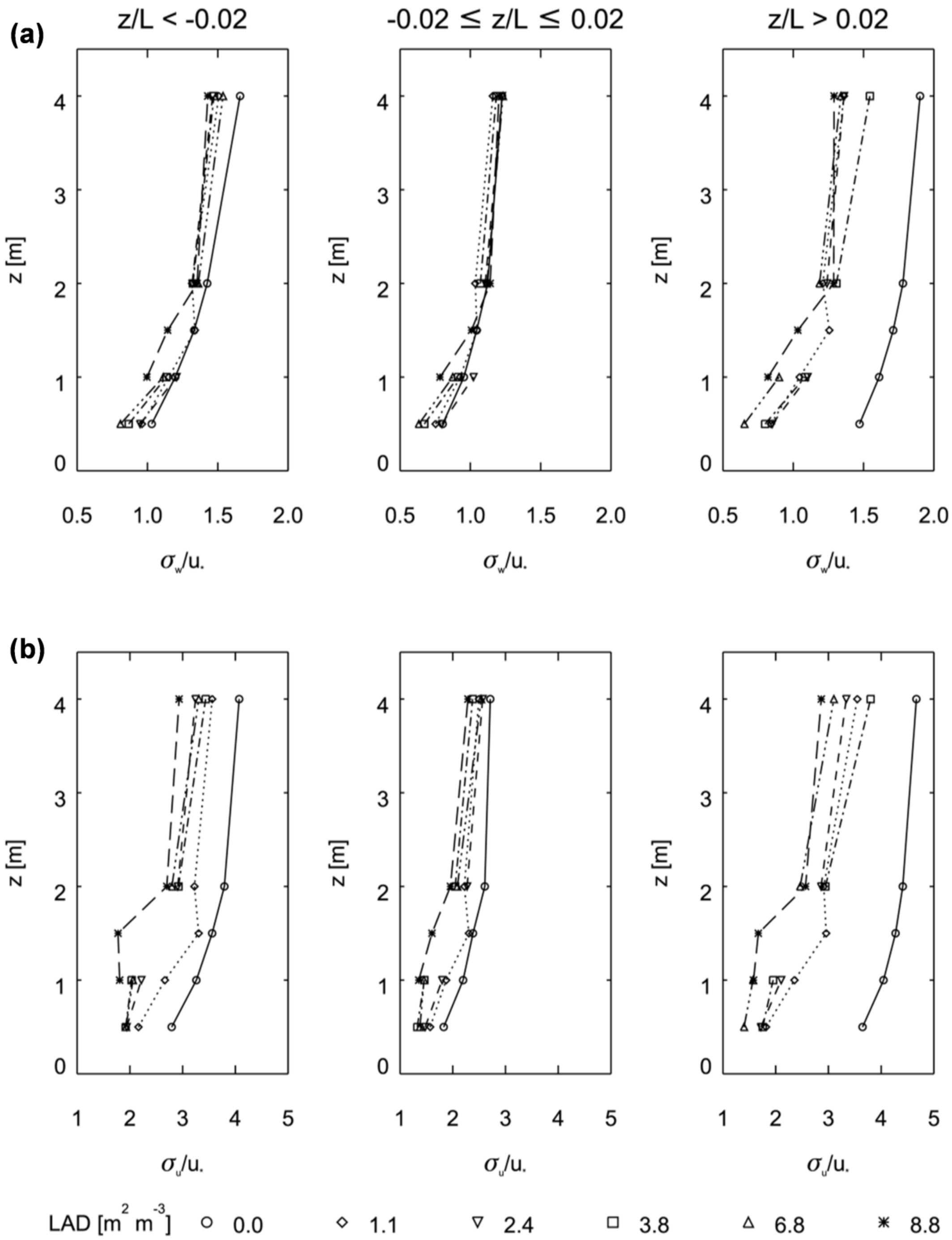

Fig. 7 Vertical profiles of normalized *w* standard deviation σ_w/u_* (a) and *u* standard deviation σ_u/u_* (b) for different stability conditions and LAD periods.

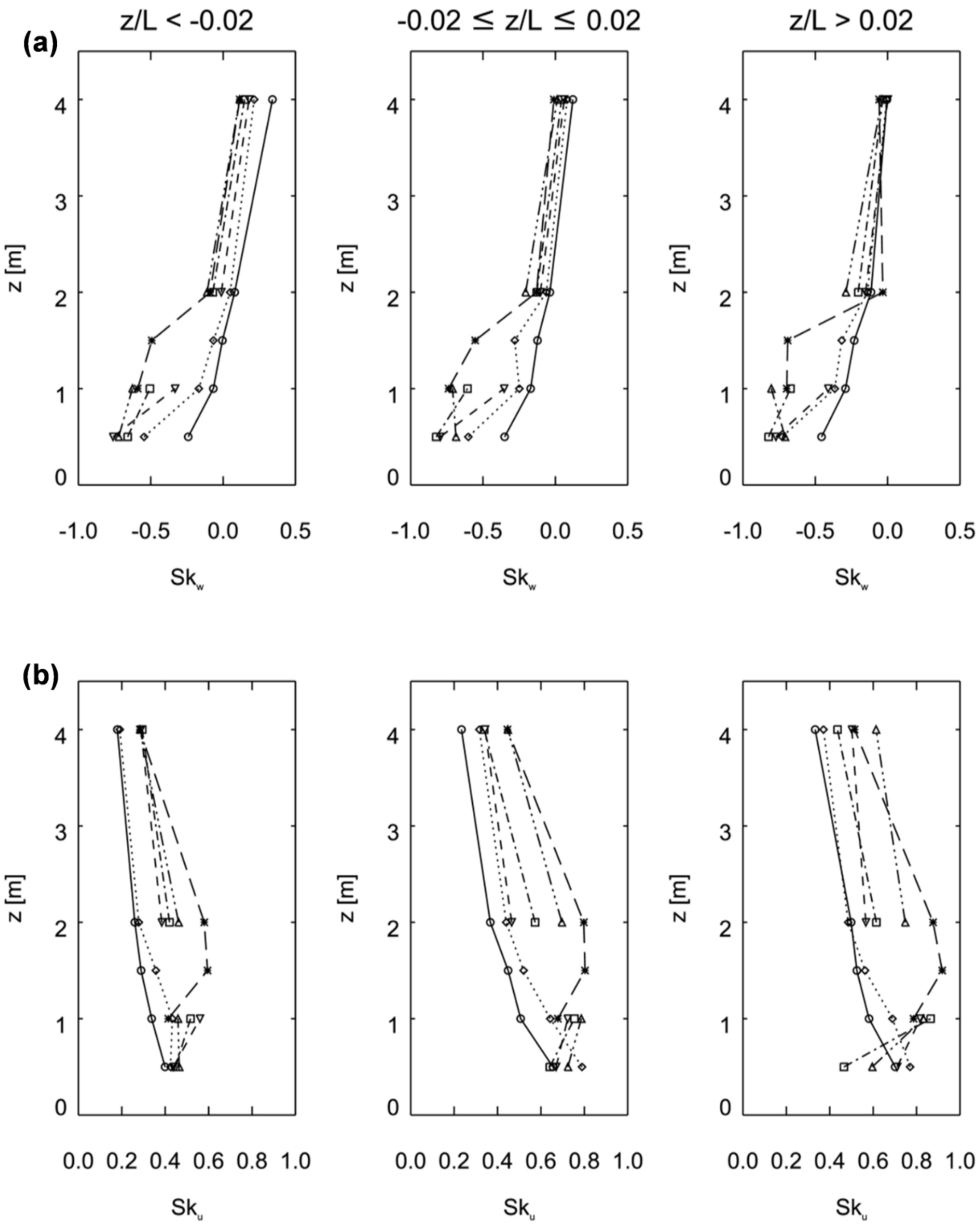

Fig. 8 Vertical profiles of *w* skewness Sk_w (a) and *u* skewness Sk_u (b) for different stability conditions and LAD periods.

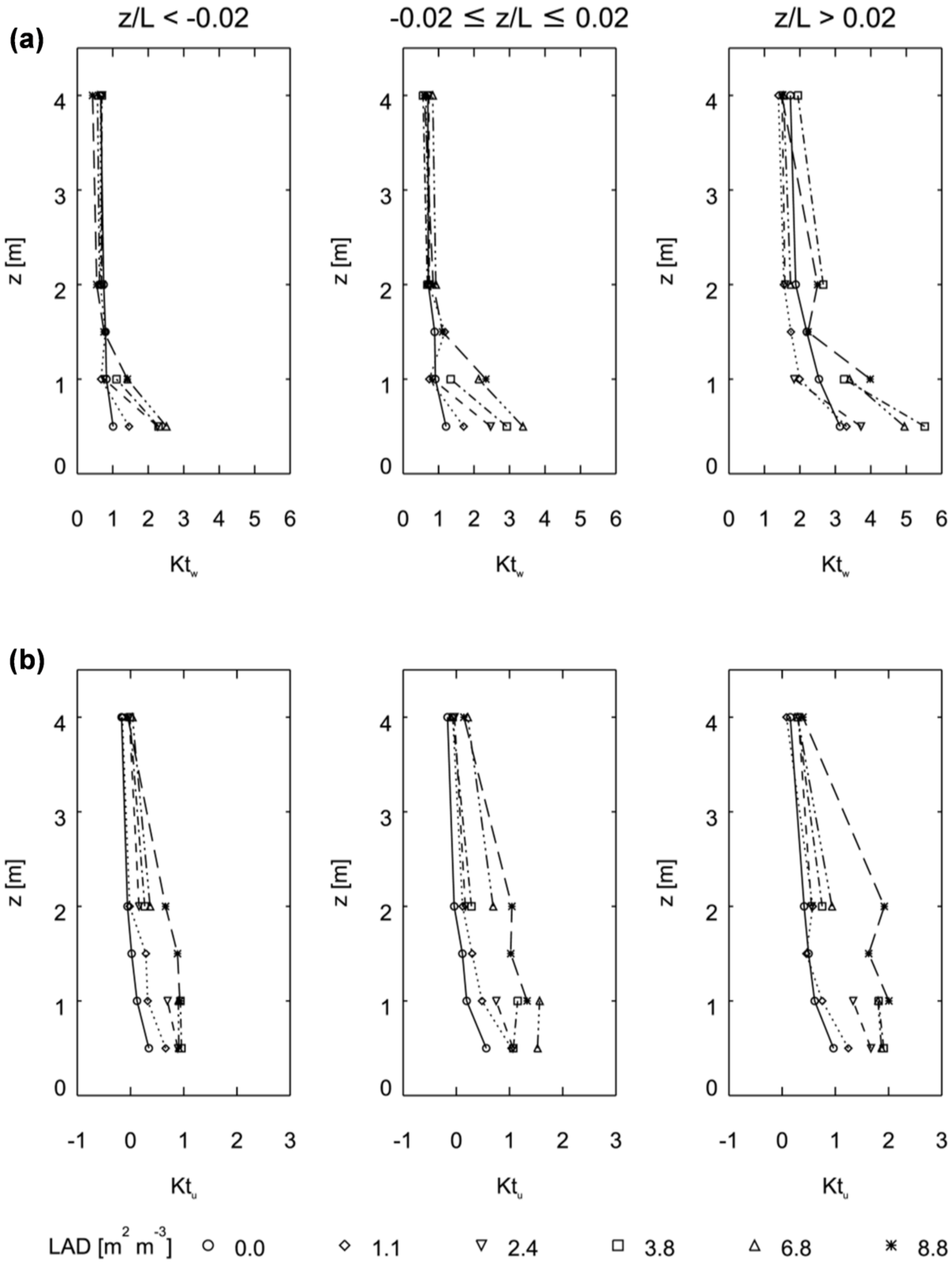

Fig. 9 Vertical profiles of *w* kurtosis Kt_w (a) and *u* kurtosis Kt_u (b) for different stability conditions and LAD periods.

The skewness is a useful statistics to evaluate the importance of intermittent but strong events in the transport of momentum. Within–canopy *w* skewness (Sk_w) was negative in all stability conditions and LAD periods, meaning that transport in this region was governed by downward strong events (Fig. 8a). On the contrary, above canopy Sk_w was close to zero in neutral and stable conditions, indicating same contribution by strong upward and downward events, whereas it was positive in unstable stratification, meaning stronger intermittent upward events. The magnitude of Sk_w progressively increased with LAD within the canopy, whereas in the trunk space it strongly augmented after first foliage development and then remained stable. On the contrary, it did not change at canopy top and above throughout the growing season.

Horizontal velocity skewness (Sk_u) is normally of opposite sign compared to Sk_w, due to the fact that momentum is progressively absorbed by vegetation drag elements getting closer to the ground and therefore the overall flux is downward. Indeed, Sk_u was always positive at all heights, but greater values were noted within the canopy compared to above (Fig. 8b). It increased with LAD within the canopy where foliage was present and at canopy top, whereas in the trunk space it did not change much along the season. Moreover, Sk_u magnitude was generally lower in unstable conditions. The combination of Sk_w and Sk_u indicated that within–canopy momentum flux was dominated by intermittent downward transport of faster air from above, with this feature becoming more accentuated with increasing foliage density.

The degree of transport intermittency can be derived from the kurtosis of *u* (Kt_u) and *w* (Kt_w) (Fig. 9). In our results kurtosis values have been subtracted by 3, so that a Gaussian distribution is characterized by zero kurtosis. Kt_w showed different patterns as LAD increased compared to Sk_w. The degree of intermittency along with foliage development was intensified only in the trunk space and lower canopy, while considerable higher values were found in stable conditions. On the other hand, Kt_u increased with LAD at all heights within the canopy and the effect of stability was similar to Kt_w, showing on average higher intermittency.

4 Discussion

Turbulent flow in a hedgerow vineyard showed to be highly influenced by canopy architecture. We were able to detect the effects of gradual vertical development of foliage density on turbulence statistics at different levels within the canopy.

The coupling between vineyard and the overlying atmosphere linearly increased with LAD. The drag coefficient was low for the empty canopy but, at maximum development, it reached values similar to those previously reported by other studies at forest sites (Cescatti and Marcolla, 2004; Shaw et al., 1988; Su et al., 2008). Shaw et al. (1988) did not found significant differences in the foliated and defoliated forest, however our results are in agreement with Su et al. (2008) which reported higher drag coefficient for the foliated forest. The same studies also showed that stable stratification has great influence on atmospheric coupling, considerably decreasing the drag coefficient. At our site this was not confirmed, since C_D was similar in neutral and stable conditions. However, we found that C_D was larger under unstable conditions, as also reported by Su et al. (2008), and the difference was more marked in the presence of foliage. A possible explanation is that convective motion enhances vertical mixing through formation of thermal plumes and this feature may be accentuated during the foliated period as the air within the canopy is warmed up during daytime by heat released from foliage or soil surface.

The increase of efficiency in absorbing momentum at canopy top was associated with a decrease of momentum penetration within the canopy, as it could be expected. Additionally, the vertical stress fraction distribution was strongly affected by vertical shape of the canopy. We showed that just the presence of few leaves in the bottom layer was sufficient to greatly reduce momentum in the trunk space, despite of low canopy density. Furthermore, when foliage entirely developed, the normalized momentum flux was close to zero already at 1 m, indicating that roughly all horizontal momentum was absorbed by leaves in the upper layer (1 – 2 m). This is in agreement with results from taller and denser canopies, showing momentum close to zero at $0.5h$ (Finnigan, 2000). The stability effects on momentum penetration in the canopy were not significant; however an unexpected increase of stress within the empty canopy in unstable conditions has been detected.

Statistics profiles confirmed the hypothesis that turbulent transport within the canopy was shifting from a rough–wall boundary layer flow in the empty canopy to a more characteristic canopy flow in the presence of foliage. In near–neutral conditions the correlation coefficient r_{uw} at canopy top without leaves was equal to the typical surface layer value of –0.32 (Garratt, 1992), whereas at the end of the growing season it increased in magnitude to –0.41, which is lower than the average canopy top value (–0.5) reported by Finnigan (2000). The same behavior was found for the corresponding values of normalized standard deviations at canopy top: $\sigma_w/u_* = 1.12$ and $\sigma_u/u_* = 2.6$ without leaves, which are similar to surface layer values of 1.25 and 2.5 respectively. For the fully–developed canopy $\sigma_w/u_* = 1.15$ and $\sigma_u/u_* = 2.0$, the latter being equal to the characteristic canopy flow value, while the vertical component being higher than the typical value of 1.0. Comparable results have been reported by Miller et al. (2015) in a foliated vineyard of similar architecture. Thus, turbulent transport in the vineyard seemed to have similar characteristics to those of denser and more homogenous canopies, even if the efficiency of momentum transport was lower. This result together with no clear presence of an inflection point may indicate that the drag exerted by vineyard rows was not sufficient to develop a well–defined turbulent mixing layer at canopy top. However, vertical and horizontal velocity skewness indicated that momentum transport within the canopy was dominated by intermittent sweeps characteristic of canopy turbulence. We suggest that a weak inflection point may have developed at a lower height than canopy top, with this level being between 0.75h and h (1.5 and 2 m). The presence of a weak inflection point at canopy top is in agreement with the results by Pietri et al. (2009) and Bailey and Stoll (2013)for low canopy density.

Without leaves the efficiency of momentum transport increased approaching the soil surface, while, in the presence of leaves, the peak shifted to the highest layer with denser foliage. r_{uw} was greatly reduced in the trunk space after development of the first layer of leaves (1 m) and, on the contrary, at this height the transport showed to be very efficient. Later in the season, with growth of the upper level, the 1 m layer was experiencing the same strong reduction in transport efficiency as the trunk space before. A more pronounced decrease of r_{uw} with increasing depth in the presence of foliage is in agreement with previous studies (Shaw et al., 1988; Su et al., 2008).

Unexpectedly, the magnitude of σ_w/u_* did not change much over the season while σ_u/u_* decreased with foliage development. Also Shaw et al. (1988) did not found any influence of foliage density on vertical velocity fluctuations, however they reported that standard deviation of horizontal component increased in the foliated forest. On the contrary, Su et al. (2008) found a pattern similar to our results, with lower σ_u in the presence of leaves. Additionally, we showed that horizontal velocity fluctuations in the lower foliage layer (1 m) were well correlated with LAD, decreasing when leaves came out at this height and further reducing after development of the upper layers. In unstable conditions the magnitude of both standard deviations was greater at all levels, whereas in stable stratification the values in the bottom canopy were similar to neutral conditions and greater in the upper canopy. However, during stable periods the efficiency of momentum transport was low, meaning that turbulent motions were still present but inactive in transporting momentum (Finnigan, 2000; Launiainen et al., 2007).

The skewness of *u* and *w* showed to increase in magnitude along the growing season within the canopy. This can be explained by reduced wind speed due to the presence of foliage, that contributes to create larger skewness (Leclerc et al., 1991). Furthermore, the skewness showed opposite sign (Sk_w negative and Sk_u positive), indicating that canopy transport was more and more dominated by strong downward transport of higher wind velocity (sweeps), a characteristic feature of canopy flow (Raupach et al., 1996). Nevertheless, horizontal and vertical skewness showed opposite vertical patterns with increasing LAD. The largest increase of Sk_u was at canopy top and it did not change in the trunk space. On the contrary, Sk_w increased in the bottom canopy and remained unvaried at canopy top with lower values. In the upper layers of the foliated vineyard, Sk_u was at its largest value, about 0.8 in neutral conditions, which is in line with previous studies (Baldocchi and Meyers, 1988; Launiainen et al., 2007; Leclerc et al., 1991; Villani et al., 2003). Sk_w peaked in the lower layers being around –0.8, in agreement with results reported by Baldocchi and Meyers (1988), Leclerc et al. (1991) and Villani et al. (2003), but differing from the decrease found in the trunk space of forest and orchard by other studies (Baldocchi and Hutchison, 1987; Dupont and Patton, 2012; Launiainen et al., 2007). The increase of Sk_w getting closer to the ground and with foliage development could be explained by the fact that only progressively stronger eddies can penetrate deeply into the foliated canopy. However, these coherent structures transported increasingly higher horizontal wind velocity compared to local mean wind only in the upper canopy. At canopy bottom it remained unvaried, probably because at this height consistently higher wind velocity was transported from above also without leaves due to proximity with the surface.

A missing peak of Sk_w at canopy top could indicate that coherent structures may penetrate deeper due to sparseness of the canopy (Bailey and Stoll, 2013; Dupont and Patton, 2012). This is confirmed by the increase of Kt_w only in the bottom canopy in the presence of foliage, indicating that vertical transport was less intermittent at canopy top and the effect of LAD was absent. However, foliage development influenced the intermittency of horizontal component, with more intermittent events along the whole profile in the presence of leaves. In general, Kt_w and Kt_u at our site showed lower values compared to experiments in denser canopies such as forests (Launiainen et al., 2007). This is in agreement with the increasing kurtosis values reported by Poggi et al. (2004) for denser canopies.

Stability conditions had different effects on skewness and kurtosis. During unstable conditions Sk_u was lower at all heights, due to increasing importance of buoyancy (Dupont and Patton, 2012) and above canopy Sk_w showed positive values, meaning that upward motions were prevailing in this layer. On the contrary, only stable stratification had a considerable effect on the kurtosis, with increased transport intermittency.

The effect of stability on turbulence statistics profile was lower compared to that of morphological changes in our vineyard. This is in agreement with results by Su et al. (2008) in the canopy crown layer of the forest, where LAD is high, but contrary to what reported by Leclerc et al. (1990) and Shaw et al. (1988) in a deciduous forest. The vineyard addresses considerable structural changes during the growing season, with foliage growth changing both height and density of the canopy, but, at the same time, vineyard is a relatively short and open canopy. Thus, diabatic effects may be less pronounced than in tall canopies because coherent structures can penetrate deeper and, consequently, weaker temperature gradients develop within the canopy.

5 Conclusions

Turbulence characteristics showed to be highly influenced by seasonal evolution of canopy foliage. Without leaves, turbulent regime was more similar to a rough–wall boundary layer flow, whereas at full foliage development it shifted to characteristics of a typical canopy flow, even if with a weak inflection point at canopy top due to sparseness of the vineyard. The overall effect of canopy morphology on within–canopy turbulence was in agreement with previous studies (Dupont and Patton, 2012; Shaw et al., 1988; Su et al., 2008). In addition, we were able to correlate turbulence profile with vertical foliage development, showing how flow characteristics within the canopy are connected with local and total foliage density during the growing season. We showed that the denser upper layer of foliage played a central role in absorbing momentum; therefore the local characteristics of turbulence at one level experience large changes between different stages of foliage development. For this reason, within–canopy microclimate conditions may be very different depending on the stage of the growing season.

6 References

Amiro, B.D., 1990. Comparison of turbulence statistics within three boreal forest canopies. Boundary-Layer Meteorol. 51, 99–121.

Aubinet, M., Feigenwinter, C., Heinesch, B., Laffineu, Q., Papale, D., Reichstein, M., Rinne, J., Van Gorsel, E., 2012. Eddy Covariance Chapter 5 Nighttime Flux Correction, in: Aubinet, M., Vesala, T., Papale, D. (Eds.), Eddy Covariance - A Practical Guide to Measurement and Data Analysis. Springer Netherlands, Dordrecht, pp. 133–157.

Bailey, B.N., Stoll, R., 2013. Turbulence in Sparse, Organized Vegetative Canopies: A Large-Eddy Simulation Study. Boundary-Layer Meteorol. 147, 369–400.

Baldocchi, D., 2014. Measuring fluxes of trace gases and energy between ecosystems and the atmosphere - the state and future of the eddy covariance method. Glob. Chang. Biol. 20, 3600–3609.

Baldocchi, D., Hutchison, B., 1987. Turbulence in an almond orchard: Vertical variations in turbulent statistics. Boundary-Layer Meteorol. 40, 127–146.

Baldocchi, D.D., Meyers, T.P., 1988. Turbulence structure in a deciduous forest. Boundary-Layer Meteorol. 43, 345–364.

Cescatti, A., Marcolla, B., 2004. Drag coefficient and turbulence intensity in conifer canopies. Agric. For. Meteorol. 121, 197–206.

Chahine, A., Dupont, S., Sinfort, C., Brunet, Y., 2014. Wind-Flow Dynamics Over a Vineyard. Boundary-Layer Meteorol. 151, 557–577.

Denmead, O.T., Bradley, E.F., 1987. On Scalar Transport in Plant Canopies. Irrig. Sci. 8, 131–149.

Dupont, S., Brunet, Y., 2008. Influence of foliar density profile on canopy flow: A large-eddy simulation study. Agric. For. Meteorol. 148, 976–990.

Dupont, S., Patton, E.G., 2012. Influence of stability and seasonal canopy changes on micrometeorology within and above an orchard canopy: The CHATS experiment. Agric. For. Meteorol. 157, 11–29.

Finnigan, J., 2000. Turbulence in plant canopies. Annu. Rev. Fluid Mech. 32, 519–571.

Finnigan, J., Raupach, M., 1987. Transfer processes in plant canopies in relation to stomatal characteristics. Stomatal Funct.

Francone, C., Katul, G.G., Cassardo, C., Richiardone, R., 2012. Turbulent transport efficiency and the ejection-sweep motion for momentum and heat on sloping terrain covered with vineyards. Agric. For. Meteorol. 162–163, 98–107.

Garratt, J.R., 1992. The Atmospheric Boundary Layer. Cambridge University Press.

Hicks, B.B., 1973. Eddy fluxes over a vineyard. Agric. Meteorol. 12, 203–215.

Hunter, J.J., Volschenk, C.G., Zorer, R., 2016. Vineyard row orientation of Vitis vinifera L. cv. Shiraz/101-14 Mgt: Climatic profiles and vine physiological status. Agric. For. Meteorol. 228–229, 104–119.

Launiainen, S., Vesala, T., Mölder, M., Mammarella, I., Smolander, S., Rannik, Ü., Kolari, P., Hari, P., Lindroth, A., Katul, G.G., 2007. Vertical variability and effect of stability on turbulence characteristics down to the floor of a pine forest. Tellus, Ser. B Chem.

Phys. Meteorol. 59, 919–936.

Leclerc, M.Y., Beissner, K.C., Shaw, R.H., Den Hartog, G., Neumann, H.H., 1991. The influence of buoyancy on third-order turbulent velocity statistics within a deciduous forest. Boundary-Layer Meteorol. 55, 109–123.

Leclerc, M.Y., Beissner, K.C., Shaw, R.H., Hartog, G. Den, Neumann, H.H., 1990. The influence of atmospheric stability on the budgets of the reynolds stress and turbulent kinetic energy within and above a deciduous forest. J. Appl. Meteorol. 29, 916–933.

Miller, N.E., Stoll, R., Mahaffee, W.F., Neill, T.M., Pardyjak, E.R., 2015. An experimental study of momentum and heavy particle transport in a trellised agricultural canopy. Agric. For. Meteorol. 211–212, 100–114.

Patton, E.G., Finnigan, J.J., 2013. Canopy Turbulence, in: Harindra, J.S.F. (Ed.), Handbook of Environmental Fluid Dynamics, Volume One. CRC Press/Taylor & Francis Group, LLC, pp. 311–328.

Pietri, L., Petroff, A., Amielh, M., Anselmet, F., 2009. Turbulence characteristics within sparse and dense canopies. Environ. Fluid Mech. 9, 297–320.

Poggi, D., Porporato, A., Ridolfi, L., Albertson, J.D., Katul, G.G., 2004. The effect of vegetation density on canopy sub-layer turbulence. Boundary-Layer Meteorol. 111, 565–587.

Raupach, M.R., Finnigan, J.J., Brunet, Y., 1996. Coherent eddies and turbulence in vegetation canopies: The mixing-layer analogy. Boundary-Layer Meteorol. 78, 351–382.

Shaw, R.H., Den Hartog, G., Neumann, H.H., 1988. Influence of foliar density and thermal stability on profiles of Reynolds stress and turbulence intensity in a deciduous forest. Boundary-Layer Meteorol. 45, 391–409.

Su, H.B., Schmid, H.P., Vogel, C.S., Curtis, P.S., 2008. Effects of canopy morphology and thermal stability on mean flow and turbulence statistics observed inside a mixed hardwood forest. Agric. For. Meteorol. 148, 862–882.

Villani, M.G., Schmid, H.P., Su, H.B., Hutton, J.L., Vogel, C.S., 2003. Turbulence statistics measurements in a northern hardwood forest. Boundary-Layer Meteorol. 108, 343–364.

Weiss, A., Allen, L.H., 1976. Vertical and horizontal air flow above rows of a vineyard. Agric. Meteorol. 17, 433–452.

Chapter IV:

Organized turbulent motions in a hedgerow vineyard: effect of evolving canopy structure

1 Introduction

Vegetation–atmosphere exchanges are determined by functional and structural properties of the plants together with environmental forcing (e.g. incoming radiation, temperature, humidity, etc.). However, a fundamental aspect is the interaction of the canopy with the lower atmosphere. The vegetation deeply alters the composition and physical properties of the air flow, exchanging energy and matter with it. These processes take place in the bottom part of the turbulent boundary layer. Therefore, turbulence is the main mechanism by which within–canopy air is transported towards upper atmospheric layers and vice versa. Turbulent flow is highly efficient in mixing the air above canopy, reducing vertical gradients. The region where the atmosphere is in equilibrium with the underlying surface and fluxes changes by less than 10% of their magnitude with height is called the *surface layer* (SL) (Stull, 1988). This layer usually extends from two times the canopy height to tens of meters above it. Here, the vertical shape of average horizontal wind speed is approximately logarithmic. Conversely, the portion of atmosphere below the surface layer is highly influenced by roughness elements and it is called the *roughness sublayer* (RSL). Below this layer, we can make a further distinction for the space actually occupied by plants, the *canopy sublayer* (CSL).

The mean velocity profile is strongly altered in the RSL, deviating from the logarithmic shape of the SL and showing a characteristic inflection point around the height of the roughness elements. At this point the drag exerted on the flow by canopy elements is very high and wind shear is maximal. The presence of the inflection point suggests the analogy of RSL turbulent motion with that occurring in a plane mixing layer (Raupach et al., 1996). The plane mixing layer is characteristic of the region where two flows of different velocities interact. As we already said, it is characterized by an inflection point in the mean velocity profile that generates hydrodynamic instability processes, which ultimately determine the formation of coherent eddies at canopy top (Finnigan, 2000). The character of the inflection point is controlled by large boundary layer eddies which break down into coherent structures of the size of canopy height (sparse canopies) or smaller (dense canopies) (Raupach et al., 1996). However, the actual interaction between the air flow and vegetation can be understood only by considering the fine–scale structure of canopy turbulence.

Previous studies were able to identify the energy containing coherent structures governing the transport of momentum in turbulent boundary layers over flat surfaces (Robinson, 1991), artificial (Raupach, 1981) and natural canopies (Baldocchi and Hutchison, 1987; Finnigan, 1979; Gao et al., 1989; Shaw et al., 1983). It was observed that turbulent transport of momentum and heat is far from being purely random, being on the contrary organized in low frequency coherent movement of the air, which are well distinguishable from high frequency random turbulence. Coherent structures consist of a sharp downward transport of higher velocity air from above (sweep or gust) and a following slow upward motion of lower velocity air from below (ejection or burst).

Several methods have been applied to identify these structures in turbulence time series, which are usually collected at a single fixed point in space. Conditional sampling techniques allow the separation of the time series into different types of events, basing on the occurrence of a particular pattern in the data. Regarding horizontal momentum flux, quadrant–hole analysis (Antonia, 1981; Lu and Willmarth, 1973) defines four quadrants based on the sign combinations of horizontal (u) and vertical (w) wind velocity. It allows the separation of the time series into four categories of events and, applying an additional threshold for momentum magnitude, the quantification of strong event contributions to overall flux. This method has been applied over several types of real canopies: crops (Finnigan, 1979; Shaw et al., 1983), orchards (Baldocchi and Hutchison, 1987) and forests (Baldocchi and Meyers, 1988; Katul et al., 1997).

Another method was proposed by Gao et al. (1989) using scalar (temperature and humidity) time series to identify coherent structures. They observed the recurrence of ramp patterns in the time series at several heights within and above canopy. The ramps were formed by a gradual rise of temperature terminated by a sharp drop and they associated this pattern with the occurrence of coherent structures. These studies leaded to characterization of momentum transport over different canopies, showing similar patterns in most vegetation types (Finnigan, 2000). Turbulent motion at vegetation–atmosphere interface is governed by intermittent large sweeps; while, moving away from the surface, sweep and ejection contribution become similar.

Coherent structures above and within canopies exist over a wide range of scales, from large boundary layer eddies to small scale within–canopy turbulence. Therefore, in order to better characterize turbulent transport, several studies attempted to investigate the spatial and temporal scales involved in the process (Brunet and Irvine, 2000; Hogstrom et al., 1996; Paw U et al., 1992; Raupach, 1981; Wang et al., 1992). Among different techniques applied (e.g. visual detection, space–time correlation function, etc.), wavelet analysis has been more frequently used because it offers an automatic method of ramp identification in the frequency and time domains of a time series (Collineau and Brunet, 1993; Thomas and Foken, 2005). The wavelet transform method has been implemented in most of the recent studies over vegetation canopies, which have been primarily conducted in forests (Eder et al., 2013; Thomas and Foken, 2007) and reported time scales of several tens of seconds.

Wavelets are able to match the shape of the ramps, successfully isolating coherent structures from random turbulence. However, this method does not include small scale turbulent transport, since a lower threshold limit has to be selected before the analysis. The choice of the appropriate smaller temporal scale is critical in order to exclude the minimum part of the flux from the analysis. Furthermore, wavelets showed to have problems in separating coherent structures that immediately follow each other, and to overestimate the number of coherent events during quiescent periods (Barthlott et al., 2007). Nevertheless, wavelet analysis is still a valuable method because it permits the individuation of the whole coherent structure, ejection and sweep portions together.

In the present work we propose a new technique for the evaluation of temporal scales, based on identification of events by quadrant analysis (section 2.4.3). In order to eliminate background noise by random turbulence and to identify coherent motions, we applied a low–pass filter on the time series (like previous wavelet analysis studies (e.g. Thomas and Foken (2005))). However, our method permits to go back to the original time series to calculate the stress faction associated with the detected event and, therefore, including most of total momentum flux. Additionally, the method proposed is potentially able to identify both short and long events, since no low–threshold is applied, except for the block averaging interval (1 s in our case) that is anyway smaller than characteristic temporal scales found in previous studies. However, quadrant analysis does not permit to follow the temporal sequence of sweeps and ejections, precluding the individuation of whole coherent structures.

Given these general features of vegetation–atmosphere interaction, canopy shape influences the organization of turbulent transport. The size of coherent structures can be related to canopy height, with larger scales as the height of vegetation increases due to lower shear at canopy top (Paw U et al., 1992). However, most of recent turbulence profile experiments have been conducted in tall canopies, such as forests, while only few considered turbulence organization in short canopies. Among them, homogenous and dense crops like wheat and maize received more attention in the past (Finnigan, 1979; Shaw et al., 1983).

Canopy architecture and vertical distribution of foliage density can play a role on turbulence characteristics in the CSL. However, only few studies investigated the influence of different canopy structures on turbulent flow organization (Bailey and Stoll, 2013; Dupont and Brunet, 2008; Huang et al., 2009; Poggi et al., 2004). They reported that as foliage density increases the characteristic inflection point at canopy top is better defined and steeper, leading to an organization of turbulence more similar to a plane mixing layer. However, most of this kind of studies were conducted in artificial canopies or using modelling simulations, while only few investigated the influence of seasonal changes in real canopy structure on turbulent motions (Dupont and Patton, 2012).

Focusing on seasonal change effects, a canopy like vineyard offers a perfect subject of study. Indeed, vineyards are characterized by large changes in leaf area density (LAD) and canopy height within few months. Furthermore, it represents a special case among short canopies, being typically organized in well–defined rows. The distance between rows is normally on the order of canopy height, making it a relatively sparse canopy, but, at the same time, foliage in the rows is very dense exerting a considerable drag on the mean flow. Previous studies reported that organization of turbulent flow over vineyards is similar to homogenous canopies (Chahine et al., 2014; Francone et al., 2012; Weiss and Allen, 1976a). However, wind direction relative to row orientation may play a role modifying the degree of penetration of above–canopy structure into the CSL (Chahine et al., 2014).

These kinds of studies are fundamental to understand canopy ventilation regime, which can be linked to several practical application in vineyard management. For example, the analysis of within–canopy turbulent motions is very important to predict small particles dispersion, like fungal spores, and minimize infection studying the effect on leaf wetness duration. Furthermore, it could lead to improvement of spraying methods, which have high application frequency during the growing season with possible heavy environmental impact.

The aims of our study are to characterize the organization of turbulent transport within and above a hedgerow vineyard and to follow the continuous evolution of turbulent motions during the growing season, from bud break to fully developed canopy. Additionally, a new method to investigate time scales of coherent structures governing momentum transport is presented.

2 Methods

2.1 Site description and experimental setup

The experiment was conducted from April to July 2015 in a flat hedgerow–trained vineyard (*Vitis Vinifera*) cv *Sauvignon Blanc* located in the North East of Italy (45°44'25.80"N 12°45'1.40"E). The vineyard is planted in rows oriented 35–125 °N, spaced 2.2 m apart and 0.5 m width; the canopy trunk space is 0.7 m and the maximum trellis height is 2 m. We decided to take the trellis height as the nominal canopy height (h) and we monitored the development of the canopy through the season. Once the vines reached 2 m, the plants were mechanically pruned to maintain this maximum height.

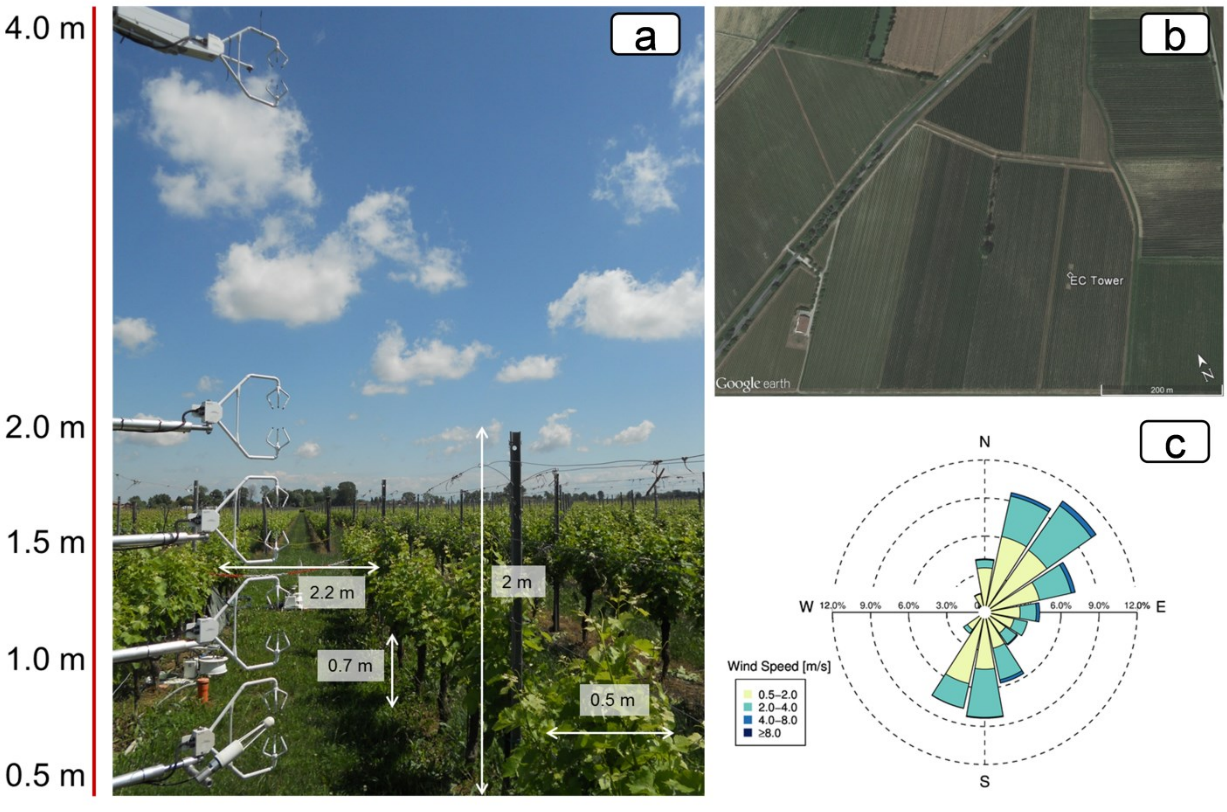

Fig. 1 Array of sonic anemometers on the 5 m tower and canopy characteristics (a), satellite image of the vineyard (b) and wind rose plot of the sonic at 4 m during the measurement period (c).

2.2 *Turbulence measurements*

A vertical profile of five Campbell Scientific sonic anemometers CSAT3 has been installed on a 5 m tower. The instrument heights were selected in order to detect the changes in turbulent flow characteristics due to vegetation growth. Four sonic anemometers have been deployed in the middle of inter–row within the canopy at 0.5 m (in the trunk space), 1 m, 1.5 m and 2 m; and one at 4 m ($2h$) as surface layer reference. The anemometers have been aligned on the vertical axis and pointed towards East.

High frequency observations of wind vector components and sonic temperature were synchronously digitally sampled at 20 Hz using a CR3000 Campbell Scientific datalogger for the four sonics in the canopy. The highest sonic was collected on a separate CR3000 datalogger as part of an eddy covariance system. The clocks of the dataloggers were synchronized using a server connection once a day at midnight. The raw data were stored in binary daily files and subdivided later in 30 minutes block files. Data processing was performed on this time interval.

2.3 *Characterization of canopy structure*

Canopy foliage and shape had been regularly monitored, ca. every 14 days, from bud break (30/04) to maximum foliage development (16/07) by optical and direct methods (Fig. 2). We assessed leaf area index (LAI) using Li-Cor LAI-2000 plant canopy analyzer. Measurements have been performed on diagonal transect in the inter–row, to better characterize the row structure of the canopy, and at several locations in the footprint area.

At the same time, direct measurements of LAI have been carried on five plants in the footprint area. The number of shoots per vine was counted and randomly selected shoots have been collected from left, center and right of the vine. During the experiment we used two different direct methods to obtain LAI. During the first month, we measured the width and length of each leaf with a ruler on selected shoots. Then, we calculated the leaf area from an empirical relation calibrated on the same vineyard. Once the canopy was more developed and the number of leaves became too large, we used a destructive sampling method, measuring leaf area directly. To better correlate canopy structure with turbulence data, the canopy crown has been subdivided into three layers (0.7–1.2 m, 1.2–1.7 m, 1.7–2 m) and LAI have been measured using direct methods for each layer.

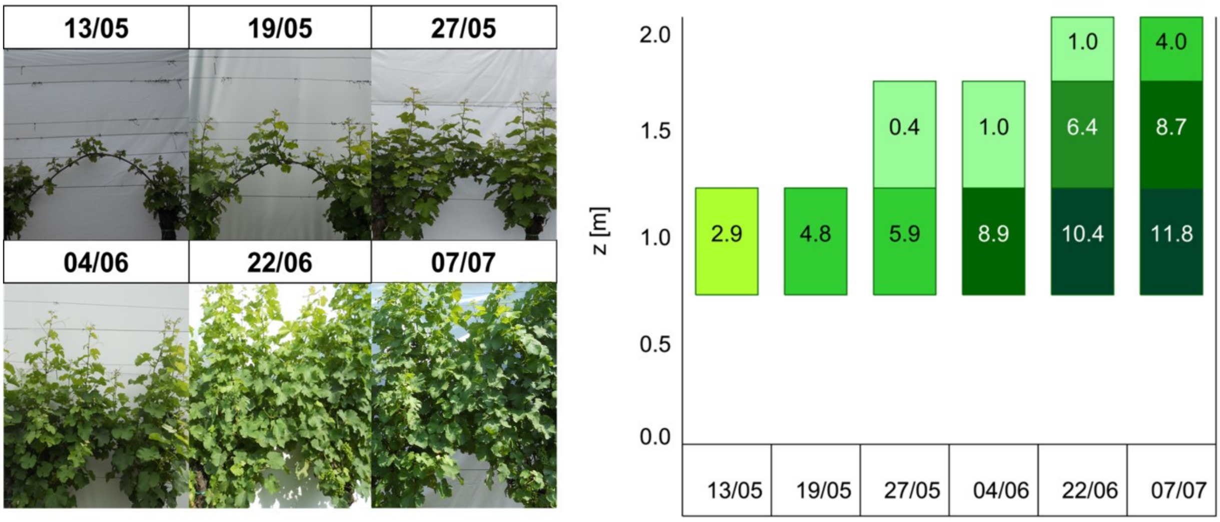

Fig. 2 Development of canopy foliage (left) and time course of Leaf Area Density [m^2 m^{-3}] for each canopy layer during the growing season (right).

In the context of turbulence characteristics analysis, a more appropriate parameter to characterize canopy structure is the leaf area density (LAD), the total leaf area in a reference volume [m^2 m^{-3}]. We calculated canopy average leaf area density as *LAD = LAI (row width) (canopy height)*, assuming a width of 0.5 m and height of 2 m (Table 3). LAD of each layer has been calculated using the height of the layer instead of canopy height (Fig. 2).

Optical and direct methods gave comparable results; thus we were confident using LAD measured with direct methods in the present work.

Table 4 Average leaf area density and canopy height during the growing season.

Sampling date	13/05	19/05	27/05	04/06	22/06	07/07
LAD [m^2 m^{-3}]	1.1	1.9	2.3	3.8	6.8	8.8
Canopy height [m]	1.0	1.2	1.3	1.5	1.9	2.0

2.4 ***Data analysis***

2.4.1 Data processing and period selection

The 20 Hz data of velocity components at each height were horizontally rotated to align mean horizontal wind to the streamlines, obtaining *u* horizontal, *v* longitudinal and *w* vertical wind velocities. For each sonic the local angle of rotation has been used. To skip disturbed flow conditions, periods with average wind direction coming from the tower (225 – 315 °N) have been discarded. Periods with rain or total number of sonic bad diagnostic flag greater than 1800 (90 sec) were not used for the analysis. Additionally, to ensure that the flow was in turbulent motion, 30–min periods with *u* or *w* standard deviations lower than 0.1 m s^{-1} were discarded. All the calculations have been performed using IDL scripts developed for the purpose.

We subdivided the dataset in seven periods of increasing LAD, starting from an "empty" canopy (LAD assumed zero) to a final LAD of 8.8 m^2 m^{-3}. Each period, of about 14 days, was associated with a LAD value measured in the middle of the period.

2.4.2 Quadrant analysis

To analyze the influence of canopy structural changes on the organization of motion, we performed a quadrant analysis (Lu and Willmarth, 1973) as described by Shaw et al. (1983). The products of the instantaneous fluctuations *u'* and *w'* (defined as $x' = x - \bar{x}$, where *x* is the instantaneous value and $\bar{x}$ is the average over the 30–min period) are separated in four quadrants according to the sign of velocity fluctuations. To each quadrant is associated a type of event: quadrant I (*q1*) *u'* > 0 and *w'* > 0, outward interactions; quadrant II (*q2*) *u'* < 0 and *w'* > 0, ejections; quadrant III (*q3*) *u'* < 0 and *w'* < 0, inward interactions; quadrant IV (*q4*) *u'* > 0 and *w'* < 0, sweeps. The events linked to downward momentum transport are sweeps and ejections, while outward and inward interactions transport momentum upward.

It is possible to isolate progressively stronger events defining an excluded region in the quadrants, the so called quadrant "hole", defined as

$$H = |u'w'| / \overline{|u'w'|} \quad (1)$$

A conditional sampling is then performed on high frequency data, the instantaneous values of *u'w'* are selected based on a conditioning function $C_{i,H}$:

$$C_{i,H} = \begin{cases} 1, & \text{if the point lies in the i}^{\text{th}} \text{ quadrant and } |u'w'| \geq H\left|\overline{u'w'}\right| \\ 0, & \text{otherwise} \end{cases} \quad (2)$$

The quadrant stress fraction $S_{i,H}$ is then calculated as

$$S_{i,H} = \overline{u'w'}_{i,H} / \overline{u'w'} \quad (3)$$

Where the conditionally averaged stress is computed as

$$\overline{u'w'}_{i,H} = \frac{1}{T}\int_0^T u'w'(t)\, C_{i,H}(t)dt \quad (4)$$

It is also possible to calculate the time fraction $T_{i,H}$ occupied by events of each quadrant:

$$T_{i,H} = \frac{1}{T}\int_0^T C_{i,H}(t)dt. \quad (5)$$

The time fraction gives information about the total time in the period where sweeps, ejections or interactions were present. This is useful to generally describe the organization of motions, but it does not give any information on the characteristics, like duration, size and stress fraction of single events. We propose a more detailed analysis, based on the principle of quadrant analysis, to better characterize events governing the transport of momentum.

2.4.3 Quadrant event duration analysis

This section will give a description of the methodology applied to identify single event characteristics. First, horizontal axis rotation and filtering of high frequency data of velocity components has been applied, as described in section 2.2.1. Afterwards, 20 Hz time series have been reduced to 1 Hz resolution by applying standard block averaging. This procedure is necessary to eliminate high frequency noise, which would not allow the identification of organized structures due to frequent crossing of quadrants when *u'w'* is very small. We are confident that the application of this low–pass filter is not removing most of the signal from the time series, since we then go back to 20 Hz data to calculate stress fraction as described later. However, a 1 Hz block averaging reduced the 30–min overall momentum flux of about 15–25%. The selection of the averaging interval is critical because it sets the minimum event time scale detected (ex. 1 Hz block average set the minimum to 1 sec) and, at the same time, it influences the identification of large scale events.

After that, quadrant analysis has been applied to 1 Hz time series of *u'* and *w'*, identifying which contiguous points lay in the same quadrant by conditional sampling as described in section 2.4.2. For each quadrant and hole size a series of $u'w'_{i,H}$ has been identified. From that, an artificial series of 1800 points (1 Hz, 30 min) has been generated with the value of $C_{i,H}$ (0 or 1) previously calculated for each point. Every group of contiguous points with value of 1 represents one event of the quadrant. By counting the number of records in each group we then calculated the duration $De_{j,i,H}$ in seconds of the event

$$De_{j,i,H} = \frac{1}{sf} \sum_{k=0}^{n} C_{i,H} \tag{6}$$

where j is the number of events for the quadrant i^{th} and hole size H; sf is the sampling frequency (1 Hz); n is the number of points in the group j of contiguous records where $C_{i,H}$ = 1. Using the same method, it is also possible to obtain time intervals between the events. We created a mask time series $G_{i,H}$ of $C_{i,H}$ with

$$G_{i,H} = \begin{cases} 1, & \text{if } C_{i,H} = 0 \\ 0, & \text{if } C_{i,H} = 1 \end{cases} \tag{7}$$

and, from that, we calculated the time interval $Ie_{l,i,H}$ between events

$$Ie_{l,i,H} = \frac{1}{sf} \sum_{k=0}^{m} G_{i,H} \tag{8}$$

with l the number of event intervals in the quadrant i^{th} and hole size H; m the number of consecutive points in the group l where $G_{i,H} = 1$.

A this point, for each quadrant and hole size we have a series of durations $De_{i,H}$ and intervals $Ie_{i,H}$. The stress fraction $Se_{j,i,H}$ associated with each event duration was calculated going back to the original 20 Hz time series values:

$$Se_{j,i,H} = \overline{u'w'}_{j,i,H} / \overline{u'w'} \tag{9}$$

Each point in j corresponds to 20 records of the original time series, thus it is necessary to use high frequency *u'w'* to not miss information. We considered all 20 high frequency records, whether or not lying in the quadrant, as part of a single event.

The frequency distributions of $De_{i,H}$ and the associate stress fraction transported by each event gives detailed information on which size of events are more frequent and/or important for momentum transport. Additionally, statistical moments of durations and intervals can be computed.

We performed the latter analysis and the standard quadrant analysis for different heights and LAD periods, in order to better characterize the properties of above and within canopy turbulent flow.

3 Results

3.1 Quadrant analysis

In this section results for standard quadrant analysis will be presented. To understand the organization of turbulent flow it is interesting to look at the stress fraction transported in each quadrant. Events in *q2* are called ejections, in *q4* are called sweeps and *q1* and *q3* are outward and inward interactions respectively. The overall 30–min momentum flux $\overline{u'w'}$ is generally negative, transporting momentum towards ground. Sweeps and ejections have negative sign and, consequently, usually dominate the transport. Interactions in *q1* and *q3* have positive sign and act as counter gradient to momentum flux.

The ratio between the sum of stress fraction in *q1* and *q3* and the sum in *q2* and *q4* is called exuberance (Shaw et al., 1983). Fig. 3a shows the vertical profiles of average exuberance calculated for different stability conditions and canopy growing stages, characterized by increasing average LAD. For the near–neutral case without leaves, the ratio increased in magnitude with height from – 0.26 at 0.5 m to – 0.35 at 4 m. As foliage developed and became denser in the bottom layer (0.7–1.2 m), the exuberance of transport increased to – 0.62 in the trunk space. At 1 m, it also increased to – 0.51, but only when upper layers of foliage became denser. At 1.5 m, measurements at beginning and end of growing season showed a constant value of about – 0.25. Similarly, at canopy top the exuberance did not vary much during the season, slightly decreasing from – 0.36 to – 0.24. The unstable and stable cases showed similar patterns with evolving LAD; however the magnitude of exuberance was slightly larger in unstable conditions and much larger in stable conditions in the bottom layers with values around – 0.8. Even if the contribution by interactions increased with stability and LAD, the ratio remained negative in all conditions, meaning that on average sweeps and ejections were governing the transport of momentum.

To evaluate the relative contribution by sweeps and ejections, the ratio between $S_{4,0}$ and $S_{2,0}$ is presented in Fig. 3b. Above canopy, the ratio slightly increased during the growing season for near–neutral and stable conditions, from 1.0 to 1.3 and 1.3 to 1.6 respectively. Instead, in unstable conditions, the ratio was always rather constant being close to 1.0.

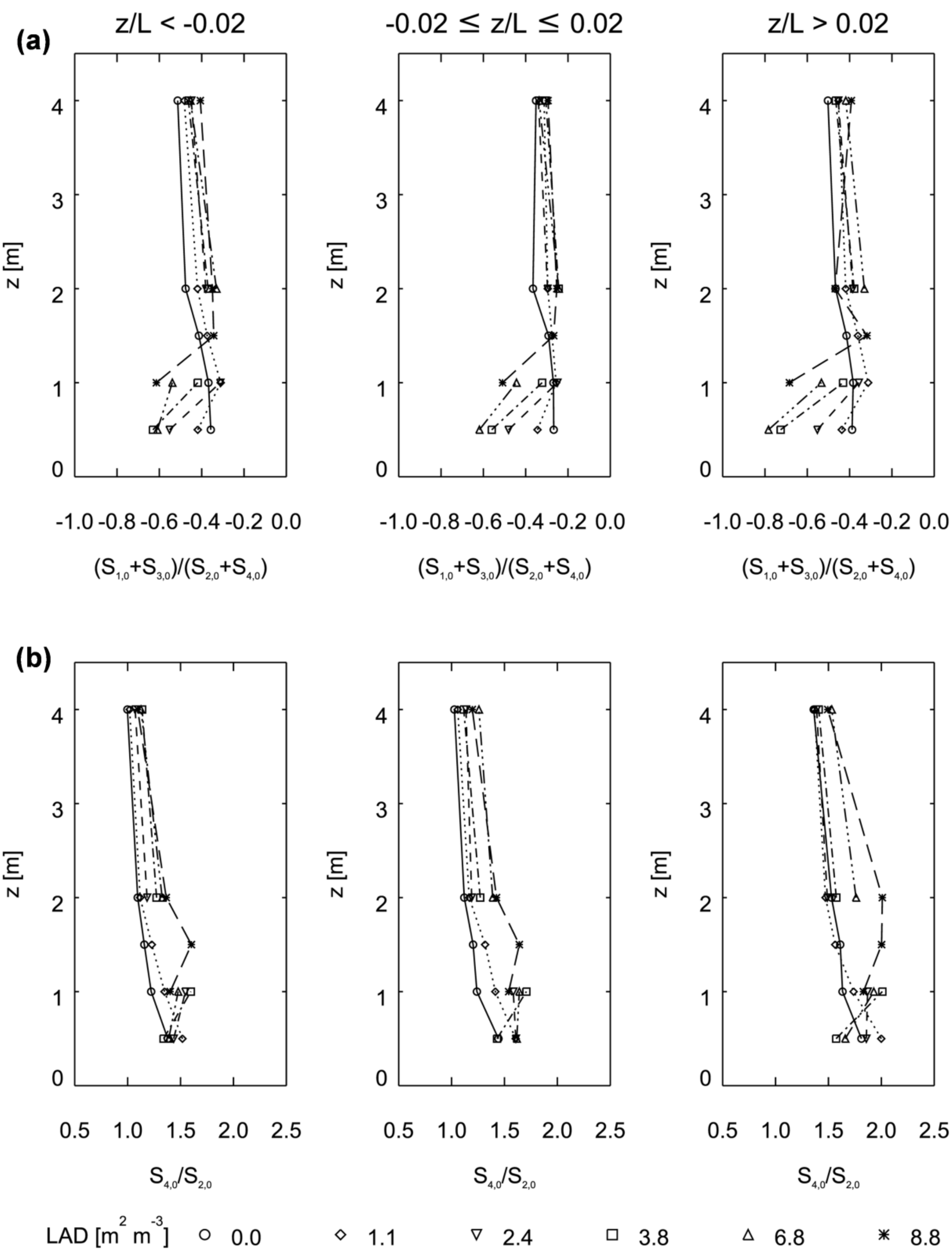

Fig. 3 Vertical profiles of wind exuberance $(\boldsymbol{S_{1,0}} + \boldsymbol{S_{3,0}})/(\boldsymbol{S_{2,0}} + \boldsymbol{S_{4,0}})$ (a) and sweeps to ejections stress fraction ratio ($S_{4,0}/S_{2,0}$) (b) for different stability conditions and leaf area density (LAD) periods.

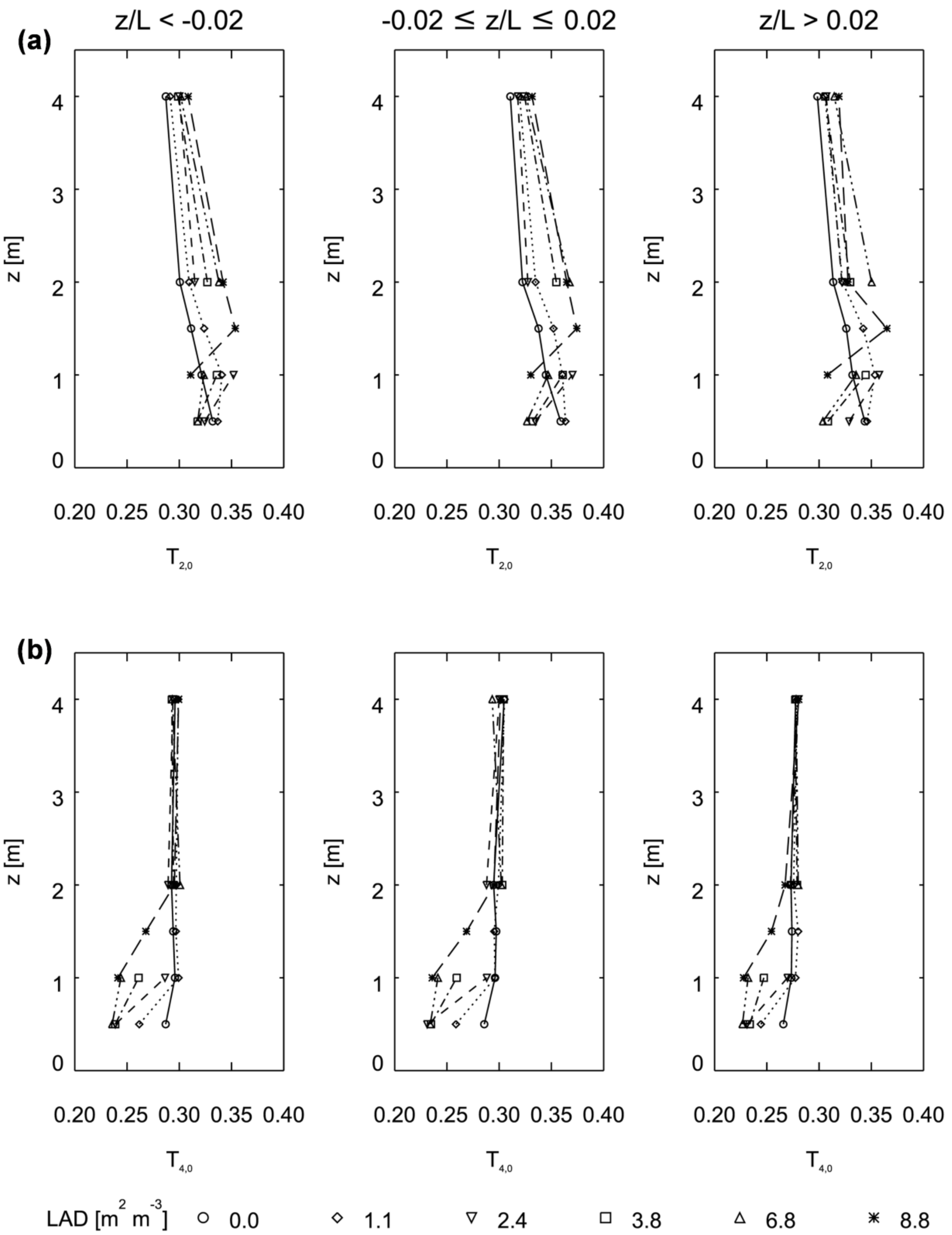

Fig. 4 Vertical profiles of ejection (a) and sweep (b) time fractions for different stability conditions and LAD periods.

At canopy top, the contribution by sweeps increased slightly more than above with foliage development and only in stable conditions the increase was significant (from 1.5 to 2.0). At

1.5 m, the ratio increased, from an empty to fully developed canopy, of about 25% in all stability cases. At 1 m, when foliage became dense at this height (LAD = 2.4 m^2 m^{-3}) sweep contribution increased from 1.2 to about 1.8, reaching the highest value of neutral conditions. As foliage became denser and the upper layers developed, the ratio at 1 m started to decrease again getting to 1.5 at fully developed canopy. In contrast, in the trunk space the contribution by sweeps and ejections was rather constant during the season for all stability cases: about 1.5 in unstable and neutral conditions and 1.7 for the stable case. In general, sweeps contribution tended to increase with LAD but showed a different behavior in the lower layer of the canopy with very dense foliage. At this height, the ratio first increased but then came back closer to no–leaves values. On the contrary, the ratio of sweeps to ejections was not particularly affected by canopy development in the trunk space and above canopy.

The relative contribution by ejections to momentum flux reduced within the canopy as foliage became denser, but the time fraction ($T_{2,0}$) occupied by these events increased in all stability conditions (Fig. 4a) from about 30 – 32% to 35 – 38%. On the other hand, sweep time fraction ($T_{4,0}$) was smaller in magnitude, being less than 30% (Fig. 4b). $T_{4,0}$ decreased within the canopy along the season where, conversely, the relative contribution by sweeps was larger.

In order to study the importance of different frequency and magnitude events in transporting momentum, we performed quadrant analysis with an excluded hole region of varying size. We selected one "gold" day for each LAD period and, within it, 30–min periods of unstable, near–neutral and stable conditions (Table 5). The stress fraction $|S_{i,H}|$ at each height was calculated normalizing the stress in quadrant i and hole size H by the 30–min momentum flux at the same height. In Fig. 5, Fig. 6 and Fig. 7 stress fraction with varying hole size for near–neutral, unstable and stable conditions respectively are presented.

Without leaves (Fig. 5a), ejections and sweeps contributed to the same amount of momentum flux above the canopy (about 80%), whereas within the canopy ejections transported 60% of the flux but sweep contribution was not reduced. With increasing hole size, sweeps remained predominant along the whole profile being more intermittent compared to ejections.

Table 5 Basic characteristics of selected 30–min periods: atmospheric stability (unstable (U), near–neutral (NN), stable (S)); wind direction (WDir) at different heights; wind speed (WSpeed) above canopy.

		z/L	WDir 4 m [°N]	WDir 2 m [°N]	WDir 1.5 m [°N]	WDir 1 m [°N]	WDir 0.5 m [°N]	WSpeed 4 m [m s^{-1}]
06/04/2015 LAD 0	U	–0.17	20	20	20	17	20	2.8
	NN	–0.004	76	77	77	71	77	2.1
	S	0.43	61	62	66	55	71	1.3
07/05/2015 LAD 1.1	U	–0.17	62	60	56	60	57	3.2
	NN	0.015	33	32	31	31	31	3.0
	S	0.32	17	12	14	11	9	1.1
28/05/2015 LAD 2.4	U	–0.18	196	207	–	203	212	2.6
	NN	–0.003	172	180	–	178	199	2.8
	S	0.28	133	130	–	112	170	1.2
08/06/2015 LAD 3.8	U	–0.14	189	203	–	198	221	1.6
	NN	–0.008	45	35	–	36	26	2.0
	S	0.12	26	19	–	28	20	1.6
17/06/2015 LAD 6.8	U	–0.2	193	209	–	203	215	1.2
	NN	–0.005	76	73	–	41	13	2.4
	S	0.2	86	77	–	37	348	1.1
09/07/2015 LAD 8.8	U	–0.15	95	92	–	55	–	2.0
	NN	–0.005	65	73	–	35	–	3.1
	S	0.11	19	39	–	29	–	1.2

Following the evolution of canopy morphology (Fig. 5b to f), it can be seen a clear effect of the increase in LAD on vertical profile. As the lower layer of foliage became denser, the stress fraction transported by sweeps in the trunk space increased relative to ejections (80% and 60% respectively). Additionally, the contribution of strong downward events became predominant at 0.5m, as showed in Fig. 5c, with 50% of momentum flux transported by events 15 times larger than the average flux. Thus, turbulent transport in the bottom canopy was characterized by strong intermittent events transporting most of the flux. At the same time, ejections also became more intermittent compared to no–foliage stage at 0.5m, but only 10% of the stress was transported by events 10 times larger than average.

These patterns were accentuated as foliage became denser and grown vertically (Fig. 5d to f). With a fully developed foliage, sweeps greater than 20 times larger than average were transporting 50% of the flux at 1 m. There was a clear effect of evolving canopy morphology on stress fraction profile: at the denser and upper layer the intermittency increased especially for sweeps, but also for ejections and outward/inward interactions. Sweeps contributed to about 80% of the flux both above and within canopy with or without leaves, whereas ejections had the same importance above canopy for the period without leaves and the contribution decreased to about 60% both above and below canopy as foliage developed. An interesting pattern is shown in Fig. 5e. With an almost fully developed canopy, the stress fractions of the four quadrants in the trunk space were less intermittent than above.

Outward and inward interactions, acting opposite to momentum transport towards ground, contributed to a smaller fraction. In general, outward interactions showed to be larger and more intermittent compared to inward interactions. Without leaves, these events were more significant above canopy, but when foliage became denser, the fraction of interactions increased in the canopy where foliage was present, with prevalence of outward movements. In denser layers and in the trunk space, inward/outward interactions reached values corresponding to 40–50% of momentum flux.

These results concerned periods of near–neutral stability, the effect of atmospheric stratification is shown in Fig. 6 and Fig. 7, for unstable and stable conditions respectively. During periods of unstable regime, the contribution by sweeps and ejections above canopy was about the same, both being around 80% at $H = 0$ during the whole period. Without leaves, Fig. 6a, sweep intermittency showed to be higher close to ground and, in general, it was greater at all heights compared to neutral conditions. Ejections showed similar patterns as neutral stability above canopy, while within the canopy the intermittency was larger.

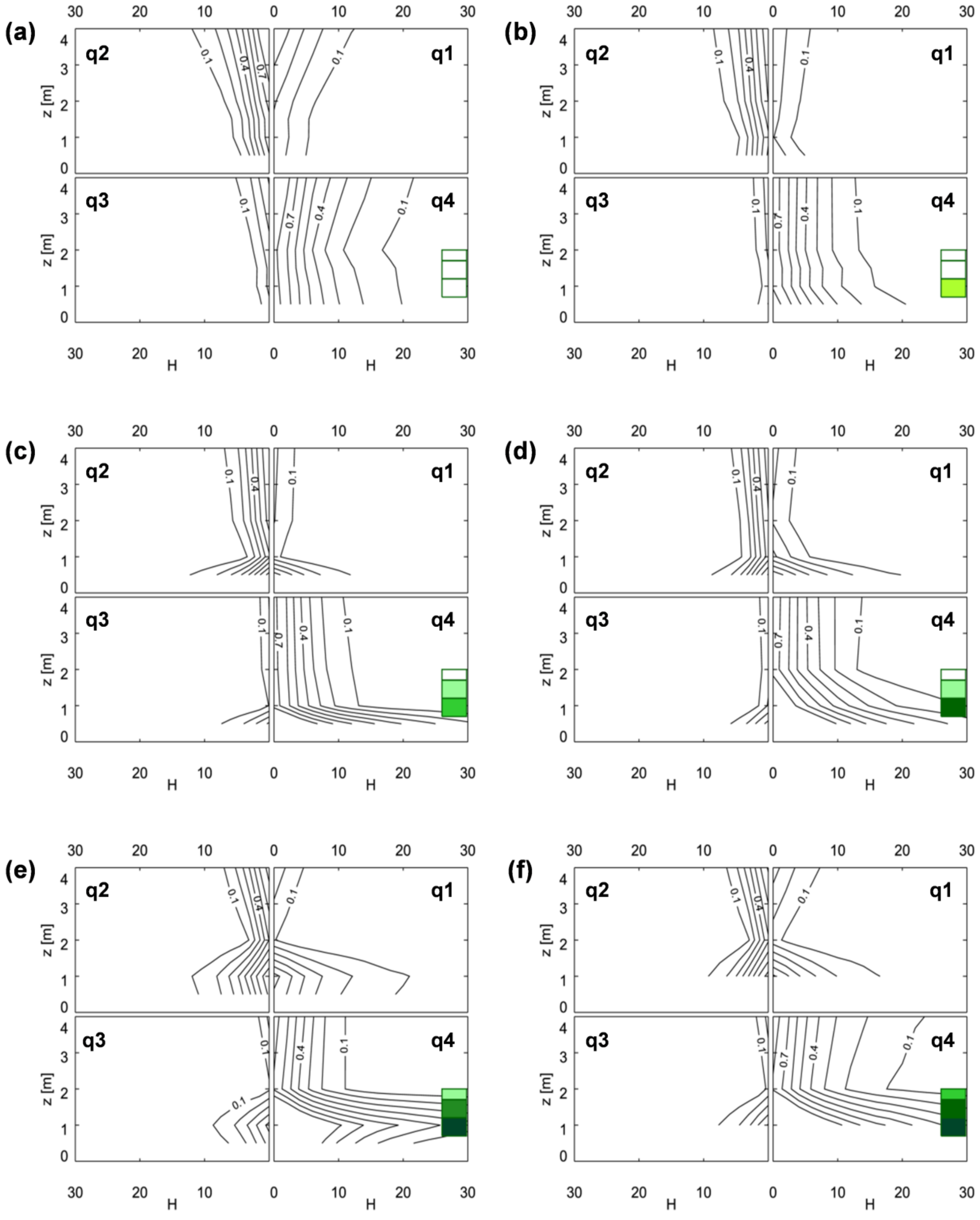

Fig. 5 Vertical profiles of stress fraction in the four quadrants with an excluded varying hole size (H) for near neutral conditions. Vertical lines are contour lines of absolute stress fraction $|S_{i,H}|$. The rectangle in *q4* represents the canopy shape subdivided into three layers of evolving LAD, darker green color means higher LAD.

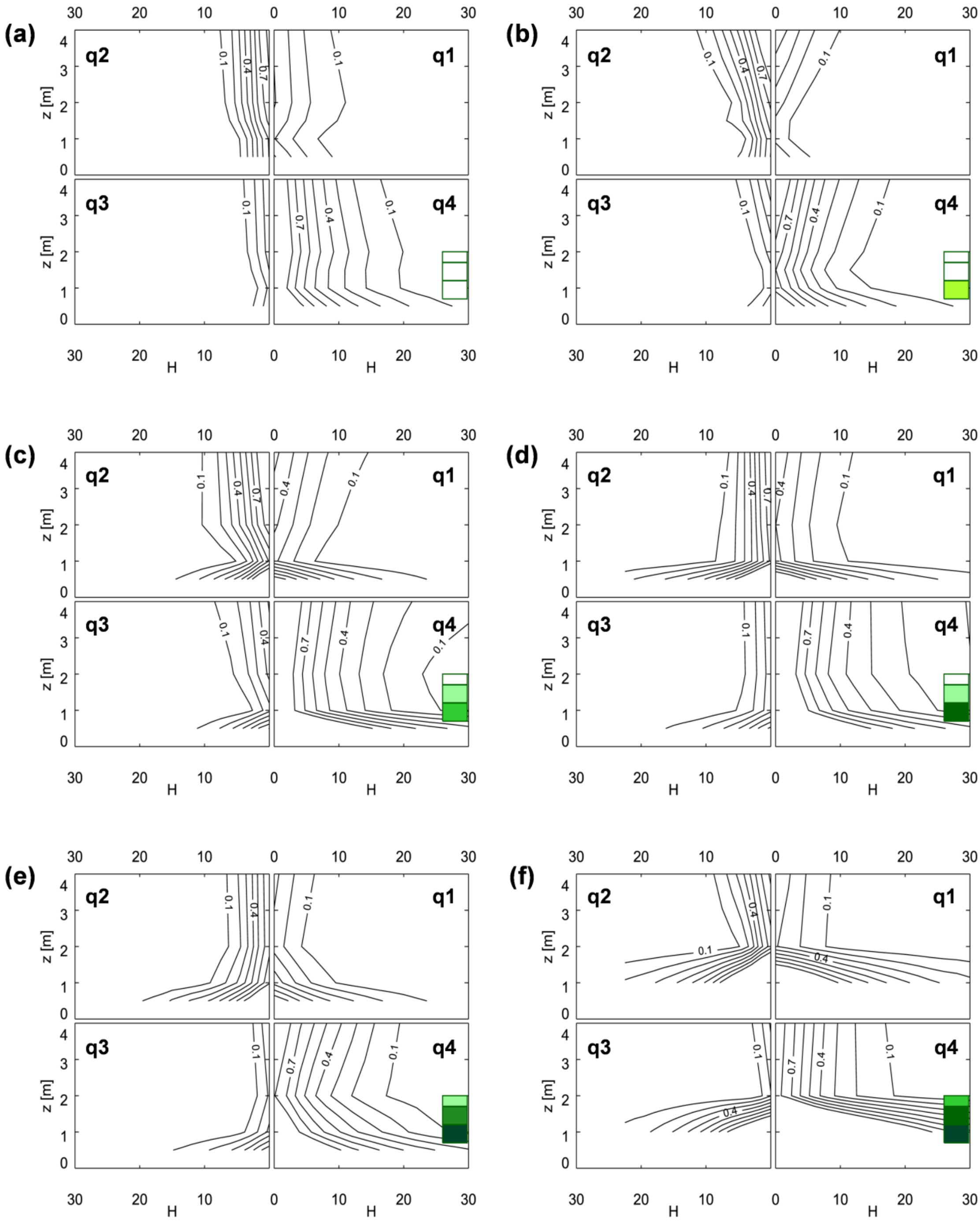

Fig. 6 Same as Fig.1 but for unstable conditions.

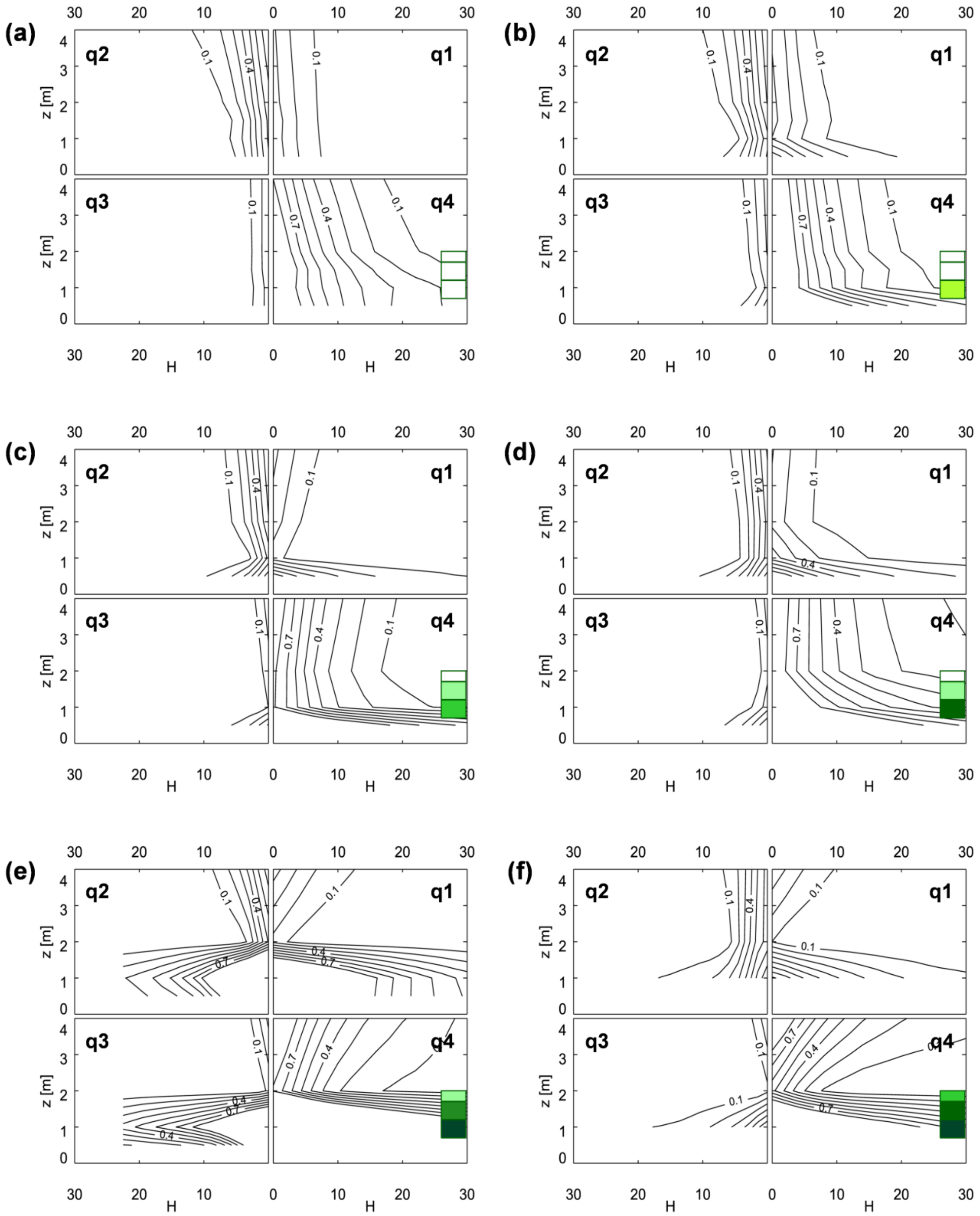

Fig. 7 Same as Fig.1 but for stable regime.

Outward interactions were transporting a greater amount of stress fraction (30–40%) compared to near–neutral conditions and were characterized by a larger number of strong events, especially in denser layers. In stable conditions (Fig. 7), sweeps were transporting a larger stress fraction compared to ejections, like in near–neutral regime, and the intermittency was much higher compared to ejections both above and below canopy. The stress fraction associated with outward/inward interactions was smaller than for unstable regime and comparable with neutral conditions, becoming greater in the canopy with increasing LAD.

The characteristics of momentum transport were also influenced by wind direction. Whether wind was coming diagonal to rows (57–102 and 147–192 °N) or parallel (12–57 and 192–237 °N), the profile of the ejection quadrant was showing different patterns, but without any particular effect on sweeps. With wind blowing diagonal to rows, ejections at the level of denser upper layer were less intermittent compare to above and below (Fig. 5d, e and d; Fig. 6c, f; Fig. 7c, e). Instead, with wind parallel to rows, ejections were transporting stress fraction with the same intermittency as above (Fig. 5d; Fig. 6d, e; Fig. 7d, f).

To better appreciate the concept of intermittency, Fig. 8 shows the patterns of stress fraction $S_{i,H}$ and time fraction $T_{i,H}$ with varying hole size for an empty canopy (a) and medium developed canopy with LAD = 3.8 m^2 m^{-3} (b) in near–neutral conditions. Stress and time were different functions of hole size in both periods for *q2* and *q4*. The transport is classified as intermittent when time fraction decreases more rapidly with hole size than stress fraction. This implies that a large fraction of stress is transported in a small fraction of time and short–lived events of large magnitude are present. Without leaves (Fig. 8a), sweep stress fraction showed the same pattern with hole sizes at all heights and sweeps were quite intermittent, with events 10 times larger than $\overline{u'w'}$ transporting about 30% of the flux in less than 2% of the time. On the other hand, ejection contribution at 4 m was larger and more intermittent than within canopy, transporting 20% of the flux in 2% of the time at H = 10, compared to less than 5% of momentum in 1% of the time in the canopy. Outward/inward interaction stress and time fractions presented a similar shape with varying hole size, except above canopy where interaction stress fractions were double than below.

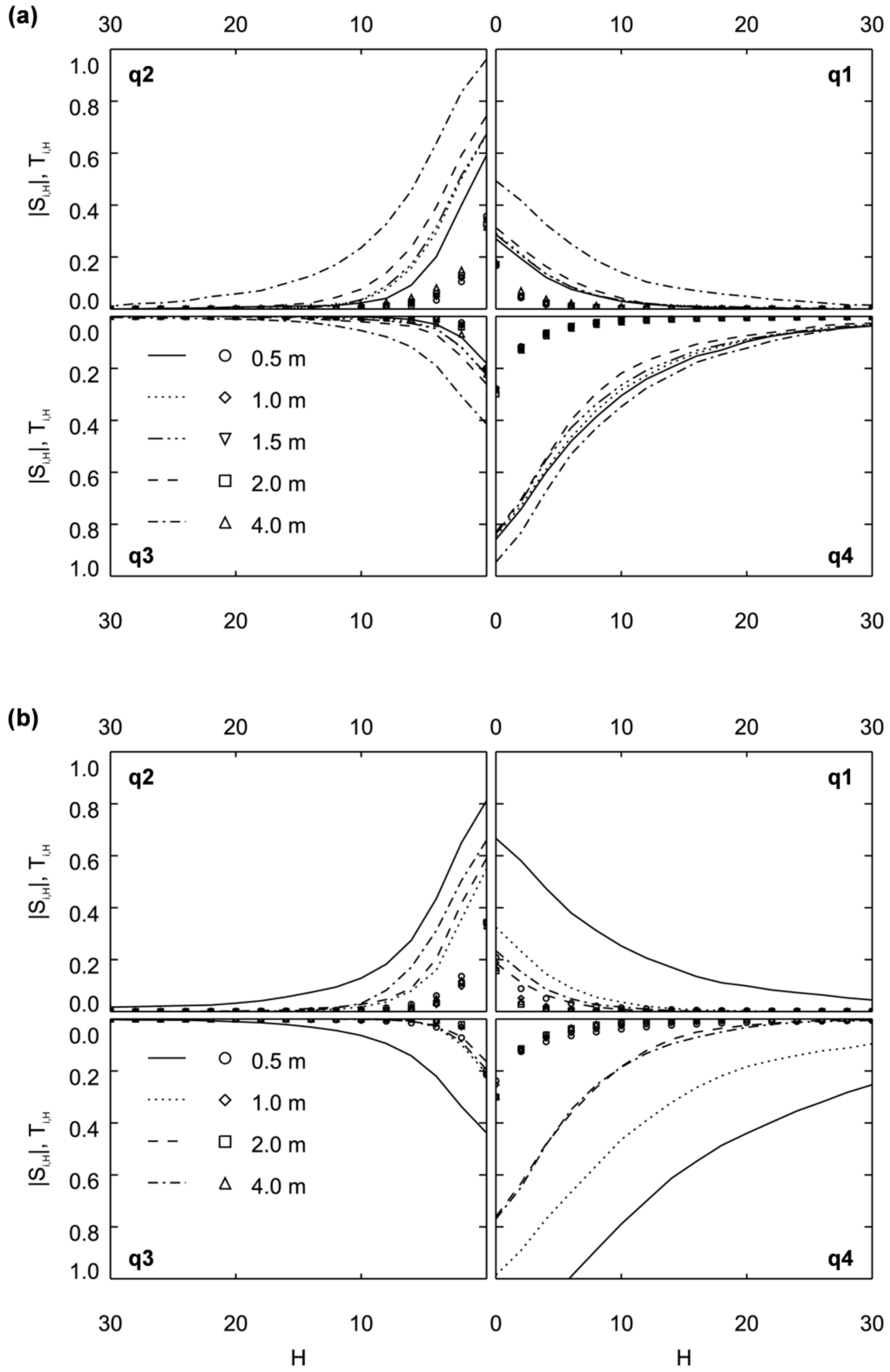

Fig. 8 Absolute stress fractions $|S_{i,H}|$ and time fractions $T_{i,H}$ .at each level for near-neutral 30–min periods with LAD = 0 (a) and LAD = 3.8 m^2 m^{-3} (b).

Fig. 8b shows the result for a medium developed canopy with dense foliage in the layer between 0.7 and 1.2 m. The presence of leaves highly influenced the transport of momentum both in and above canopy. In the trunk space, all quadrants contributed to a rather large amount of stress and were characterized by high intermittency; nevertheless sweeps were predominant in transporting momentum. At 1 m, where foliage was very dense, transport was strongly dominated by highly intermittent sweeps, accounting for 50% of flux at $H = 10$ in 2% of the time. Ejections were still important, transporting 60% of total flux but only with relatively weak events, at $H = 10$ only 2% of the stress was due to ejections. The transport at 2 and 4 m was presenting the same features as for the empty canopy: sweeps were still more significant than ejections, but less intermittent than below, and interactions were playing a minor role.

3.2 ***Quadrant event duration analysis***

Traditional quadrant analysis allows for a description of the organization of turbulent transport, identifying the type of events involved and their relative magnitude to overall momentum flux and frequency. However, the events are not defined individually in their absolute duration. In this section results from a study of event temporal scales based on adapted quadrant analysis are presented.

The analysis, described in section 2.4.3, allows for the calculation of single event duration (*De*) in each quadrant. From event durations, a frequency distribution of quadrant events in each time class was derived. The maximum time class was set to 20 s, which is enough to include most or all the events in the 30–min period, with 1 s bin size. At the same time, stress fraction associated with the events in each class can be calculated.

Frequency and stress fraction distribution for sweeps and ejections over duration classes are presented for near–neutral 30–min period without leaves (Fig. 9a) and for a well–developed canopy (Fig. 9b). The most frequent events were of short duration (1–2 s); however these events were transporting only a minor fraction of total momentum flux. The dominant temporal scales in momentum transport were between 2 and 4 s for both sweeps and ejections. However, sweeps were carrying larger stress fraction compared to ejections of the same duration. Without leaves no clear difference between heights could be detected, whereas, with a developed canopy, events of 2–4 s at canopy bottom were transporting higher stress fraction compared to above. This is in agreement with what found using traditional quadrant analysis.

The daily time course of *De* frequency distribution for a middle season day (June, 8) at 1 m is presented in Fig. 10. Sweeps exhibited a more compact pattern, with highly frequent events of 2–4 s and maximum duration lower than 10 s during most of the day. The ejection durations were more spread: frequent events were distributed over a wider range (2–7 s) and with maximum *De* around 15 s. The onset of stable conditions clearly increased the maximum length of both sweeps and ejections. Additionally, events were distributed over a wider range of durations without any clear pattern. The presence of both short and long events could be interpreted as a signal of high intermittency and low organization of turbulent flow.

The effect of LAD and stability on event durations (*De*) and intervals (*Ie*) is summarized in Fig. 11 and Fig. 12 respectively. In order to eliminate short semi–random events not involved in momentum transport, data with an excluding hole size $H = 2$ are presented. Ejections were characterized by longer durations (5–6 s) compared to sweeps (3–4 s), with higher values in unstable and stable conditions (Fig. 11). The duration was slightly larger above canopy and it decreased approaching the ground. No significant effect of LAD evolution was detected; only in stable conditions ejection *De* increased at the top and within canopy as foliage became denser.

Similar patterns were exhibited by time intervals between events (Fig. 12). Sweeps had shorter intervals compared to ejections on average (20 and 25 s respectively) and no clear influence of LAD was found. However, there was a visible effect for time intervals between ejections in stable conditions: *Ie* increased at canopy top from 20 to 36 s during the growing season. A similar pattern was shown in unstable conditions, but with a more limited increase (from 20 to 30 s).

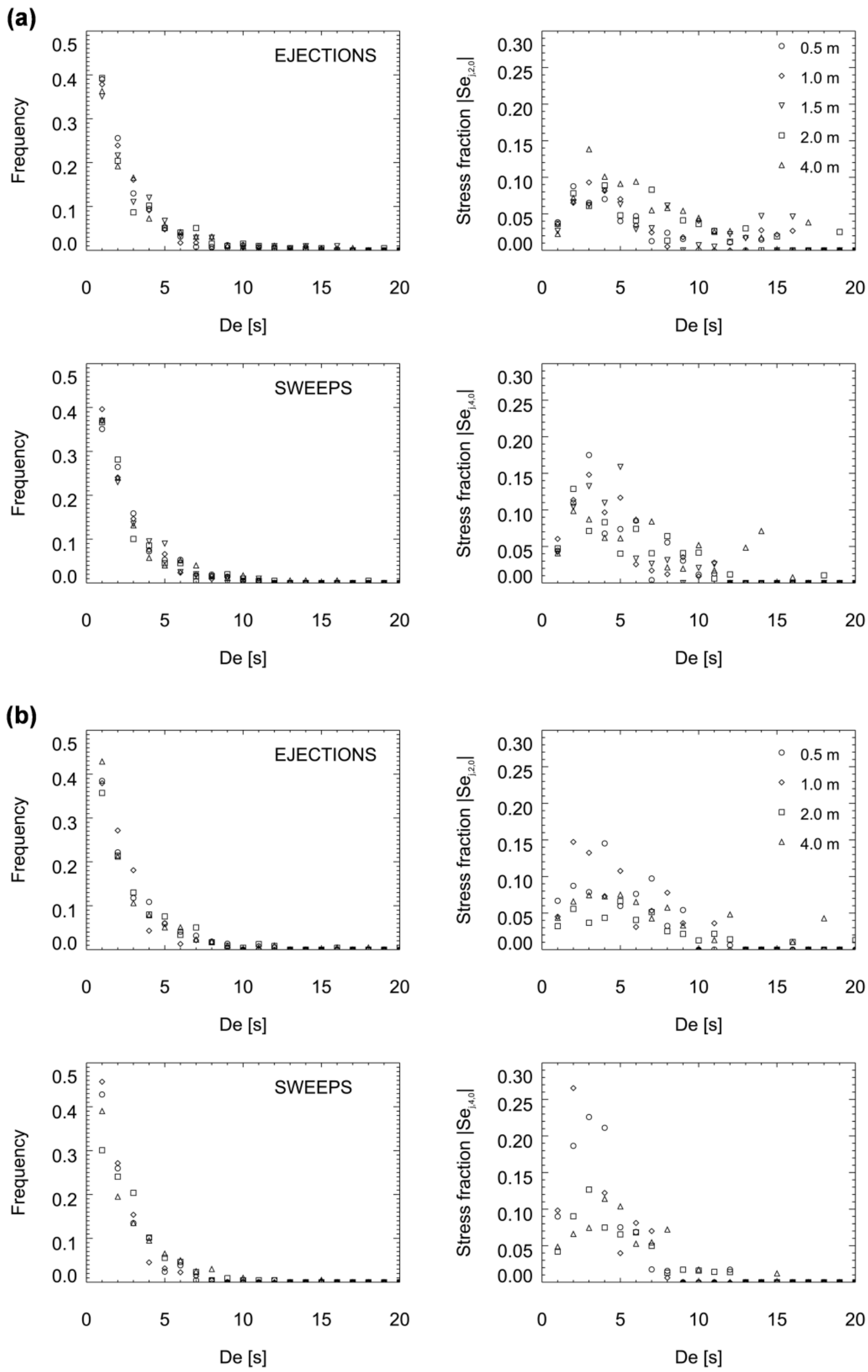

Fig. 9 Frequency (left) and stress fraction (right) distribution for sweeps and ejections over duration classes; without leaves (a) and with LAD = 6.8 (b).

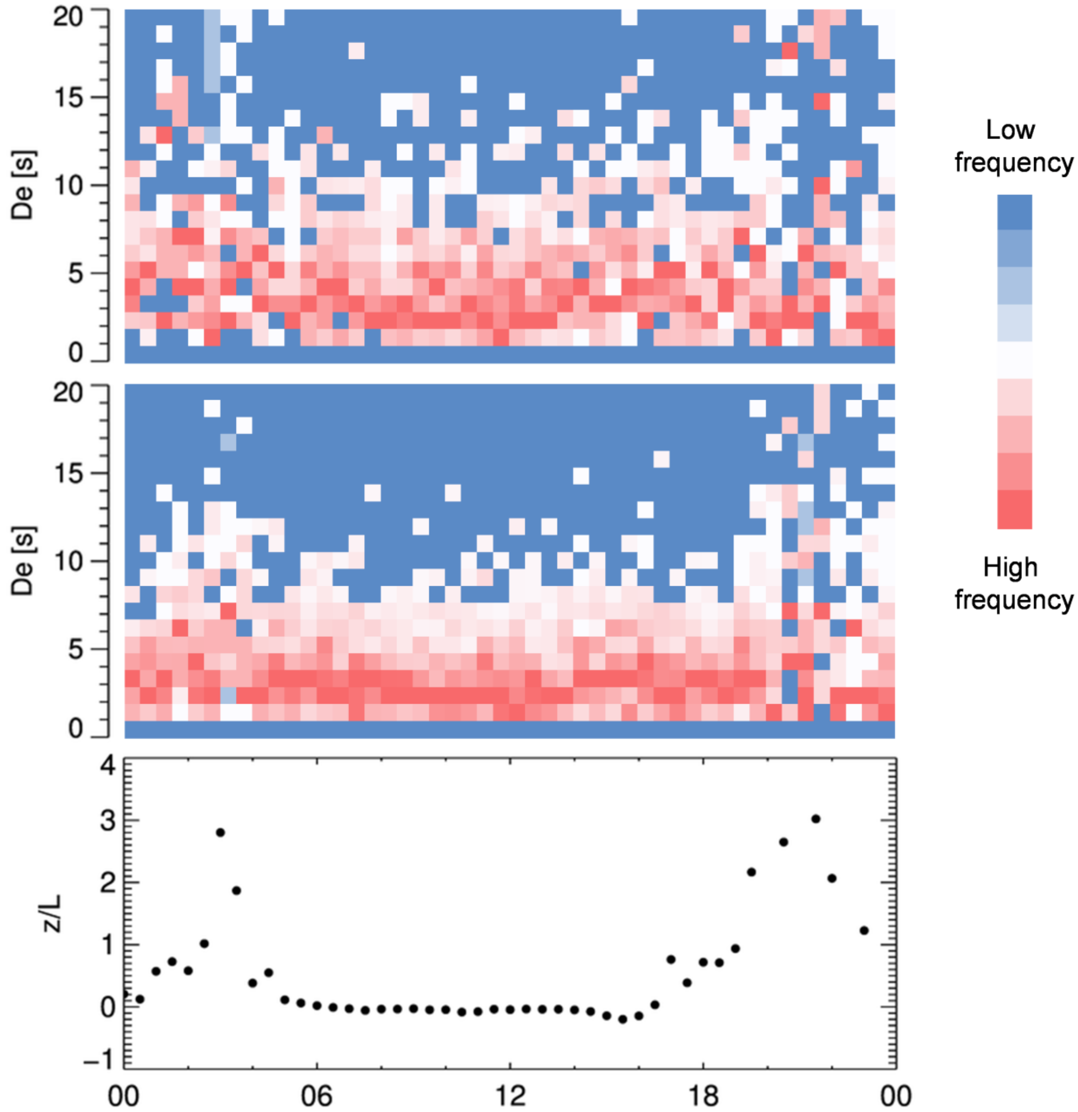

Fig. 10 Daily time course of duration frequency distribution of ejections (top) and sweeps (middle) for a medium–developed canopy (June, 8) at 1 m and daily pattern of stability parameter *z/L* (bottom). Red and blue colors represent high and low frequent events respectively.

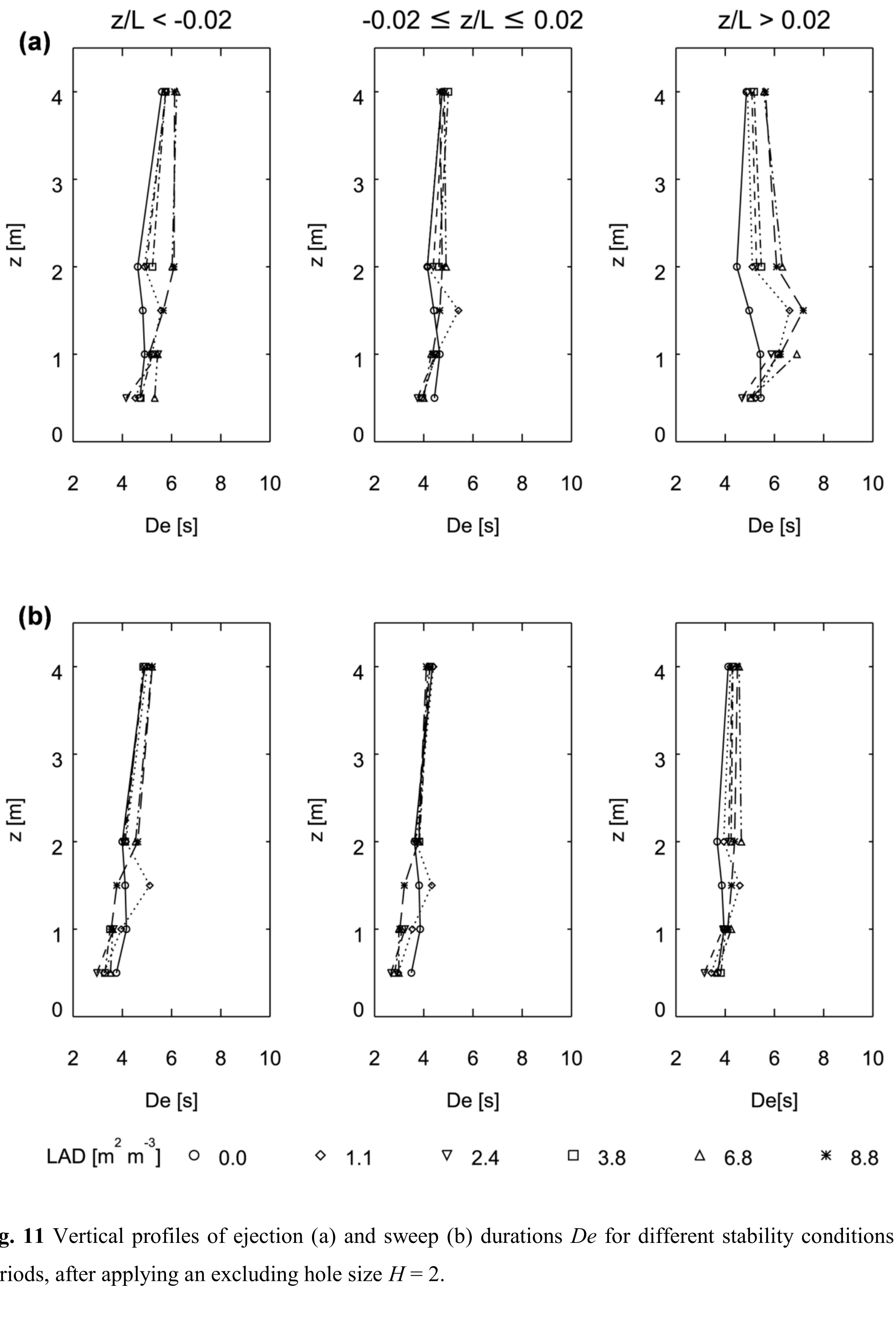

Fig. 11 Vertical profiles of ejection (a) and sweep (b) durations *De* for different stability conditions and LAD periods, after applying an excluding hole size $H = 2$.

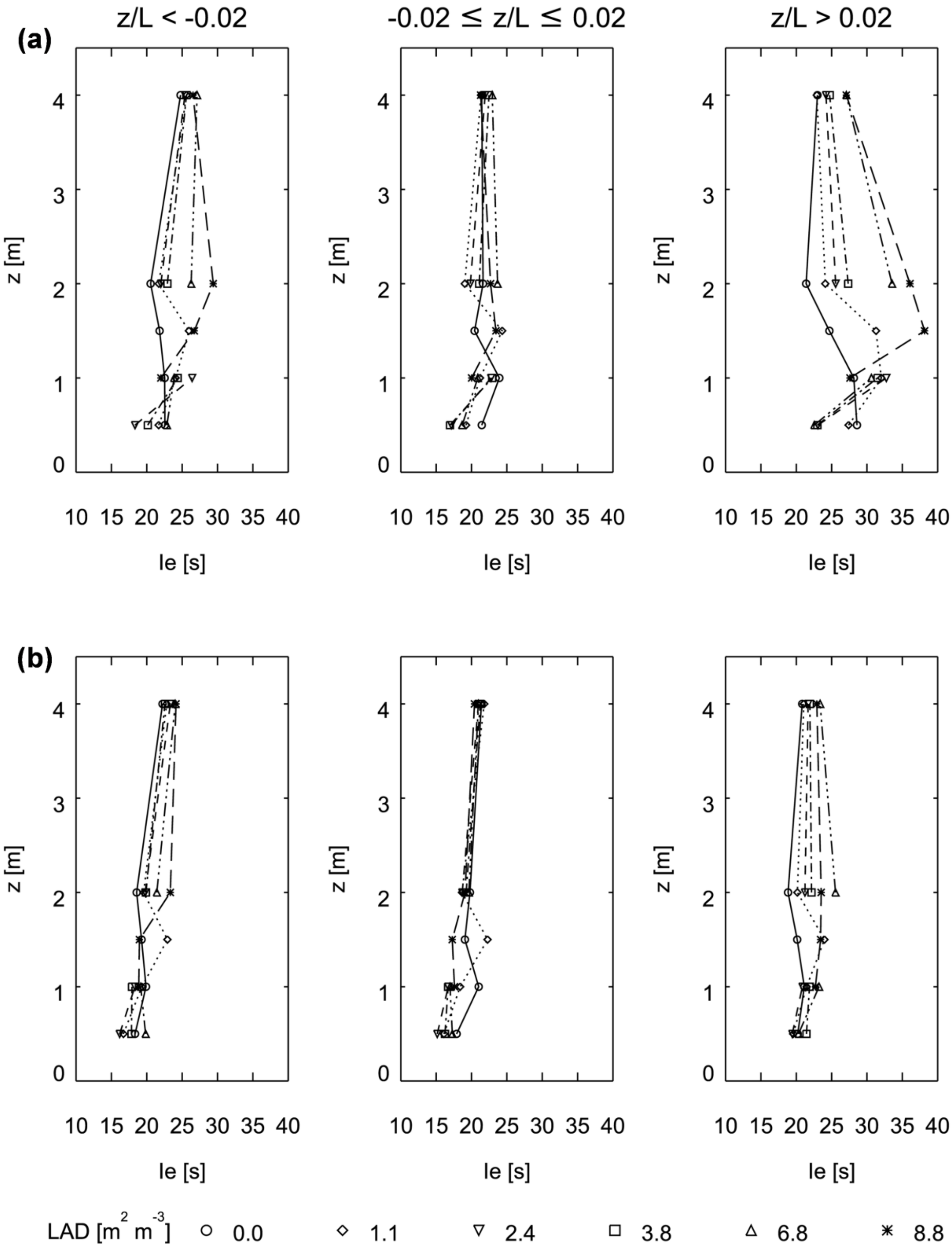

Fig. 12 Vertical profiles of intervals *Ie* between ejections (a) and sweeps (b) for different stability conditions and LAD periods, after applying an excluding hole size $H = 2$.

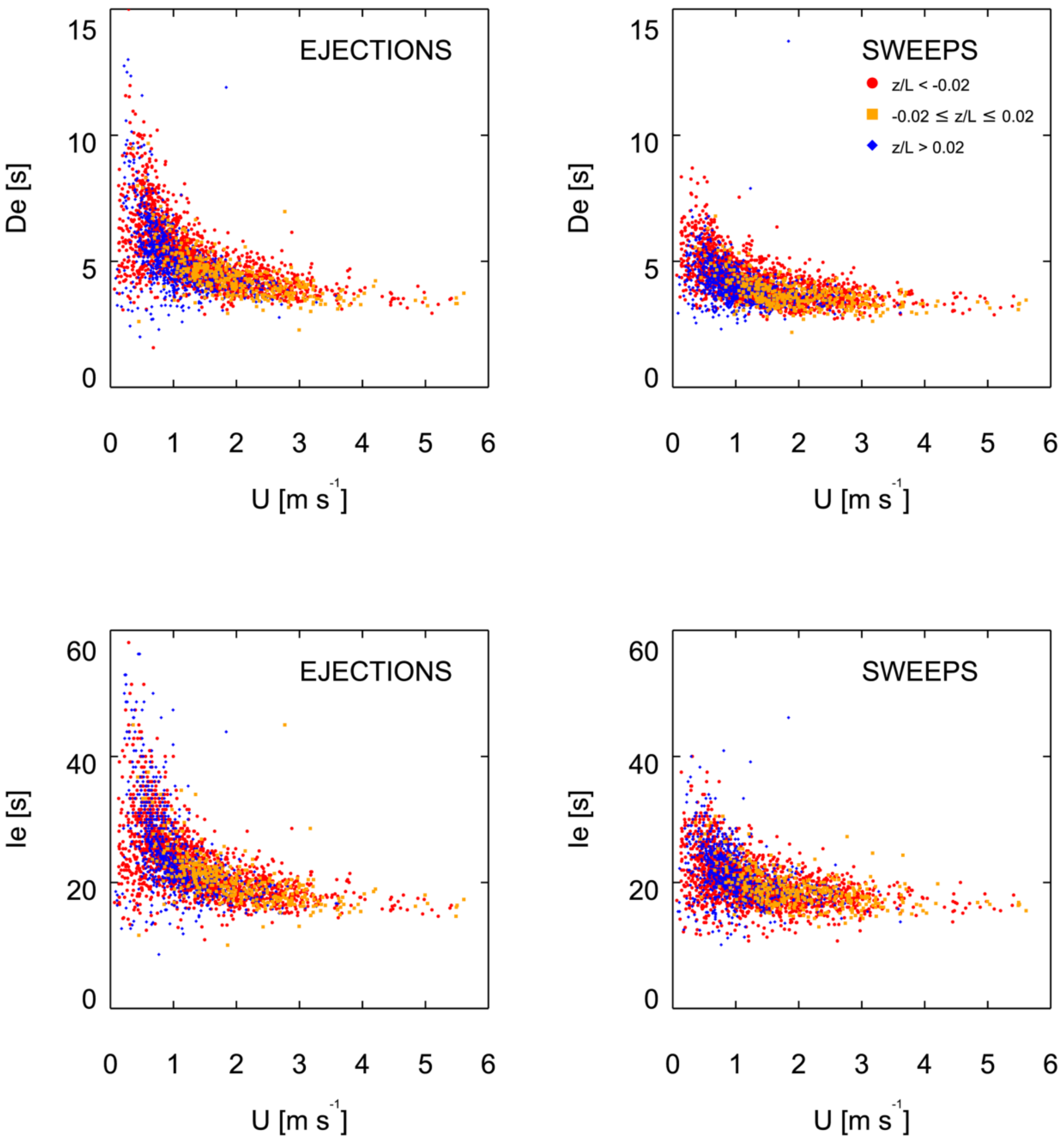

Fig. 13 Relationship of event duration *De* (top) and intervals *Ie* (bottom) with wind speed *U* at canopy top (2 m), after applying an excluding hole size *H* = 2. Different colors represent atmospheric stability classes: unstable (red); near–neutral (orange); stable (blue).

Stable and unstable conditions are often characterized by low wind velocity, so we analyzed the relationship between mean wind velocity (U) and event duration/intervals at canopy top (Fig. 13). Durations and intervals decreased as wind speed increased following a hyperbolic function. However, different patterns were found for sweeps and ejections at low wind speeds ($U < 1$ m s^{-1}). Ejections showed a wider range of durations and intervals, reaching larger values of *De* and *Ie*. Maximum sweep duration was around 8 s, while for ejections 14 s. Intervals between sweeps did not go over 40 s, whereas ejection intervals extended up to 60 s. At wind speeds greater than 2 m s^{-1} the durations and intervals were not varying with increasing shear. *De* was within the range 3–5 s and 4–6 s, while *Ie* 15–20 s and 17–22s, for sweeps and ejections respectively.

Periods of near–neutral conditions had $U > 1$ m s^{-1}, thus duration and intervals did not vary much with wind speed. Stable periods were confined mostly in low wind conditions with larger durations and intervals, whereas unstable periods covered the whole range of wind speeds and event temporal scales.

4 Discussion

The study of turbulent flow organization above and within canopy with an evolving canopy structure was performed using classical quadrant analysis. Additionally, temporal scales of events have been investigated using a new method also based on conditional sampling.

Our results showed that the relative importance of sweeps to ejections in transporting momentum increased from above to within the canopy, confirming the transition from boundary–layer to canopy flow, characterized by mixing–layer organization of motion (Finnigan, 2000; Raupach et al., 1996). Above canopy the sweep to ejection ratio was close to unity during the whole experiment, meaning that the organization of the flow at 4 m was not affected by canopy development and this level being in the surface layer.

The magnitude of sweeps to ejection ratio at different level in the canopy changed as foliage developed. Without leaves, the ratio was greater close to ground while during successive canopy stages the highest value was recorded at the closest level below the presence of denser foliage. In the trunk space the relative contribution of sweeps to ejections remained constant during the whole season, while at canopy top sweep importance slightly increased during each stage. These patterns suggest that turbulent flow in the empty canopy was more similar to a rough–wall boundary layer, whereas as foliage developed in density and height the flow evolved to a characteristic canopy regime, with the level of transition from free air flow to canopy flow shifting up during the season.

Previous studies addressed the change of turbulent transport organization above and within canopies characterized by different densities (Dupont and Brunet, 2008; Poggi et al., 2004), but only few investigated the change in turbulent flow between a foliated and non–foliated canopy (Dupont and Patton, 2012; Francone et al., 2012). In addition, we were able to study the vertical variation of turbulence organization due to minimal structural changes in the same canopy.

The effect of increasing foliage density was consistent with the transition between open and denser canopies (Dupont and Brunet, 2008; Poggi et al., 2004). As foliage developed, the organization of turbulent transport in the lower canopy decreased as indicated by greater flow exuberance at 0.5 and 1 m. Our values ranged between – 0.2 and – 0.8, which is in agreement with the exuberance reported by Baldocchi and Meyers (1988) in a deciduous forest. Interactions were always minor compared to sweeps and ejections; however their contribution increased in the trunk space as the first layer of leaves came out and, once the upper layers developed, it increased also in the lower foliated layer. The intensification of the interaction terms can be related to the complexity of within–canopy flow, which could have been generated also by wake turbulence and secondary circulations (Baldocchi and Meyers, 1988).

The change in wind field characteristics between top and bottom canopy was significant. In the low canopy, where wind speed is weak, the flux was composed by the small sum of large contributions by all quadrants, including interactions. Similar results were found by Baldocchi and Hutchison (1987), however they reported stress fractions larger than unity and in our case this value was exceeded only by sweeps. Dupont and Patton (2012) detected a decrease of sweep contribution in the trunk space of an almond orchard when the canopy was foliated, probably because structures do not penetrate as deeply under this condition. This is not our case, stress fraction transported by sweeps was still dominant, most likely because the row architecture of the canopy allows organized structures to enter more deeply. Nevertheless, in the bottom canopy they transported small momentum flux and the strength of sweeps was dampened.

On the other hand, the exuberance slightly decreased during the growing season at canopy top, meaning that at this level the coherency of turbulent transport slightly increased with canopy development. The same behavior, with marginal increase of sweep contribution and transport efficiency, was observed by Francone et al. (2012) in the roughness sublayer above the canopy of three different vineyards from early vegetative season to fully developed foliage. Thus, we can argue that turbulent flow organization was not strongly affected by canopy development in the layer just above roughness elements, while the greatest effects were experienced within the canopy.

Canopy turbulent transport is known to be highly intermittent: most of the stress is transported during period of strong turbulence, which occupy a small fraction of the time (Raupach, 1981). This characteristic has been confirmed by several studies in natural (Baldocchi and Hutchison, 1987; Finnigan, 1979; Shaw et al., 1983) and artificial canopies (Poggi et al., 2004; Raupach et al., 1986). Our results showed that transport intermittency increased during the growing season within the canopy where foliage was present. Sweeps were more intermittent than ejections, with significant amount of stress fraction transported by strong events at large hole sizes. On average, sweeps had smaller time fractions than ejections, confirming their intermittent character, and their presence decreased within the canopy as foliage density increased. Nevertheless, at canopy top and above, sweeps were present during about 30% of the time throughout the whole season.

Above canopy, ejection time fraction had roughly the same magnitude through the season, in agreement with values reported by previous studies in different canopies (Katul et al., 1997; Launiainen et al., 2007; Shaw et al., 1983). On the contrary, ejection time fraction increased in the upper canopy and decreased in the lower canopy when the overhead layers became very dense. This behavior can be associated to a higher organization of turbulent transport in the upper layers and lower organization at the bottom, where weak turbulence is present.

The degree of intermittency at the highest level with foliage was dependent on wind direction. When wind was blowing across rows, the transport was less intermittent compare to above and, in contrast, for winds parallel to rows, the pattern was the same as above. However, this behavior was shown only by ejections and interactions. A possible explanation is that transversal wind, impacting directly on the row, establishes a motion where turbulence is enhanced and organized in strong sweeps and weak ejections. Increasing the excluding hole size, many ejections are too weak to be included and their contribution to overall stress fraction is underestimated, even if part of the same coherent structure with intermittent sweeps (Gao et al., 1989). On the contrary, row parallel winds have a different interaction with the canopy: the air enters at canopy top without being subjected to strong distortion and momentum is transported more efficiently along the vertical profile, as confirmed by the correlation coefficient of u and w (not shown here).

The analysis of event time scales revealed that momentum transport in the vineyard was dominated by sweeps of 2–4 s and ejections of 4–6 s, which can be summed to estimate an average duration of dominating coherent structures in the order of 6–10 s. Our result is of the same order of magnitude of time scales calculated using other methods in canopies of similar height (Table 2 in Feigenwinter and Vogt (2005)). Paw U et al. (1992) found time scales of 7–50 s in a maize field of 2.6 m using temperature drop algorithm and visual detection, Brunet and Collineau (1994) obtained shorter time scales (3–4 s) for a maize crop of 1.55 m applying the wavelet detection method, while Qiu et al. (1995) detected longer structures (15–25 s) in another maize field 2.6 m height with ramp detection and wavelet function method. The agreement with previous studies, obtained applying other methods, gives us confidence to rely on our event detection approach. In addition, we were able to calculate event frequency and stress fraction transported by the same duration class. Ejections covered a wider range of classes in the 30–min period compared to sweeps and this can explain the longer average duration. The same result, with longer ejections compared to sweeps, was found by Qiu et al. (1995).

The events transporting most of stress fraction were in the range of 2–5 s, while shorter events were the most frequent but not involved in momentum transport. Thus, small scale events could be linked to inactive random turbulence. The evolution of canopy morphology did not have any clear influence on structure duration. Nevertheless, an effect of LAD could be detected for ejections during periods of stable conditions with larger duration when foliage was present.

The variation of atmospheric stability had an effect on the organization of turbulent transport, but the influence was more pronounced during stable rather than unstable conditions. This confirms the hypothesis of Raupach et al. (1996), who considered the buoyancy effect negligible within and just above short canopies. Still, a departure from the neutral state intensified the importance of interaction terms and increased transport intermittency within the canopy. During periods of stable stratification, sweep contribution was greater compared to neutral and unstable conditions at all measurement heights.

The relative importance of ejections did not increase in unstable periods compared to near–neutral, as it could be expected due to buoyancy transport in daytime boundary layer. Li and Bou-Zeid (2011) found similar results over vineyard and lake for momentum transport, but at the same time they demonstrated that upward thermal plumes are predominant in transporting sensible heat. Therefore, they suggested that buoyancy–produced thermals significantly alter the distributions of scalars but hardly alter the distribution of momentum.

From our results, we can say that the effect on sweep/ejection transport by transition from an empty to fully developed canopy was similar in magnitude to the change from unstable/neutral to stable stratification.

The onset of stable stratification caused the coexistence of different time scale events, from short to very long, with consequent longer average duration especially within the canopy where foliage was present. However, the latter could be more related to typical low winds of very stable stratification and free convection. This is confirmed by increasing event durations as wind speed approached zero. A possible explanation is that very weak turbulence is associated to low winds. In these conditions the drag exerted at canopy top is low, with a consequent decrease in wind shear. Thus, weak but long–lived boundary layer eddies tend to retain their characteristics and the flow is only slightly modified by interaction with canopy structure.

We want to point out that the large effect of leaf density on ejection duration during stable conditions (or very low winds) may be an artefact due to the use of a non–zero excluding hole size in the analysis. As said before, the selection of a non–zero hole size could lead to the elimination of weak ejections from the results, even if the event is part of a coherent structure with a strong sweep which was included (Gao et al., 1989). Therefore, during stable conditions, where momentum flux is small and ejections very weak, only long ejections can exceed the imposed threshold. Even if we selected the smallest hole size used in the analysis ($H = 2$), this effect was clearly impacting the results. A smaller H should be used for ejections compared to sweeps, but this would mean to use $H = 0$, including also background turbulence not involved in transport of momentum. This is a limitation of quadrant analysis compared to other methods used to identify coherent structures, like wavelets or visual detection. However, this is an automatized method and it can be applied on large dataset, giving a wide picture of the organization of turbulence under different conditions.

5 Conclusions

The organization of within–canopy turbulent transport evolved throughout the growing season along with vertical foliage development. Momentum flux was dominated by sweeps and their contribution relative to ejections increased in the presence of foliage. In the empty trunk space the ratio did not change during the season and, at the same time, the intermittency of transport increased at all heights. Atmospheric stability showed to have similar effects on the organization of turbulent transport as structure development.

The analysis of event time scales revealed that momentum transport within the canopy was dominated by sweeps of 2–4 s and ejections of 4–6 s, which can be summed to estimate an average duration of dominating coherent structures in the order of 6–10 s. The evolution of canopy morphology did not have any clear influence on structure duration; however event durations, especially ejections, showed to increase in low wind conditions. The new method to detect temporal scales demonstrated to be robust and applicable to large dataset, in spite of some limitations related to the choice of excluding hole size.

This kind of studies can have practical applications in vineyard management. For example, the understanding of canopy turbulence regime is directly related to small particle dispersion, like fungal spores. Additionally, infections can be minimized studying the effect of canopy ventilation on leaf wetness duration.

6 References

Antonia, R.A., 1981. Conditional sampling in turbulence measurement. Annu. Rev. Fluid Mech. 13, 131–156.

Bailey, B.N., Stoll, R., 2013. Turbulence in Sparse, Organized Vegetative Canopies: A Large-Eddy Simulation Study. Boundary-Layer Meteorol. 147, 369–400.

Baldocchi, D., Hutchison, B., 1987. Turbulence in an almond orchard: Vertical variations in turbulent statistics. Boundary-Layer Meteorol. 40, 127–146.

Baldocchi, D.D., Meyers, T.P., 1988. Turbulence structure in a deciduous forest. Boundary-Layer Meteorol. 43, 345–364.

Barthlott, C., Drobinski, P., Fesquet, C., Dubos, T., Pietras, C., 2007. Long-term study of coherent structures in the atmospheric surface layer. Boundary-Layer Meteorol. 125, 1–24.

Brunet Y., Collineau, S., 1994. Wavelet analysis of diurnal and nocturnal turbulence above a maize crop. In: Foufoula- Georgiou E, Kumar P (eds) Wavelets in geophysics. San Diego: Academic Press, pp 129–150.

Brunet, Y., Irvine, M., 2000. The control of coherent eddies in vegetation canopies: streamwise structure spacing, canopy shear scale and atmospheric stability. Boundary-Layer Meteorol. 94, 139–163.

Chahine, A., Dupont, S., Sinfort, C., Brunet, Y., 2014. Wind-Flow Dynamics Over a Vineyard. Boundary-Layer Meteorol. 151, 557–577.

Collineau, S., Brunet, Y., 1993. Detection of turbulent coherent motions in a forest canopy part I: Wavelet analysis. Boundary-Layer Meteorol. 65, 357–379.

Dupont, S., Brunet, Y., 2008. Influence of foliar density profile on canopy flow: A large-eddy simulation study. Agric. For. Meteorol. 148, 976–990.

Dupont, S., Patton, E.G., 2012. Momentum and scalar transport within a vegetation canopy following atmospheric stability and seasonal canopy changes: The CHATS experiment. Atmos. Chem. Phys. 12, 5913–5935.

Eder, F., Serafimovich, A., Foken, T., 2013. Coherent Structures at a Forest Edge: Properties, Coupling and Impact of Secondary Circulations. Boundary-Layer Meteorol. 148, 285–308.

Feigenwinter, C., Vogt, R., 2005. Detection and analysis of coherent structures in urban turbulence. Theor. Appl. Climatol. 81, 219–230.

Finnigan, J., 2000. Turbulence in plant canopies. Annu. Rev. Fluid Mech. 32, 519–571.

Finnigan, J., 1979. Turbulence in Waving Wheat: II. Structure of Momentum Transfer. Boundary-Layer Meteorol. 16, 213–236.

Francone, C., Katul, G.G., Cassardo, C., Richiardone, R., 2012. Turbulent transport efficiency and the ejection-sweep motion for momentum and heat on sloping terrain covered with vineyards. Agric. For. Meteorol. 162–163, 98–107.

Gao, W., Shaw, R.H., Paw U, K.T., 1989. Observation of organized structure in turbulent flow within and above a forest canopy. Boundary-Layer Meteorol. 47, 349–377.

Hogstrom, U., Bergstrom, H., Högström, U., 1996. Organized turbulence structures in the near-neutral atmospheric surface layer. J. Atmos. Sci. 53, 2452–2464.

Huang, J., Cassiani, M., Albertson, J.D., 2009. The effects of vegetation density on coherent turbulent structures within the canopy sublayer: A large-eddy simulation study. Boundary-Layer Meteorol. 133, 253–275.

Katul, G., Hsieh, C.-I., Kuhn, G., Ellsworth, D., Nie, D., 1997. Turbulent eddy motion at the forest-atmosphere interface. J. Geophys. Res. 102, 13409–13421.

Launiainen, S., Vesala, T., Mölder, M., Mammarella, I., Smolander, S., Rannik, Ü., Kolari, P., Hari, P., Lindroth, A., Katul, G.G., 2007. Vertical variability and effect of stability on turbulence characteristics down to the floor of a pine forest. Tellus, Ser. B Chem. Phys. Meteorol. 59, 919–936.

Li, D., Bou-Zeid, E., 2011. Coherent structures and the dissimilarity of turbulent transport of momentum and scalars in the unstable Atmospheric surface layer. Boundary-Layer Meteorol. 140, 243–262.

Lu, S.S., Willmarth, W.W., 1973. Measurements of the structure of the Reynolds stress in a turbulent boundary layer. J. Fluid Mech. 60, 481.

Paw U, K.T., Brunet, Y., Collineau, S., Shaw, R.H., Maitani, T., Qiu, J., Hipps, L., 1992. On coherent structures in turbulence above and within agricultural plant canopies. Agric. For. Meteorol. 61, 55–68.

Poggi, D., Porporato, A., Ridolfi, L., Albertson, J.D., Katul, G., 2004. The effect of vegetation density on canopy sub-layer turbulence. Boundary-Layer Meteorol. 111, 565–587.

Qiu, J., KT, P.U., Shaw, R., 1995. Pseudo-wavelet analysis of turbulence patterns in three vegetation layers. Boundary-Layer Meteorol. 72, 177–204.

Raupach, M.R., 1981. Conditional statistics of Reynolds stress in rough-wall and smooth-wall turbulent boundary layers. J. Fluid Mech. 108, 363–382.

Raupach, M.R., Coppin, P.A., Legg, B.J., 1986. Experiments on scalar dispersion within a model plant canopy part I: The turbulence structure. Boundary-Layer Meteorol. 35, 21–52.

Raupach, M.R., Finnigan, J.J., Brunet, Y., 1996. Coherent eddies and turbulence in vegetation canopies: The mixing-layer analogy. Boundary-Layer Meteorol. 78, 351–382.

Robinson, S.K., 1991. Coherent Motions in the Turbulent Boundary Layer. Annu. Rev. Fluid Mech. 23, 601–639.

Shaw, R.H., Tavangar, J., Ward, D.P., 1983. Structure of the Reynolds Stress in a Canopy Layer. J. Clim. Appl. Meteorol. 22, 1922–1931.

Stull, R.B., 1988. An Introduction to Boundary Layer Meteorology. Kluwer Academic Publishers.

Thomas, C., Foken, T., 2007. Organised motion in a tall spruce canopy: Temporal scales, structure spacing and terrain effects. Boundary-Layer Meteorol. 122, 123–147.

Thomas, C., Foken, T., 2005. Detection of long-term coherent exchange over spruce forest using wavelet analysis. Theor. Appl. Climatol. 80, 91–104.

Wang, Y., Miller, D., Anderson, D., 1992. A spatial length scale analysis of turbulent temperature and velocity fluctuations within and above an orchard canopy. Boundary-Layer Meteorol. 59, 125–139.

Weiss, A., Allen, H., 1976. Air-flow patterns in vineyard rows. Agric. For. Meteorol. 16, 329–342.

Summary and conclusions

Vineyard is a complex ecosystem with several sources/sinks of scalars, where vines and soil surface combine to give the overall flux of the canopy. The highly structured canopy of vineyards determines both a peculiar radiative regime and a characteristic turbulent mixing around foliage. Furthermore, the combination and strength of sources and sinks evolves throughout the year, driven by the annual cycle of grapevine. At the same time, the morphological structure of the vineyard is greatly variable over the year, shifting from an empty canopy during vine dormancy to dense foliage in summer.

We focused on the study of the carbon budget of the vineyard and its partitioning between vine and grassed soil inter–row. In 2015, the annual ecosystem carbon budget was about – 80 g C m^{-2} y^{-1}, however the largest part of carbon assimilation was due to grassed soil compartment (– 60 g C m^{-2} y^{-1}). Therefore, we showed that vineyards can act as net sink of CO_2 with an appropriate management (e.g. grassed inter–row), giving an additional value of sustainability to viticulture. In any case, the interannual variability and the increasing frequency of extreme events (high intensities rainfall, summer heat–waves, etc.) are challenging this important role of vineyards.

Disentangling the vineyard carbon budget using the combination of micrometeorological methods and soil chambers proved to be useful but the coherency was not always clear. Actually, EC and soil chamber measurements were often different, even during periods where sources/sinks accounted by the two methods should have been similar. This behavior can be partly related to different soil conditions between the chamber collars and the larger eddy covariance footprint area. However, it could also be explained by particular conditions of turbulent transport in the canopy sublayer, especially in stable stratification.

The vertical transport of scalars released/absorbed at the ground towards/from the overlying atmosphere is driven by canopy turbulence. We showed that turbulence characteristics were greatly influenced by canopy structure. Without leaves, turbulent regime was more similar to rough–wall boundary layer flow, whereas at full foliage development it assumed the characteristics of a typical canopy flow, even if with a weak inflection point at canopy top due to sparseness of the vineyard. The row structure of the vineyards allowed deep penetration of coherent eddies within the canopy sublayer compared to denser canopies. However, most of momentum was absorbed by the upper layers of foliage and consequently turbulent motion in the lower canopy was still present but characterized by inactive turbulence.

The organization of turbulent transport in coherent structures was also highly affected by vertical foliage development. The contribution by sweeps to momentum transport increased during the growing season where foliage was present. In the empty trunk space sweeps became more intermittent when upper layers developed, but their importance relative to ejections did not change. However, the level of turbulence organization decreased at this height, confirming that transport in the trunk space of the fully developed canopy was characterized by weak and inactive turbulence.

Atmospheric stability showed to have a weaker effect on canopy turbulence statistics compared to morphological changes. However, diabatic and structural effects had almost the same impact on the organization of transport, both increasing intermittency and decreasing the level of organization, especially in stable conditions. The duration of sweeps and ejections, detected with the new method proposed, showed to decrease approaching the surface but it was not particularly influenced by canopy morphology. Nevertheless, event durations increased at low wind speed, typical of nighttime stable conditions.

From our results we can argue that in the non–foliated canopy vertical mixing close to the ground was similar to upper layers, with deeper penetration of coherent structures. On the contrary, in the presence of foliage, ventilation in the lower canopy decreased due to drag exerted by the upper layers, dampening vertical transport of momentum and decoupling the trunk space from the overlying atmosphere. Thus, in the foliated period soil chambers may have experienced\ lower mixing of the surrounding air, especially in nighttime stable conditions, with a consequent build–up of CO_2 concentration opposing to diffusive transport. This would lead to an underestimation of soil respiration measured by this technique. Nevertheless, additional studies are needed to evaluate the similarity between momentum and scalar transport in order to extend these results to explain the nature of scalar fluxes.

Today, the availability of precise measuring techniques, associated with powerful processing capacity, allows the study of vegetation–atmosphere interactions with an unprecedented detail. However, plant canopies still represent a complex subject where a range of phenomena and processes interact. There, the complexity of plant physiology, the intricacy of turbulence and the beauty of plant architecture merge in one picture that will continue to stimulate the keen attention of researchers for many years.

Ringraziamenti

Sono stati tre anni intensi che mi hanno vista cambiare e crescere, trovare una nuova strada che mi ha portato ad appassionarmi ed impegnarmi nello studio di alcuni aspetti di cui prima a malapena conoscevo i concetti generali. È tutto cominciato un po' per caso, non avevo ancora un'idea chiara di cosa "volessi fare nella vita", ma giorno dopo giorno è cresciuta la consapevolezza che questo potrebbe essere quello che sarebbe giusto per me e che vorrei fare. Non è stato un percorso facile, ma ho avuto di fianco delle persone straordinarie che mi hanno sempre dato forza nei momenti di sconforto e con cui ho riso e scherzato ogni giorno.

Comincio ringraziando la mia famiglia, i miei genitori perché mi hanno sempre sostenuto e continuano a credere in me, nonostante non sia ben chiaro cosa stia facendo. Mia sorella per avermi sempre spinto ad andare oltre, non accontentarmi e cercare nuove esperienze all'estero. Ci sono poi le mie amiche che anche se distanti ho sempre sentito vicine.

Passando all'ambiente di "lavoro", il primo ringraziamento va alla persona senza cui tutto questo non sarebbe stato possibile, che mi ha dato un'opportunità pur non conoscendomi e che mi ha poi seguito con grande dedizione, passione e pazienza, investendo lunghi pomeriggi tra spiegazioni e discussioni. Voglio ringraziare Andrea, il mio tutore, non solo per avermi insegnato gran parte di quello che so, ma anche per aver sempre agito cercando il meglio per me con grande generosità e altruismo, facendo nascere in me l'interesse e la passione verso la ricerca e, in particolare, verso lo studio delle interazioni tra vegetazione e atmosfera. Una presenza fondamentale per me è stata anche quella di Luca, il mio compagno di ufficio e di lunghe giornate sotto il sole (non al mare purtroppo). Lo ringrazio per esser stato la mia valvola di sfogo, per avermi sostenuto e dato coraggio, per aver reso tutto più divertente e facile. Ringrazio Franco per essere stato sempre disponibile e pronto a dare una mano. Grazie a Francesca, Giulio, Fabio e Andrea per il loro supporto post-lavorativo.

Ringrazio la mia coinquilina di Davis, Katharina, che ha reso la mia esperienza li indimenticabile, per avermi incluso nella sua vita ed essere un'amica su cui so posso contare. Allargo questo ringraziamento anche a Nina e Miles, che mi hanno fatto scoprire le bellezze della California. Grazie al prof. Kyaw Tha Paw U per avermi guidato, dato utili consigli e fatto sentir parte del suo gruppo di ricerca, di cui ringrazio tutti i dottorandi che mi hanno accolto tra loro.

Sperando di non essermi dimenticata nessuno, un grazie va a tutte le belle persone che ho conosciuto in questi anni girando per il mondo tra corsi e convegni perché grazie anche a loro ho trovato la voglia di continuare e provare a farmi strada in questa direzione.

Acknowledgements

It has been a long way, three intense years during which I learned and changed a lot. Even if at the beginning I was not sure about what to do with my life, day by day I have developed interest and passion about my research work, finally realizing that this could be the right path for me. It was not easy, but I had a lot of people around who supported me during sad moments and laughed with me during most of the time.

I want to start thanking my family, my parents which always supported me and continue to believe in me, even if it is not very clear what I am doing. Thanks to my sister that pushed me to go further and make new experiences abroad. Thanks to my friends, which I always felt close even if they are not.

Skipping to "work", I want to first thank the person without whom nothing of this could have been possible, that gave me a chance without knowing me and then guided me with dedication, passion and perseverance, spending many afternoons in explanations and discussions. I thank Andrea, my supervisor, not just because he taught me most of what I know, but also because he always behaved for my best with great generosity and altruism, making grow in me the interest and passion for research and, in particular, for the study of vegetation–atmosphere interactions. Another important person for me has been Luca, my mate in the office and during long days in the sunshine (not at the beach unfortunately). I thank him for the continuous support and encouragement, making everything easier and nicer. Thanks to Franco for his willing to help.

Thanks to my Davis housemate, Katharina, who made my experience there unforgettable, including me in her life and being a friend I know I can count on. Thanks also to Nina and Miles, who let me discover a lot of beautiful places around California. I want to thank prof. Kyaw Tha Paw U for his advice and to have made me feel part of his research group, and all the PhD students who welcomed me.

Thanks to all the nice people I met during these years at courses and conferences around the world, because they also contributed to convince me to continue working in this direction.